

Efforts towards the Total Synthesis of Azaspiracid-3

DISSERTATION

Presented in Partial Fulfillment of the Requirements for the Degree Doctor of Philosophy
in the Graduate School of The Ohio State University

By

Zhigao Zhang

Graduate Program in Chemistry

The Ohio State University

2013

Dissertation Committee:

Dr. Craig J. Forsyth, Advisor

Dr. Jon R. Parquette

Dr Anita E. Mattson

Copyright by
Zhigao Zhang
2013

Abstract

Azaspiracid, a structurally complex marine toxin isolated from the mussel *Mytilus edulis* in Killary Harbor, Ireland, represents a new class of marine metabolites unrelated to any previous known agent of diarrhetic shellfish poisoning. As such, the natural product has spurred considerable interest among organic community. The thesis details the study towards the total synthesis of azaspiracid-3.

The C1-C21 domain and C22-C40 domain have been synthesized, which aims to assemble the molecule through Yamaguchi esterification. The ABCD domain involved an efficient NHK coupling reaction between C1-C12 segment and C13-C22 segment. The trioxadispiroketal skeleton was constructed under the influence of acid catalysis. The EFGHI domain highlighted a chelate controlled Mukaiyama aldol reaction to produce C22-C40 linear precursor, and a DIHMA process to assemble the bridged ketal.

With the recognition of bridged ketal and spiroaminal functionality in the FGHI domain, the gold-catalysis to achieve these moieties has been proposed. A novel gold-catalyzed spiroaminal formation has been systemically developed. The gold-catalyzed ketalization was then successfully implemented to construct the bridged ketal, while an inevitable elimination could not deliver the desired spiroaminal under gold conditions.

A NHK reaction to couple the C1-C21 and C22-C40 domains has also been proposed. The revised C22-C40 domain was achieved with a similar synthetic route.

Dedication

This document is dedicated to my family.

Acknowledgments

First of all, I would like to thank my advisor, Prof. Dr. Craig J. Forsyth, for allowing me to join his research group and explore the challenges of organic synthesis. I am very grateful to Dr. Forsyth for his extensive support, advice and help throughout my graduate research in the azaspiracid project.

I am thankful to my committee members: Professors Jon Parquette, Anita Mattson and Birgit Alber for devoting their precious time.

I would like to thank Dr. Jianyan Xu and Dr. Yue Ding. During my first couple years in Ohio State, they unconditionally offered me a lot of help in my graduate study and personal life. I also would like to thank Dr. Ting Wang and Dr. Chao Fang for their helpful discussions and comments on my research.

I highly appreciate and honor those researcher who have made critical contributions to this project: Dr. Junliang Hao, Dr. Son Nguyen, Dr. Jianyan Xu, Dr. Yue Ding for their pioneering work. I am also thankful to my current sub-group member: Mr. Yong Chen, Mr. Daniel Adu-Ampratwum, and Mr. Antony Okumu. Especially, I would like to thank Mr. Yong Chen, who provided me materials for later-stage synthesis. Thank to Dr. Dan Carper, Dr. Baoyu Wang and many other people from other groups for generously lending me some reagents and solvents.

Thank to Dr. Yue Ding, Mr. Daniel Adu-Ampratwum for proof reading my dissertation.

I would also like to thank my friends: Dr. Jianyan Xu, Dr. Yue Ding, Dr. Ting Wang, Dr. Chao Fang, Mr. Yong Chen, Dr. Dimao Wu, Dr. Bo Wang, Dr. Yucheng Pang, and Dr. Feng Zhou, who shared with me lots of fun inside and outside of the lab. Dr. Yue Ding and Mr. Yong Chen are my teachers of evolution theory and the world-wide history. I learned a lot of knowledge from them other than chemistry. Thank to Dr. Daniel Wherritt, Dr. Matt Jackel, Dr. Brandon Van Ness, and all of other group members for providing me the friendly environment in this group.

Last but not the least, I sincerely thank my family, especially my wife Qinqin Zhu, my daughter Boxuan Zhang, my parents, my brother Zhikuan Zhang, who gave me unconditional love, support and encouragement. It is them who made me whom I am today!

Vita

October 1985.....Born in Qingfeng, Henan Province, China
June 2003.....Qingfeng No. 1 High School
June 2007B.S. Chemistry, University of Science and
Technology of China
September 2007 to presentGraduate Teaching and Researching
Associate, Department of Chemistry, The
Ohio State University

Publications

1. Zhao, Q. R.; Xie, Y.; Zhang, Z. G.; Bai, X. *Crystal Growth & Design*, **2007**, *7*, 153.
2. Zhao, Q. R.; Xie, Y.; Dong, T.; Zhang, Z. G. *J. Phys. Chem. C*. **2007**, *111*, 11598.
3. Zhao, Q. R.; Zhang, Z. G.; Dong, T.; Xie, Y. *J. Phys. Chem. B*. **2006**, *110*, 15152.

Fields of Study

Major Field: Chemistry

Table of Contents

Abstract.....	ii
Dedication.....	iii
Acknowledgments.....	iv
Vita.....	vi
Publications.....	vi
Field of Study.....	vi
List of Tables.....	ix
List of Figures.....	x
List of Schemes.....	xi
List of Abbreviations.....	xiv
Chapter 1: Introduction.....	1
1.1. Shellfish Poisoning.....	1
1.2. Discovery of Azaspiracid.....	5
1.3. Structure Revision of Azaspiracid-1.....	6
1.4. Analog of Azaspiracid.....	9
1.5. Origin of Azaspiracid.....	10
1.6. Biological Activity.....	11
Chapter 2: Synthetic Efforts.....	14

2.1. Synthetic Study on the Originally Proposed Structure.....	14
2.1.1. Forsyth's Approach.....	14
2.1.2. Nicolaou's Approach.....	16
2.2. Synthetic Study on Revised Structure.....	19
2.2.1. Nicolaou's Total Synthesis of Azaspiracids.....	20
2.2.2. Evans' Total Synthesis of (+)-Azaspiracid-1.....	27
2.2.3. Forsyth's Approach.....	31
2.2.4. Carter's Approach.....	37
Chapter 3: Research Progress and Discussion.....	42
3.1. Yamaguchi Esterification Route.....	42
3.1.1. ABCD Domain Synthesis.....	43
3.1.2. EFGHI Domain Synthesis.....	51
3.2. Efforts on FGHI Domain Synthesis with Gold (I) Catalysis.....	57
3.2.1. Gold-Catalyzed Ketalizations.....	58
3.2.2. Gold-Catalyzed Spiroaminal Formation.....	61
3.2.3. Efforts on FGHI Domain Synthesis.....	70
3.3. NHK Route for the Total Synthesis of AZA3.....	77
Experimental Data.....	83
References.....	126
Appendix A. Selected NMR Spectra.....	132

List of Tables

Table 1. Conditions Tested to Construct Spiroaminals	64
Table 2. Optimization of Gold Conditions.....	65
Table 3. Spiroaminal Formation Using Alcohols as Solvent.....	66

List of Figures

Figure 1. Domic Acid.....	2
Figure 2. DSP Toxins.....	3
Figure 3. Saxitoxin.....	4
Figure 4. Brevetoxin 1.....	5
Figure 5. Proposed Structure of Azaspiracid-1.....	6
Figure 6. Corrected structure of azaspiracid-1.....	8
Figure 7. Analogs of Azaspiracids.....	9
Figure 8. <i>Protoperidinium crassipes</i> under a Microscopic view	10
Figure 9. the Origin of Azaspiracids: <i>Azadinium Spinosum</i>	11
Figure 10. Explanation of the Stereoselectivity.....	50
Figure 11. Ketal and Spiroaminal in FGHI Domain.....	57
Figure 12. Substrate Scope.....	68
Figure 13. DIHMA Process.....	82

List of Schemes

Scheme 1. Key Degradation Intermediates of Natural Azaspiracid-1.....	7
Scheme 2. Forsyth's C5-C20 Domain Synthesis.....	15
Scheme 3. Forsyth's C26-C40 Domain Synthesis.....	16
Scheme 4. Nicolaou's 1 st Attempt towards the ABCD Domain.....	17
Scheme 5. Nicolaou's 2 nd Attempt towards the ABCD Domain.....	18
Scheme 6. Nicolaou's Synthesis of the FGHI Domain.....	19
Scheme 7. Nicolaou's Retrosynthetic Analysis of Azaspiracid-1.....	20
Scheme 8. Nicolaou's Synthesis of the ABCD Domain.....	23
Scheme 9. Nicolaou's FGHI Domain Synthesis.....	24
Scheme 10. Nicolaou's Total Synthesis of Azaspiracid-1.....	26
Scheme 11. Evans' Retrosynthetic Analysis.....	27
Scheme 12. Evans' ABCD Domain Synthesis.....	28
Scheme 13. Evans' EFGHI Domain Synthesis.....	30
Scheme 14. Evans' Total Synthesis of (+)-Azaspiracid-1.....	31
Scheme 15. Forsyth's Synthesis of Trioxadispiroketal 80	33
Scheme 16. Forsyth's Gold-Catalyzed ABCD Domain Synthesis.....	35
Scheme 17. Forsyth's FGHI Synthesis.....	37
Scheme 18. Carter's C1-C26 Domain Synthesis.....	39

Scheme 19. Carter's FGHI Domain Synthesis.....	41
Scheme 20. Retrosynthetic Analysis.....	43
Scheme 21. Retrosynthetic Analysis of the ABCD Domain.....	44
Scheme 22. Synthesis of 138	45
Scheme 23. Synthesis of 143	46
Scheme 24. Synthesis of the Iodide 129	47
Scheme 25. Synthesis of the Aldehyde 149 and the Silyl Enol Ether 154	48
Scheme 26. CD Fragment Synthesis.....	49
Scheme 27. Synthesis of the C1-C21 Carboxylic Acid 126	51
Scheme 28. Retrosynthetic Analysis of the EFGHI Domain.....	52
Scheme 29. Synthesis of the Aldehyde 164	53
Scheme 30. Synthesis of the EFG aldehyde 166	54
Scheme 31. Synthesis of the C21-C40 Domain of AZA3.....	56
Scheme 32. Examples of Gold-Catalyzed Ketal Formations ^{65, 66, 67}	59
Scheme 33. Examples of Applications Examples of Applications of Gold-Catalyzed Transformations in Natural Product Synthesis ^{41, 68, 69}	61
Scheme 34. Summary of Synthetic Route for Spiroaminals.....	62
Scheme 35. Synthesis of Spiroaminal Model Compound.....	63
Scheme 36. Proposed Mechanism of Gold-Catalyzed Spiroaminal Formation.....	70
Scheme 37. Synthetic Analysis.....	72
Scheme 38. Synthesis of the Alkyne 224	73
Scheme 39. Construction of FG Bridged Ketal under Gold Conditions.....	75

Scheme 40. Attempted Construction of the Spiroaminal in the FGHI Domain.....	76
Scheme 41. NHK-Based Retrosynthetic Analysis.....	78
Scheme 42. Revised Synthesis of the E Fragment.....	79
Scheme 43. Synthesis of the C22-C40 Linear Precursor.....	80
Scheme 44. Synthesis of the C22-C40 Domain of AZA3.....	81

List of Abbreviations

Ac	acetyl
ADmix- α	commercial reagent for asymmetric dihydroxylation
ADmix- β	commercial reagent for asymmetric dihydroxylation
BAIB	bis(acetoxy)iodobenzene
Boc	<i>tert</i> -butoxy carbonyl
BocON	2-(<i>tert</i> -butoxycarbonyloxyimino)-2-phenylacetonitrile
Bn	benzyl
Bu	butyl
brsm	based on recovery of starting material
Bz	benzoyl
COD	cyclooctadiene
CSA	camphosulfonic acid
Cy	cyclohexyl
dba	dibenzylidene acetone
DBU	1,8-Diazabicycloundec-7-ene
DCC	dicyclohexyl carbon diimide
DDQ	dichlorodicyano quinone
DEAD	diethyl azodicarboxylate

DHP	3,4-dihydro-2- <i>H</i> pyran
DIBAL	diisobutyl aluminum hydride
DIPT	diisopropyl tartrate
DMAP	4- <i>N,N</i> -dimethyl amino pyridine
DMF	<i>N,N</i> -dimethyl formide
DMP	Dess Martin periodinane
DMSO	dimethyl sulfoxide
Et	ethyl
<i>ee</i>	enantiomeric excess
ESI	electrospray ionization
h	hours
HMDS	hexa methyl disilyl amide
Hz	hertz
Im	imidazole
Ipc	isopinocampheyl
IR	infrared specscopy
LC	liquid chromatography
LDA	lithium diisopropyl amide
<i>m</i> CPBA	<i>meta</i> -chloro peroxy benzoic acid
min	minute
Me	methyl
modp	1-morpholino-carbamoyl-4,4-dimethyl-1,3-pentanedionato

MS	molecular sieves
MTM	methyl thio methyl
NHK	Nozaki-Hiyama-Kishi
NIS	<i>N</i> -iodo succinimide
NMO	<i>N</i> -methyl morpholine <i>N</i> -oxide
NMP	<i>N</i> -methyl morpholine
NMR	nuclear magnetic resonance
NOE	nuclear Overhauser effect
OSu	<i>N</i> -oxysuccinimide
PFP	pentafluoro phenyl
Ph	phenyl
Piv	pivaloyl
PMB	<i>p</i> -methoxy benzyl
PMP	<i>p</i> -methoxy phenyl
PPTS	pyridinium <i>para</i> -toluene sulfonate
Pr	propyl
Py	pyridine
R _f	retention factor
rt	room temperature
SAD	Sharpless asymmetric dihydroxylation
SAE	Sharpless asymmetric epoxidation
TBAF	tetra butyl ammonium fluoride

TBAI	tetra butyl ammonium iodide
TBDPS	<i>tert</i> -butyl diphenyl silyl
TBS	<i>tert</i> -butyl dimethyl silyl
TCA	trichloro acetamide
Teoc	trimethyl silyl ethoxy carbonyl
TEMPO	2,2,6,6-tetramethyl-1-piperidinyloxy
TES	triethyl silyl
Tf	trifluoro methyl sulfonyl
TFA	trifluoro acetate
TFAA	trifluoro acetic anhydride
TFP	trifuranyl phosphine
THF	tetrahydro furan
THP	tetrahydro pyran
TIPS	triisopropyl silyl
TMS	trimethyl silyl
TMSE	trimethyl silyl ethyl
TPAP	tetrapropyl ammonium perruthenate
Tris	triisopropyl phenyl sulfonyl
Ts	toluene sulfonyl
Xc	Evans auxiliary

Chapter 1: **Introduction**

1.1 Shellfish Poisoning

Algae are very important to marine ecosystems, and normally most of algae are not harmful. Algal blooms occur in natural waters when certain types of algae grow quickly due to the changes in the levels of chemicals stimuli. Algal blooms can deplete oxygen and block the sunlight that other organisms need to live and some can produce toxins, which have been called harmful algal blooms (HABs). More importantly, the toxins can be accumulated in bivalve molluscs (such as mussels, clams, oysters and scallops) without being degraded. Normally, these toxins are harmless to the shellfish themselves, while they are very toxic to human being. As early as 1927,¹ the first shellfish poisoning was reported in San Francisco, California. To date, there are five different types of shellfish poisoning that has been recognized: Amnesic shellfish poisoning (ASP),² diarrhetic shellfish poisoning (DSP),³ paralytic shellfish poisoning (PSP),² neurotoxic shellfish poisoning (NSP),⁴ and the newly discovered azaspiracid shellfish poisoning (AZP).⁵

Amnesic shellfish poisoning (ASP). The first incident of shellfish poisoning associated with ASP was reported in 1987 when a serious outbreak food poisoning occurred in eastern Canada.² Quickly after the incident, a team of scientists discovered the cause,⁶ which was consumption of the marine biotoxin called domoic acid. The toxin is produced by marine diatoms, which belongs to the genus *Pseudo-nitzschia* and *Nitzschia*

navis-varingica. Domoic acid can cause permanent short-term memory loss, brain damage, and death in severe cases.

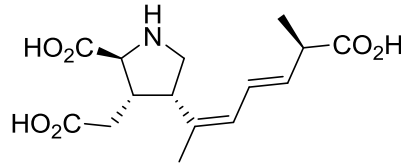
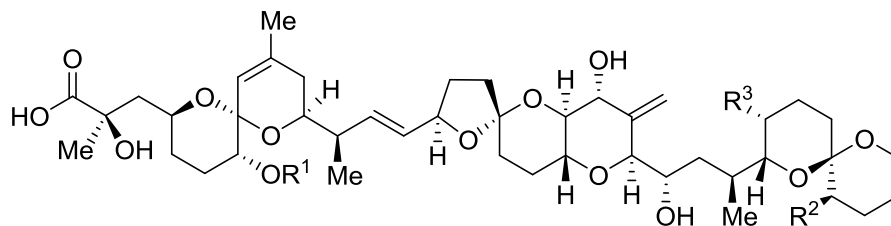
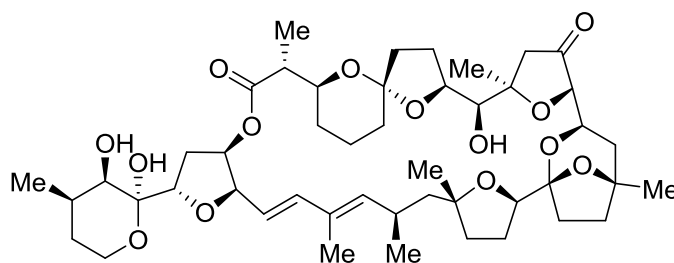


Figure 1. Domoic Acid

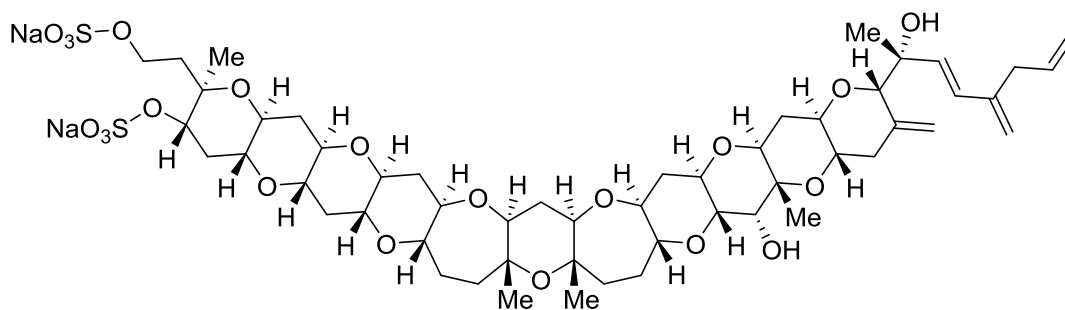
Diarrhetic shellfish poisoning (DSP). The first DSP incident were in Netherlands in 1960s, followed by similar reports in late 1979 from Japan.⁷ DSP toxins can be divided into three different groups based on chemical structures. The first group, acidic toxin, includes okadaic acid (OA)⁸ and its derivatives dynophysistoxins (DTXs).⁹ The second group, neutral toxins, includes polyether lactones pectenotoxins (PTXs).¹⁰ The third group includes disulfated ployethers yessotoxins (YTXs).¹¹ These toxins usually produced by dinoflagellates species of *Dinophysis spp.* and *Prorocentrum*. As the name implies, the syndrome manifests itself as diarrhea, although nausea, vomiting and abnormal cramps are all common.



Toxin	R ¹	R ²	R ³
Okadaic acid	H	H	Me
Dinophysis toxin 1	H	Me	Me
Dinophysis toxin 2	H	Me	H
Dinophysis toxin 3	Acyl	H	Me



Pectenotoxin 2



Yessotoxin

Figure 2. DSP Toxins

Paralytic shellfish poisoning (PSP). The main toxins associated with PSP are saxitoxins (STX)¹² which are neurotoxins. STX are naturally produced by

dinoflagellates (genera *Alexandrium*, *Gymnodinium* and *Pyrodinium*) and cyanobacteria (*Anabaena*, *cylindroermopis*, *Lyngbya*, etc).¹³ The major symptoms are neurological, including tingling, numbness in the mouth and fingertips, ataxia, giddiness, drowsiness, fever, rash. Similar to ASP, PSP can be fatal in some extreme cases, especially in immunocompromised individuals.

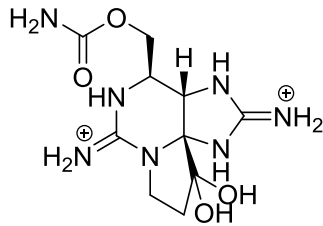


Figure 3. Saxitoxin

Neurotoxic shellfish poisoning (NSP). NSP is normally associated with the red tides in Florida, Texas, North Carolina, and Mexico. The cause of NSP is the consumption of shellfish, which are contaminated by brevetoxins (PbTx).¹⁴ These toxins are produced naturally by the dinoflagellate *Karenia brevis*. Moreover, PtTx can bind to voltage-gated sodium channels in nerve cells, which can lead to disruption of normal neurological process. Symptoms caused by NSP include vomiting, nausea, and a variety of neurological symptoms, such as slurred speech, abdominal pain, while NSP is not fatal to humans.

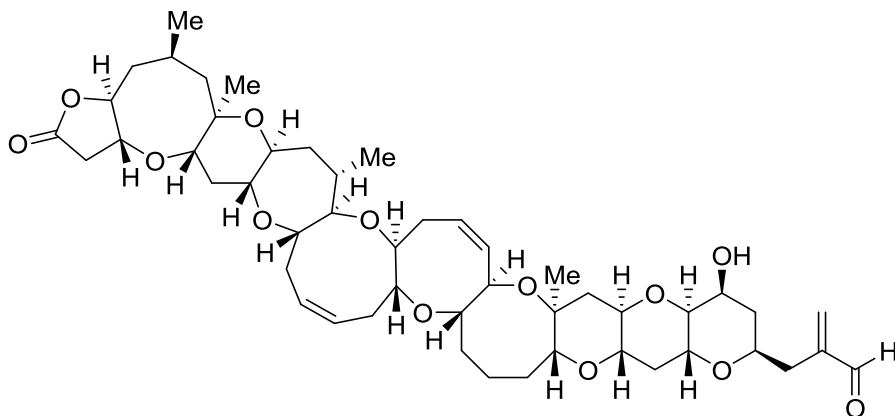


Figure 4. Brevetoxin 1

Azspiracid shellfish poisoning (AZP). AZP is newly defined shellfish poisoning syndrome, which is associated with marine toxin azaspiracid.

1.2 Discovery of Azaspiracid

The discovery of Azaspiracid started with a seafood-poisoning incident in Netherland, in 1995. At least eight people became sick after consumption of blue mussel *Mytilus edulis*, which was collected in Killary Harbor, Ireland. The symptoms were very similar to that of diarrhetic shellfish poisoning (DSP), including nausea, vomiting, diarrhea and stomach cramps.¹⁵ But further analysis showed that the contaminations of the major DSP toxins okadaic acid (OA) and dinophysistoxins (DTXs) were very low, which means that the cause must be an unknown toxin.

In order to solve this puzzle, Yasumoto and co-workers collected 20 kg of whole mussel meat at Killary Harbor in February 1996⁵ and succeeded in isolating 2 mg of the causative toxin named azaspiracid, which was a colorless amorphous solid. They also

proposed the structure (Figure 5) based on the extensive study of $^1\text{H-NMR}$, $1\text{H-}^1\text{H}$ Cosy, $^{13}\text{C-}$ NMR, ROESY, HSQC, TOCSY, HMBC, FAB MS/MS, and (CID) MS/MS. As shown, azaspiracid-1 ($\text{C}_{47}\text{H}_{71}\text{NO}_{21}$) has 47 carbons (40 on the parent chain), 9 rings, and 20 stereogenic centers. The unique array of molecular frameworks includes a trioxadispiroketal fused with a *trans* tetrahydrofuran ring (ABCD domain), a six-membered hemiketal bridge (E domain), and a spiroaminal fused with a 2,9-dioxabicyclo[3.3.1] nonane ring (FGHI domain). At the point of isolation, the absolute configuration of azaspiracid was unknown.

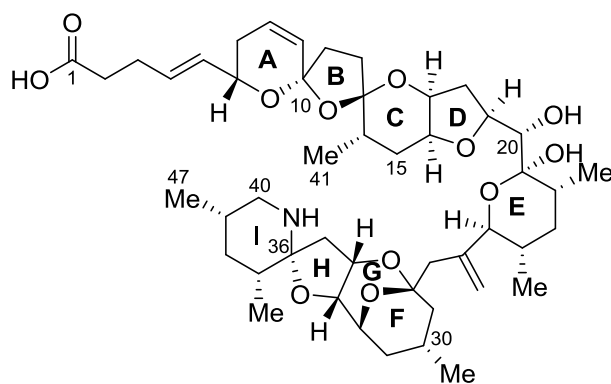
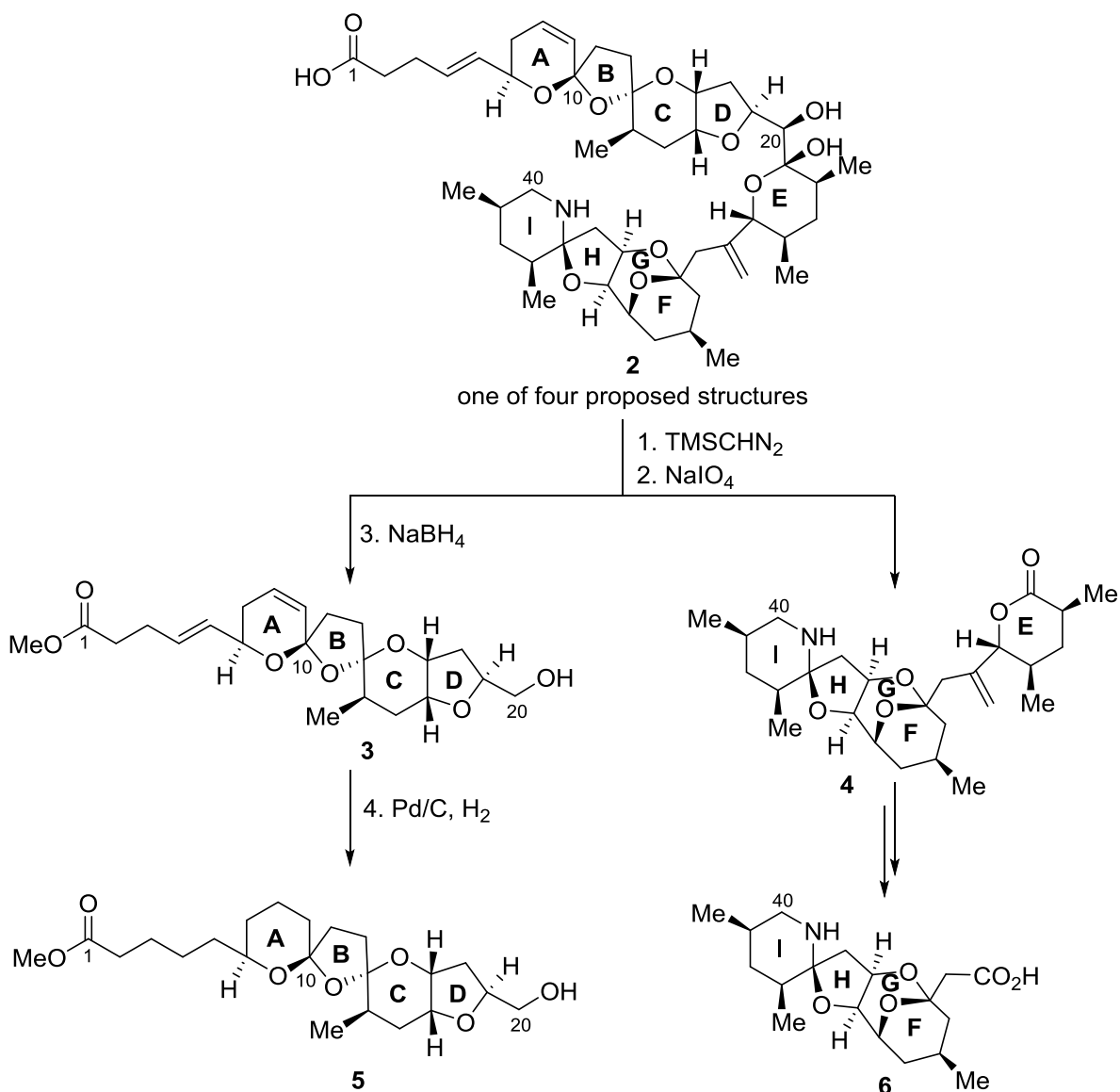


Figure 5. Proposed Structure of Azaspiracid-1

1.3 Structure Revision of Azaspiracid-1

Due to the uncertainty of the intriguing chemical structure and the scarcity in nature, azaspiracid has spurred considerable interest among the organic chemistry community. After extensive synthetic studies, the Nicolaou group claimed to have completed the total synthesis of proposed azaspiracid-1,¹⁶ but to their disappointment, all of the isomers **1**, *FGHI-epi-1*, *C20-epi-1* and *C20-epi-FGHI-epi-1* did not match the data, by TLC and

HPLC, from the naturally derived sample of azaspiracid-1, which indicated that the original proposed structure was in error.



Scheme 1. Key Degradation Intermediates of Natural Azaspiracid-1

In collaboration with the Satake group, the Nicolau group then utilized degradation of natural samples into smaller fragments, whose chemical synthesis could narrow down

the location of structure error between synthetic and natural compounds.¹⁷ As shown in scheme 1, the natural sample was degraded into three key intermediates: **3**, **4**, **5**, and **6**. After comparing ¹H-NMR spectrum from **4**, the relative stereochemistry for EFGHI domain of azaspiracid-1 was predicated as the structure FGHI-*epi-4*. The absolute stereochemistry was further established as FGHI-*epi-4*, by comparison of optical rotation and ¹H-NMR spectrum of the derived ester from **6**. The biggest challenge for the structure elucidation was the ABCD part. With the huge difference in the ¹H-NMR spectra and clue from another marine natural product lissoketal, the Nicolau group first suspected the endocyclic double bond between C8-C9 should be moved to C7-C8 in **3**. Through further extensive synthetic study on **5**,¹⁸ the relative stereochemistry of the ABCD domain was settled down, as AB-*epi-5*, to further accommodate the thermodynamic stability and NOE effect between 6-H and the methyl group on C13. Finally, the absolute stereochemistry (Figure 6) between the ABCD and EFGHI domains was established by total synthesis.

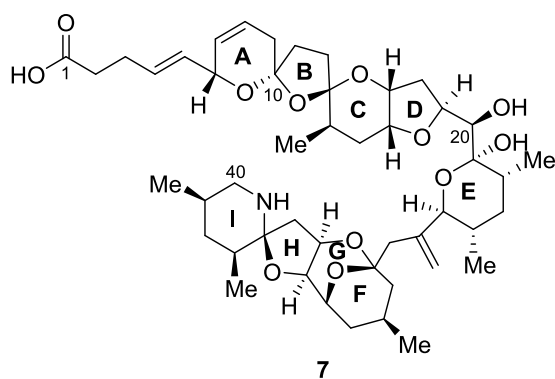


Figure 6. Corrected Structure of Azaspiracid-1

1.4 Analog of Azaspiracid

Shortly after the isolation of azaspiracid-1 (AZA1), four additional analogs of this toxin were isolated,^{19, 20} and the structures of these four analogs were also determined by MS and NMR spectroscopy techniques. Compared to AZA1, AZA2 possesses an additional methyl group on C8, and AZA3 has a C22-demethyl structure. The other two analogs (AZA4 and AZA 5) proved to have oxidized structures of AZA3, showing the presence of an additional OH at either C3 (AZA4) or at C23 (AZA5).

Up to now, only AZAs 1 to 5 have had their structures verified with NMR techniques, while there are over 30 analogues²¹ in this toxin family, which spread from west Europe to the east coast of United States. The structures of other analogs have been solely predicted based on the analysis of fragmentation patterns of MS/MS spectra. As shown in Figure 7, the most abundant 11 analogs have been listed. The structures of AZA 6 to 11 were proposed based on those of AZA 1 to 5. Interestingly, all of them share the same FGHI domain, while the differences are mainly at the C3, C8, C22, and C23 positions.

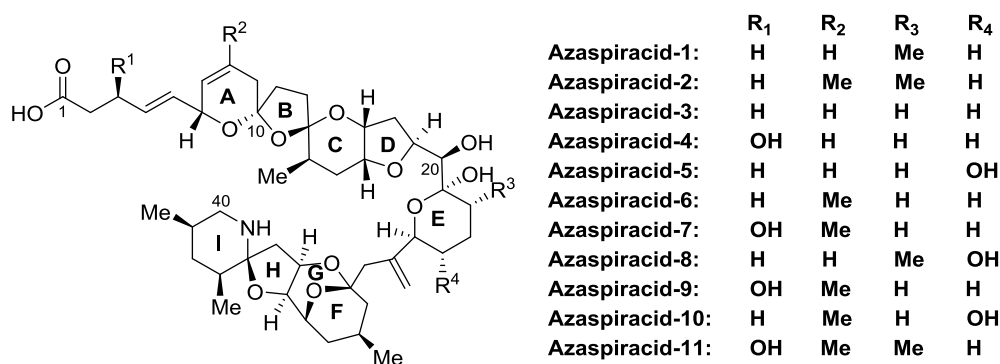


Figure 7. Analogs of Azaspiracids

1.5 Origin of Azaspiracid

The polyether structures of azaspiracids suggest that this neurotoxin may be produced by some kind of dinoflagellate. There have been several attempts to discover the progenitor of azaspiracids. The James Group collected the dinoflagellate sample in the southeast coast of Ireland.²² Each species of dinoflagellate was tested for the existence of azaspiracid. Only *protoperidium crassipes* (Figure 8), were found to be positive. More interestingly, only AZA1, AZA2, and AZA3 were found in the dinoflagellate, so it is believed that AZA1, AZA2 and AZA3 are likely to be the genuine products of a causative marine organism and the other analogs may be the degradation products in shellfish.

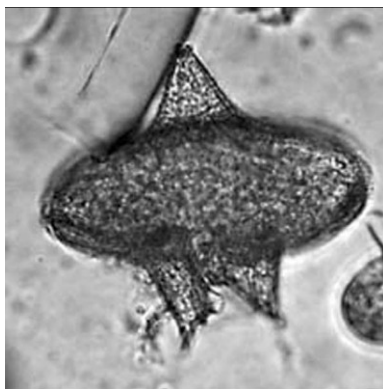


Figure 8. *Protoperidium crassipes* under a Microscopic view

Nevertheless, detailed investigation have been conducted by the Irish Marine Institute, which failed to show any correlation between occurrence of azaspiracids in shellfish and blooms of *Protoperidium crassipes* in a four year period (2002-2006).²³ The role of *Protoperidium crassipes* was proposed by Krock and Tillmann to be an AZA

vector following grazing upon a proximal source.²⁴ At the same time, they discovered a new species named *Azadinium spinosum* (Figure 9). They also proved that this newly discovered dinoflagellate did produce azaspiracids in cell culture.²⁵ More interestingly, they only found AZA1 and AZA2 in the species. The question of origin of AZA3 is still unanswered.

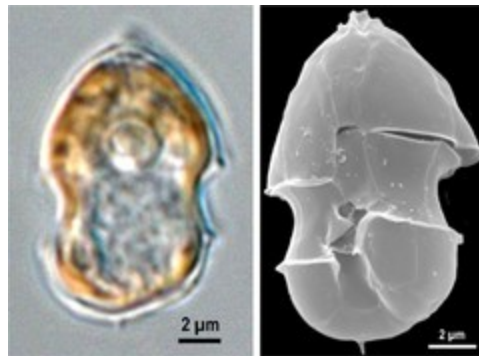


Figure 9. the Origin of Azaspiracids: *Azadinium spinosum*

1.6 Biological Activity

In vivo toxicology

Before people realized the causative toxin for the food poisoning incident, toxicological studies had been carried out in mice.¹⁵ The intraperitoneally (IP) injected acetone extracts of contaminated blue mussels caused sluggishness, respiratory difficulties, spasms, progressive paralysis, and even death within 20-90 mins. When the partially purified azaspiracids were used in the study, it shows that IP injection of a lethal dose ($> 150 \mu\text{g}/\text{kg}$) caused swelling of the stomach and liver concurrent with reduction in size/weight of the thymus and spleen.²⁶ With the assumption of the same purity degree,

the order of azaspriacid analog potency seems to be AZA2 > AZA3 > AZA1 > AZA4 > AZA4.

In an accurate oral administration, the study showed that an approximate oral minimum lethal dose was 500 µg/kg. Lower doses (300 µg/kg) induced fatty acid droplet accumulation in the liver, followed by sporadic degeneration and erosion of the small intestinal microvilli, vacuole degeneration in epithelial cells, and atrophy of the lamina propria. With mid-level doses (500 to 700 µg/kg), AZA1 could cause the injuries of both T and B lymphocytes in the spleen.²⁷

In another series of *in vivo* studies, mice were monitored for recovery, while orally administered with repeated doses of AZA1. The recovery times for each tissue: liver = 7 days; lymphoid = 10 days; lung = 56 days, and the stomach => 12 weeks, which were much slower, compared to that associated with DSP. As far as the chronic effects, low doses repeated exposures to AZA1 could cause the lung tumor formation, which potentially poses a threat to human health.²⁸

In vitro toxicology

Compared to okadaic acid (OA), AZA1 did not show any inhibition effect on PP1²⁹ or PP2A.³⁰ However, OA and genistein could modulate the cytosolic calcium response induced by AZA1 in human lymphocytes cells.³¹ With the neuroblastoma cells tested, it has been shown that AZA1 disrupts cytoskeletal structure and induces a time and dose dependent decrease of F-actin pools.³⁰

The effects of azaspiracids on the cytosolic [Ca²⁺], intracellular pH in human T lymphocytes cells were also investigated. AZA1 induces a significant increase of [Ca²⁺],

both in calcium-free and a calcium-containing medium. AZA2 could also increase the $[Ca^{2+}]$ level, while only in a calcium-free medium. AZA 3 could also increase the calcium levels, while AZA4 has an opposite effect, by reducing the calcium influx. However, AZA5 has no effect on intracellular calcium homeostasis.³² The intracellular pH also has response with AZAs. AZA1 and AZA2 did not modify intracellular pH both in calcium-free and a calcium-containing medium. AZA3 slightly increased pH by 0.16 units with the presence of extracellular calcium. AZA4 inhibited the basal pH increase, while AZA5 did not have any effect on intracellular pH.³³

Unlike DSP toxins, the fact that different AZA analogs show distinct different biological activities is interesting and unusual for a marine toxin series of toxins, since each series generally show the same mechanism of action but with different potencies. Their different mechanistic behavior opens attractive possibilities to further SAR studies.

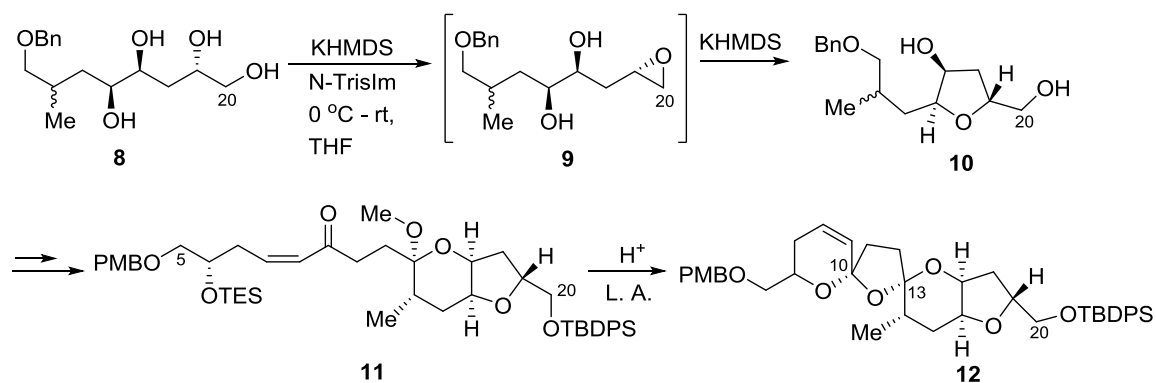
Chapter 2: Synthetic Efforts

2.1 Synthetic Study on the Originally Proposed Structure

Before 2004, the relative stereochemistry between the ABCDE and the FGHI domains was unknown. Moreover, the biological study of azaspiracids indicated that the basis of the toxicity also remained a mystery which made the structure-activity relationship study urgent for both of chemists and biologists. Several research groups had contributed to solve the structure puzzle through extensive synthetic studies.

2.1.1 Forsyth's Approach

In 2001, the Forsyth group reported first synthetic study on construction of the C5-C20 trioxadispiroketal domain,³⁴ which was considered the earliest publication on this topic (Scheme 2). The synthetic study highlighted a novel method for construction of highly substituted *trans*-tetrahydrofuran in a one-pot conversion (scheme 2). In the presence of KHMDS, the C20 primary hydroxyl group in **8** was selectively sulfonylated, which was followed by base-induced epoxide formation and intramolecular *trans* ring closure to furnish **10**. After a series of manipulations, enone **11** was synthesized in high yields, which was planned to form the ABCD skeleton under acidic conditions.

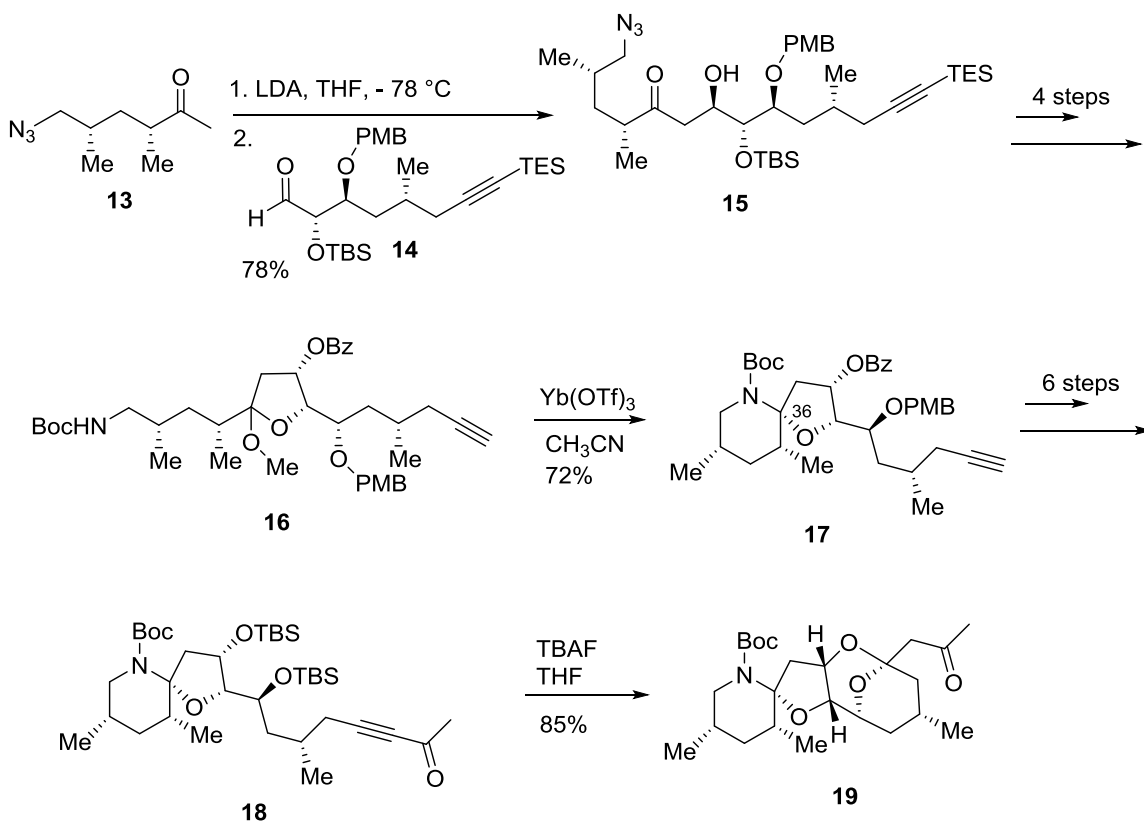


Scheme 2. Forsyth's C5-C20 Domain Synthesis

Treatment of **11** with numerous Brønsted or Lewis acids in a variety of solvents resulted in trioxadispiroketal **12**. The configurations at C10 and C13 were assigned as 10-*R* and 13-*S*, based on the NOE studies and X-ray crystallography of a C5-OH derivative. Compared to the proposed ABCD structure (10*R*,13*R*), molecular mechanics calculations indicated that spiroketal **12** actually was thermodynamically favored because of a double anomeric stabilization from the bis-spiroketal.

The Forsyth group also reported their synthetic effort on the C26-C40 domain of AZA1 (Scheme 3).³⁵ The F-I linear precursor was synthesized through a Felkin aldol reaction between a C27-C34 aldehyde **14** and C35-C40 methyl ketone **13**. A four-step transformation provided **16**. After screening a variety of Lewis acid and solvent combinations, treatment of **16** with Yb(OTf)₃ in CH₃CN efficiently yielded spiroaminal **17** as a single diastereoisomer. The relative configuration of the newly formed C36 stereogenic center was further confirmed by NOE studies. After a series of protecting group manipulations and E ring model coupling, a novel double intramolecular hetero-

Michael addition (DIHMA) was applied to construct the F and G rings of AZAs, which involved fluoride-induced *in situ* desilylation-bis conjugate addition.

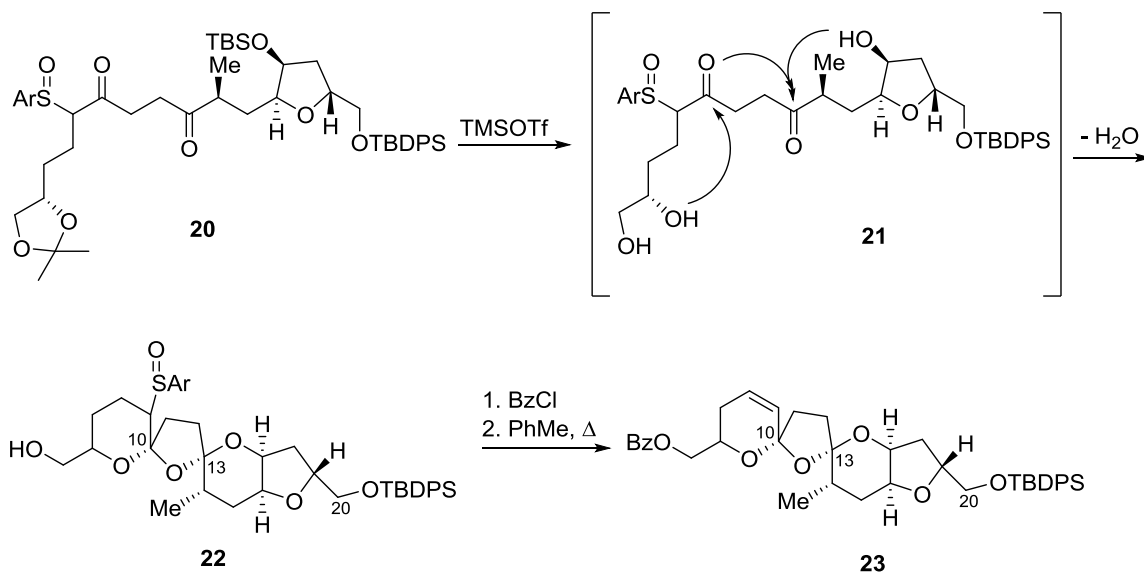


Scheme 3. Forsyth's C26-C40 Domain Synthesis

2.1.2 Nicolaou's Approach

In 2001, the Nicolaou group also reported a synthetic study on the fragment synthesis.³⁶ With the result from Forsyth's group about the ABCD domain synthesis in mind, two different synthetic routes were tested to get the desired 13*R*-dispiroketal. As shown in Scheme 4, the first hypothesis was tested to use a tolyl sulfoxide (ArSO) as an

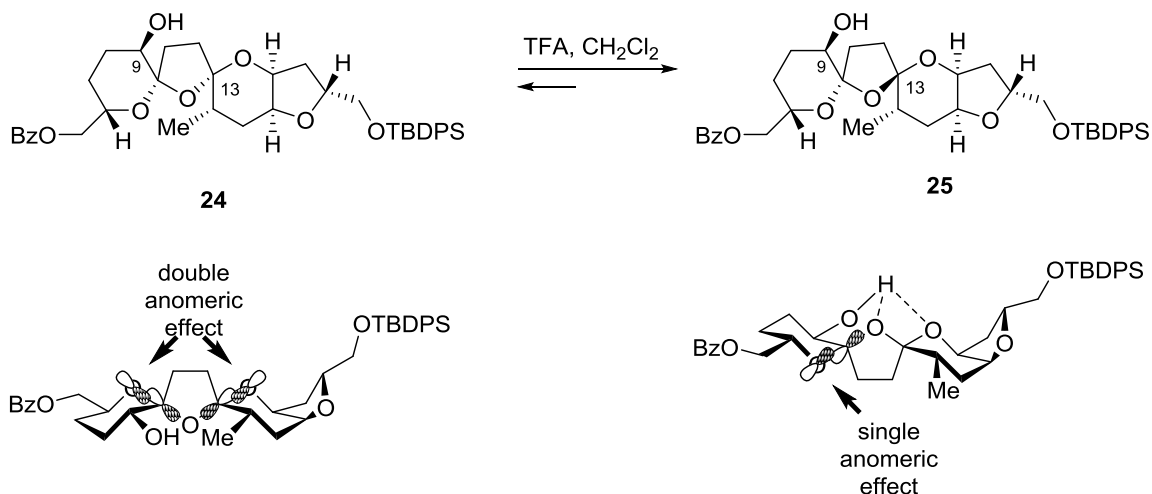
auxiliary group to construct spiroketals. Treatment of **20** with TMSOTf removed the acetonide and TBS groups, and led to a tetracyclic system **22**. NOE studies of the derived **23** showed that **22** was an undesired stereoisomeric product, which meant that the bulky tolyl sulfoxide group did not overcome the double anomeric effects.



Scheme 4. Nicolaou's 1st Attempt towards the ABCD Domain

The second hypothesis was to utilize a hydrogen bonding effect to invert the 13*S* configuration of the double spiroketal system of the ABCD domain to the 13*R* form (Scheme 5). By a similar synthetic route, a hydroxyl group was installed at the C9 position in **24**. Epimerization at C13 was achieved with acid catalysis. Upon exposure of **24** to TFA in CH_2Cl_2 at ambient temperature, an equilibrium was soon reached, providing the desired 13*R* product **25** in 56% yield. Recycling the starting material twice raised the yield up 80%, which made the synthetic route scalable. The structural assignment of **25**

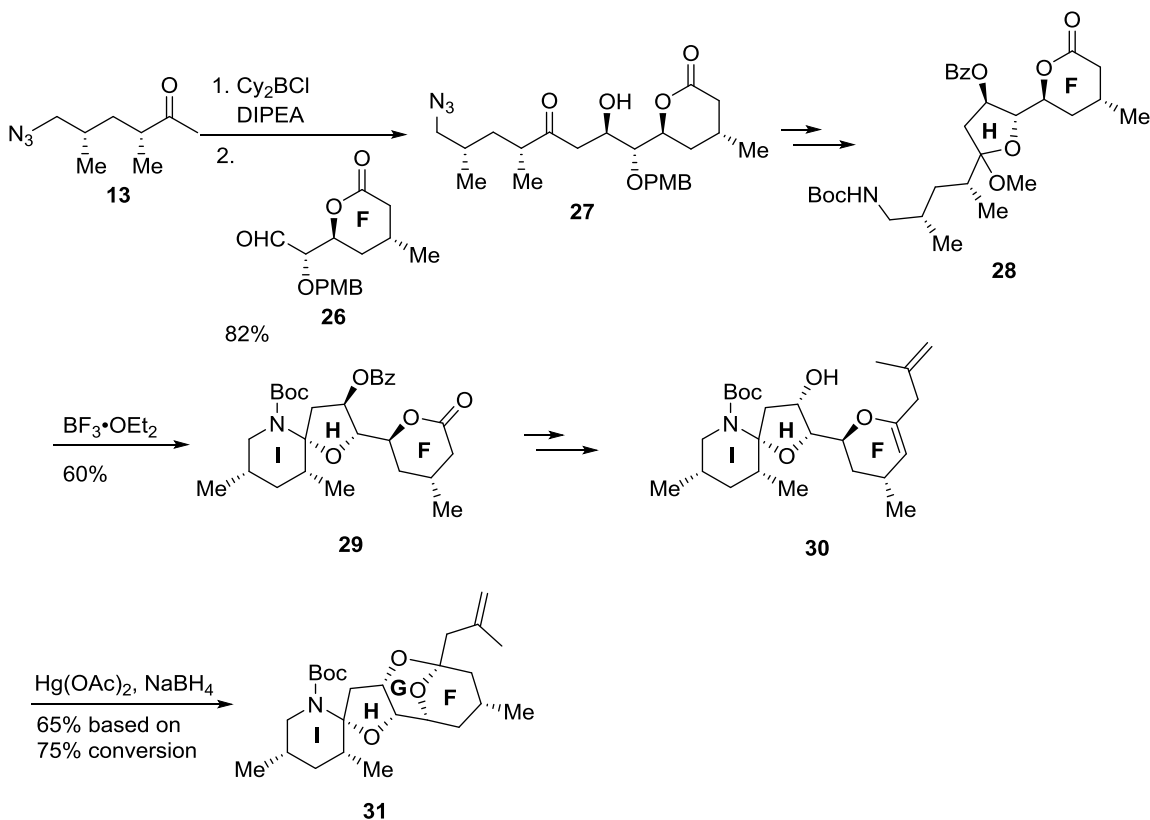
was also confirmed by observing the expected NOEs. The conformations of the two epimers **24** and **25** showed the hydrogen bonding effect between the C9 hydroxyl and the oxygen inside the BC rings with only a single anomeric effect to stabilize the desired isomer, compared with the undersired, but thermodynamically favored product **24**.



Scheme 5. Nicolaou's 2nd Attempt towards the ABCD Domain

Nicolaou's approach towards the FGHI domain is shown in Scheme 6.³⁶ The C26-C40 precursor was synthesized through a boron-mediated aldol reaction between aldehyde **26** and ketone **13**, while a chelation-controlled Mukaiyama aldol only resulted in extensive decomposition of the aldehyde **26**. After a series of transformations, the spiroaminal functionality was assembled under $\text{BF}_3 \cdot \text{OEt}_2$ conditions. After several steps of protecting group manipulations and C34 stereogenic center inversion, the final intramolecular ketalization was planned to furnish the FGHI skeleton of AZA1. The

condition of $\text{Hg}(\text{OAc})_2$ in THF/ H_2O (3:1) followed by quenching with NaBH_4 was found to be optimal for G ring formation, providing the desired product in 65%.



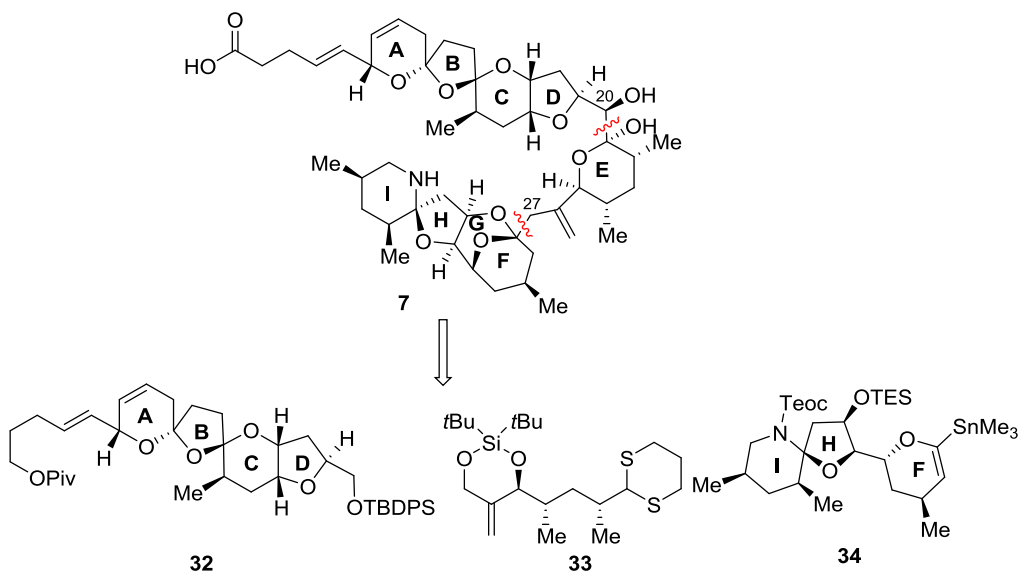
Scheme 6. Nicolaou's Synthesis of the FGHI Domain

2.2 Synthetic Study on Revised Structure

In 2004, the Nicolaou group finally settled the debate about the structure of azaspiracid-1 through collaborative degradation and total synthesis, but the synthetic efforts towards the total synthesis never stopped, due to the challenging chemistry involved and interesting biological activity that requires SAR studies.

2.2.1 Nicolaou's Total Synthesis of Azaspiacids

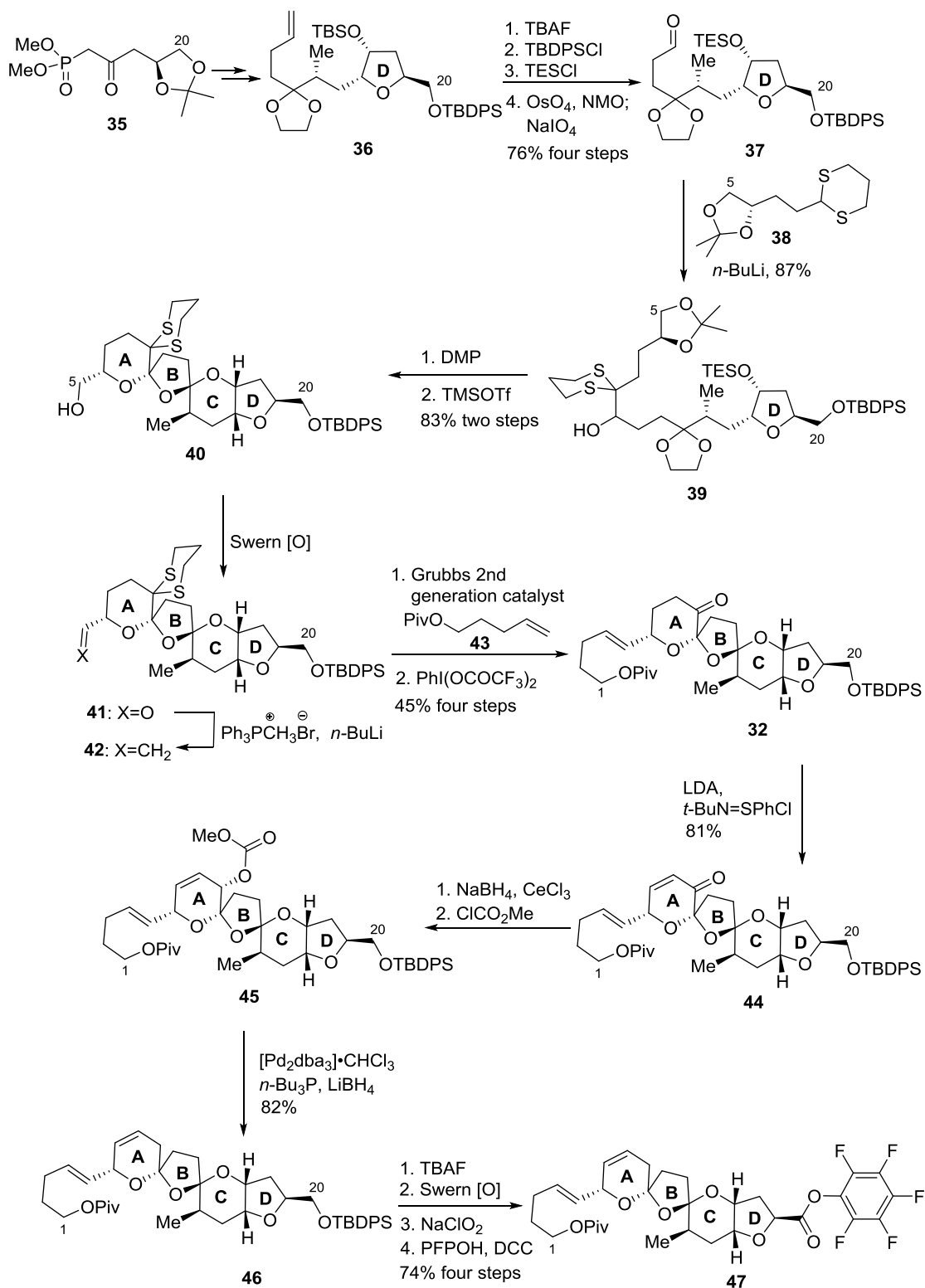
The correct structure of azaspiacid-1 was finally assigned through Nicolaou's first total synthesis, although the synthetic route was quite similar to previously published synthetic work towards the natural product with the originally proposed structure.¹⁸ As shown in Scheme 7, the strategic disconnections were at C20-C21 and C27-C28, providing the key synthetic precursors **32** (C1-C20 ABCD domain), **33** (C21-C27 E domain), and **34** (C28-C40 FGHI domain). The lithiated dithiane coupling strategy was planned to couple the ABCD and E domains, and a C(sp²)-C(sp³) Stille coupling was applied to link ABCDE and FGHI domains. The main benefit of this synthetic plan was to allow the necessary flexibility to address the relative stereochemistry issue of the natural product.



Scheme 7. Nicolaou's Retrosynthetic Analysis of Azaspiacid-1

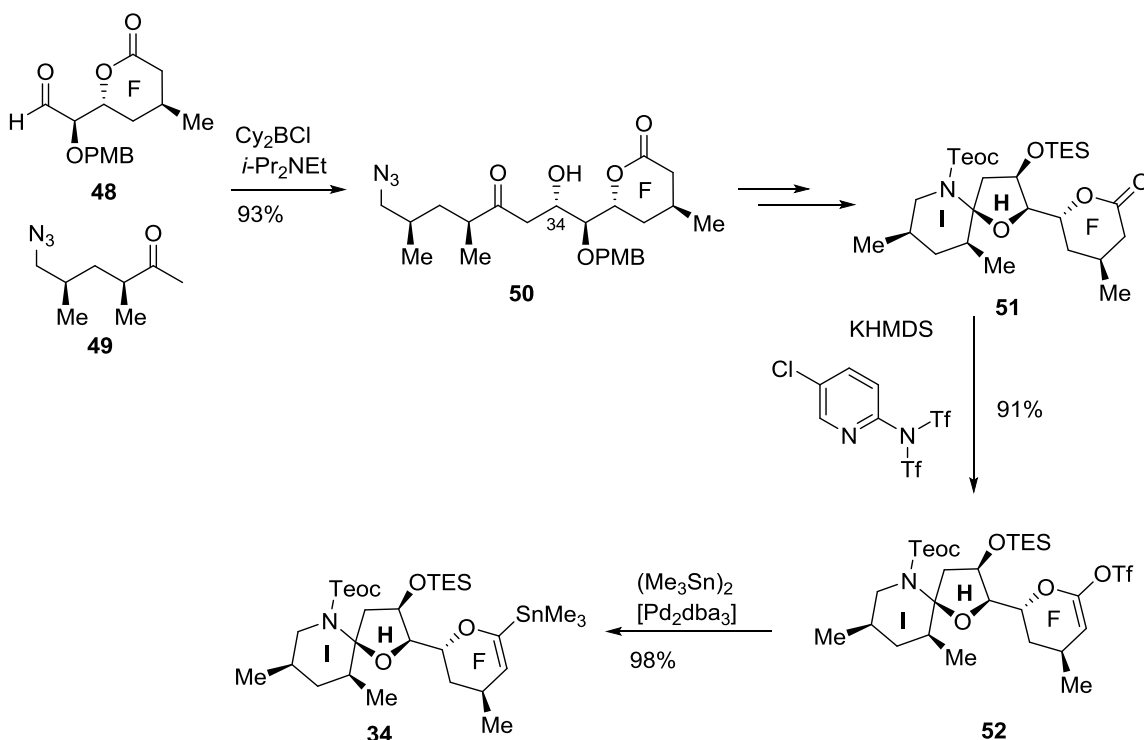
Construction of the ABCD domain started with phosphonate **35**, which was synthesized from L-malic acid (Scheme 8). Following the previously reported synthetic route,³⁶ intermediate **36** was prepared in 12 steps in good yields. To facilitate the cyclization to the ABCD domain, the C17-*O*-TBS group of **36** was converted into an *O*-TES by a deprotection and selective reprotection process, followed by cleavage of the terminal olefin to give aldehyde **37**. Lithiated dithiane coupling between C10-C20 domain **37** and C5-C9 domain **38** produced **39** as 1:1 mixture of diastereomers, which was then oxidized to a ketone with DMP. Exposure of the resultant ketone moiety to TMSOTf at low temperature (-90 °C) successfully triggered the deprotection-double spirocyclization process, which delivered the tetracyclic product **40** as a single stereoisomer. A following Swern oxidation converted the C5 primary alcohol to aldehyde **41**, followed by a Wittig olefination to furnish the desired terminal olefin **42**. Cross-metathesis of **42** with the side chain **43** was executed with the 2nd generation Grubbs catalyst, yielding the corresponding *E*-olefin **32** as the major product. Treatment of **32** with PhI(OCOCF₃)₂ removed the dithiane functionality, leading to the ketone **44**. The endocyclic C7-C8 double bond was then set up through a Mukaiyama method with 81% yield. The C9 ketone moiety was then reduced in three steps, involving conversion of the ketone into allylic ester **45** and the application of a palladium-catalyzed reductive protocol to furnish **46**. The C20 TBDPS protecting group was removed under TBAF conditions. The resulting primary alcohol was then oxidized into a carboxylic acid in two steps. After screening different leaving groups for the later dithiane coupling, the pentafluorophenyl ester **47** was chosen to be the C21-C40 coupling partner, which was

synthesized through DCC-catalyzed esterification between the resulting carboxylic acid and pentafluorophenol.



Scheme 8. Nicolaou's Synthesis of the ABCD Domain

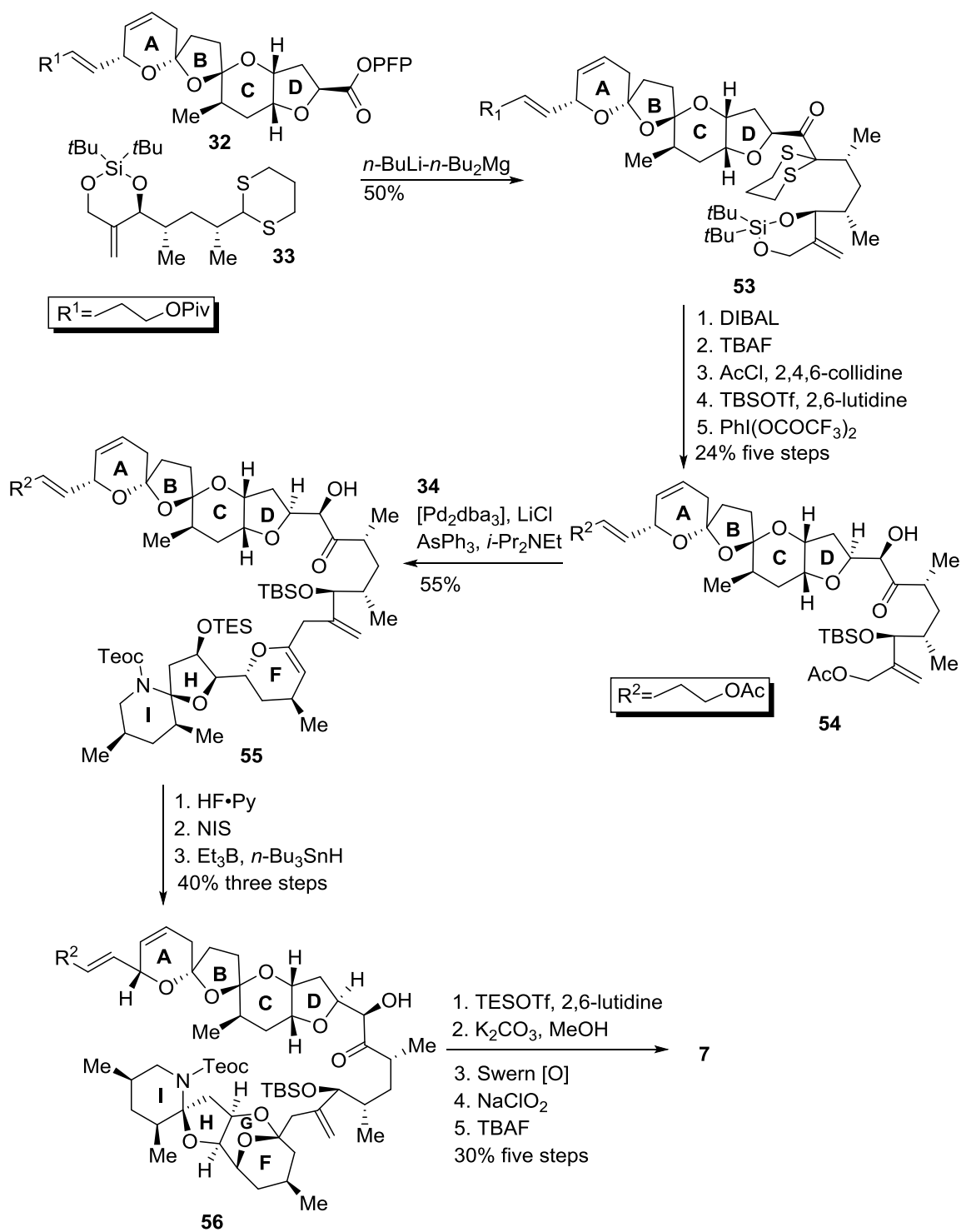
The preparation of the FGHI domain started with the same boron mediated aldol reaction between aldehyde **48** and ketone **49**. The FGHI framework was constructed through a previously reported synthetic route.³⁷ The ketone moiety was then functionalized into an enol triflate with the Comin's reagent. The enol triflate was then converted into vinyl stannane **34** under palladium conditions.



Scheme 9. Nicolaou's FGHI Domain Synthesis

Scheme 10 shows the final part of the Nicolaou's total synthesis. The dithiane-based coupling was applied to link the ABCD domain **32** and **33**. Initially, traditional bases ($t\text{-BuLi}$, $n\text{-BuLi}$) were applied to generate a carbon anion, which led to no product containing both domains in various solvents and different temperatures. Control

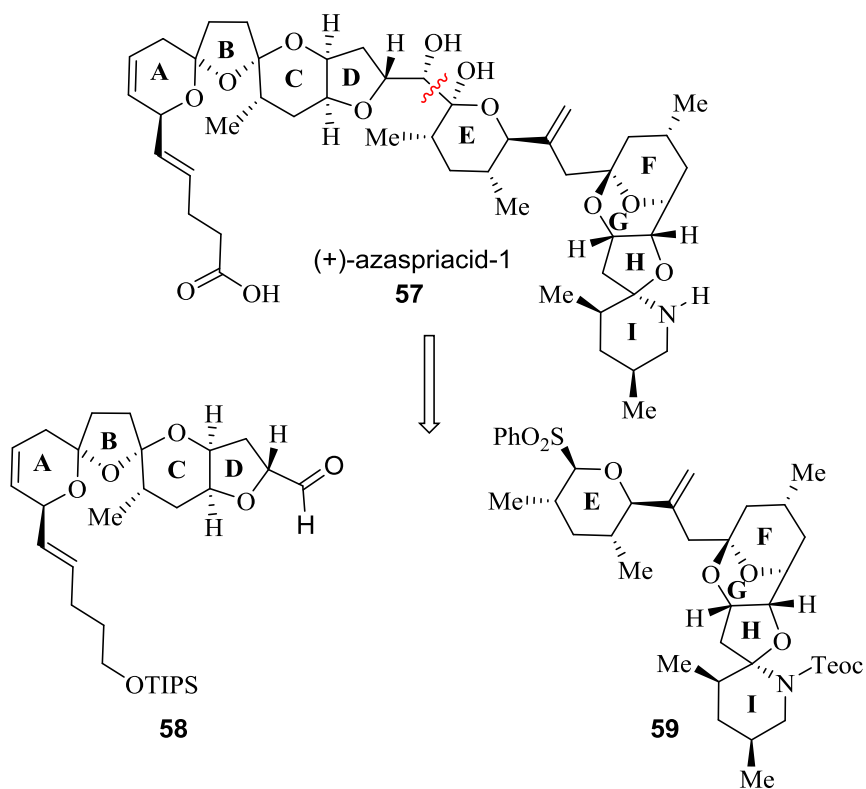
experiments revealed the reason that the derived anion could not be trapped with the ABCD aldehyde is due to a short lifetime of the anion itself. Then *n*-BuLi-*n*-Bu₂Mg was employed to provide a longer lived organometallic intermediate which delivered the desired product in 50% yield. The reduction of the C20 ketone functionality was then stereoselectively achieved under DIABL conditions, affording a diol intermediate formed by concomitant cleavage of the pivaloate ester at C1. A three-step protecting group manipulation produced **54**. The Stille reaction was then planned to couple ABCDE domain **54** and FGHI domain **34**. After screening conditions of catalysts and ligands, AsPh₃ was chosen to be an additional ligand which would result in the desired compromise between the reaction rate increment and stereochemical integrity preservation at C25. Under buffered condition of HF•Py, the TES group was then selectively removed, which was then followed by closure of the G ring promoted by NIS to produce the azaspiracid skeleton. The resulting iodide was then removed effectively. The C20 hydroxyl was then protected as TES ether. The C1 alcohol was revealed under basic conditions, and converted into a carboxylic acid in a two-step sequence. Finally, a global deprotection delivered the natural product. The Nicolaou group also completed the total synthesis of AZA2 and AZA3 with similar synthetic strategies.³⁸



Scheme 10. Nicolaou's Total Synthesis of Azaspiracid-1

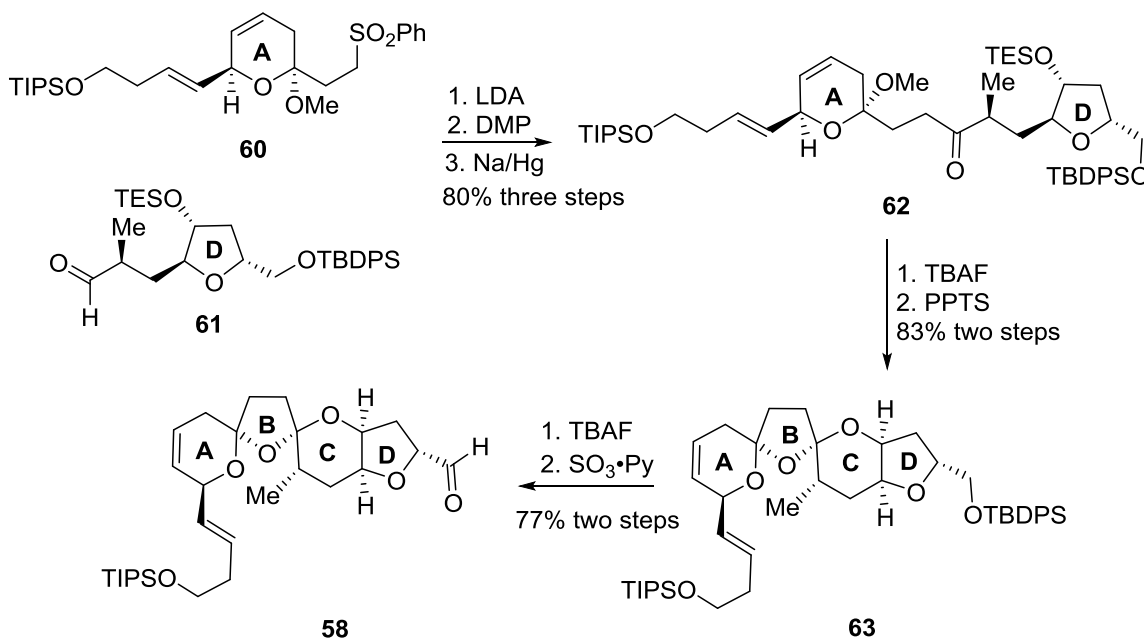
2.2.2 Evans' Total Synthesis of (+)-Azaspiacid-1

In 2007, the Evans group finished the total synthesis of unnatural (+)-azaspiacid-1 in 26 linear steps and 2.7% overall yield from the aldol reaction between the siloxyfuran and ethyl glyoxalate in the FG fragment synthesis.³⁹ As shown in Scheme 11, the disconnection was between C20 and C21 to provide precursors **58** and **59**. The addition of an anomeric sulfone derived from **59** to the ABCD domain **58** was planned to give the azaspiacid skeleton. In the synthetic plan, all of the nine rings are fully constructed prior to the coupling, which reduced the number of manipulations after the coupling step.



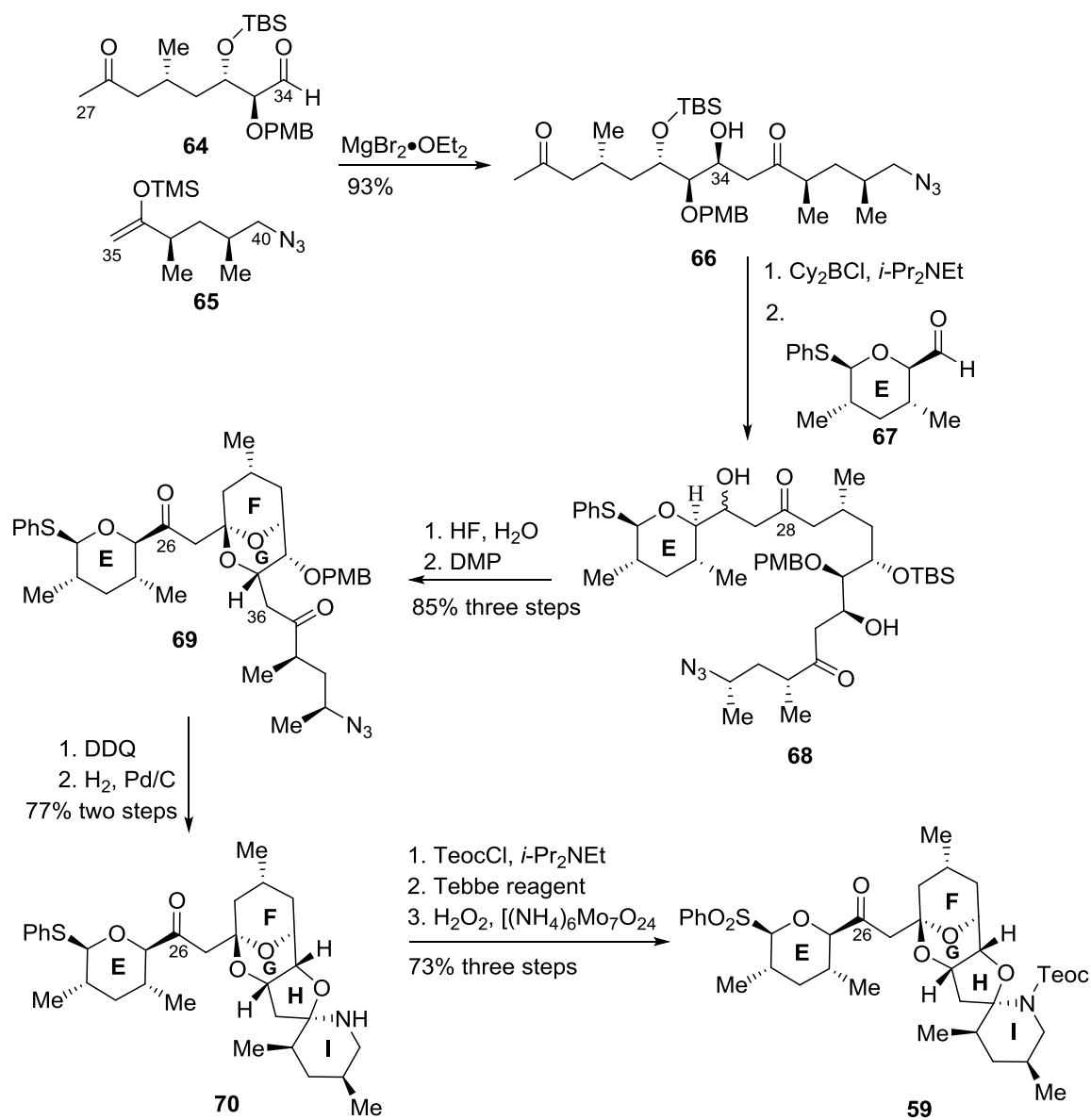
Scheme 11. Evans' Retrosynthetic Analysis

Scheme 12 shows the synthetic work on the ABCD domain. The A ring (pyran) and D ring (*trans*-furan) were set up before the sulfone coupling between **60** and **61**. The sulfone deprotonation with LDA and addition to aldehyde **61** provided a C1-C20 precursor as a mixture of four hydroxyl sulfone, which was oxidized to produce a ketosulfone intermediate. Exposure of resulting ketone to sodium amalgam removed the sulfone moiety, providing the ketone **62** as a single diastereomer. For the later spiroketal cyclization, the TES ether was then selectively removed with one equivalent of TBAF at low temperature (-20 °C). The ABCD domain skeleton was then constructed under acidic conditions (PPTS, CH₂Cl₂). The chemoselective cleavage of the TBDPS ether and subsequent Parikh-Doering oxidation afforded the aldehyde **58**.



Scheme 12. Evans' ABCD Domain Synthesis

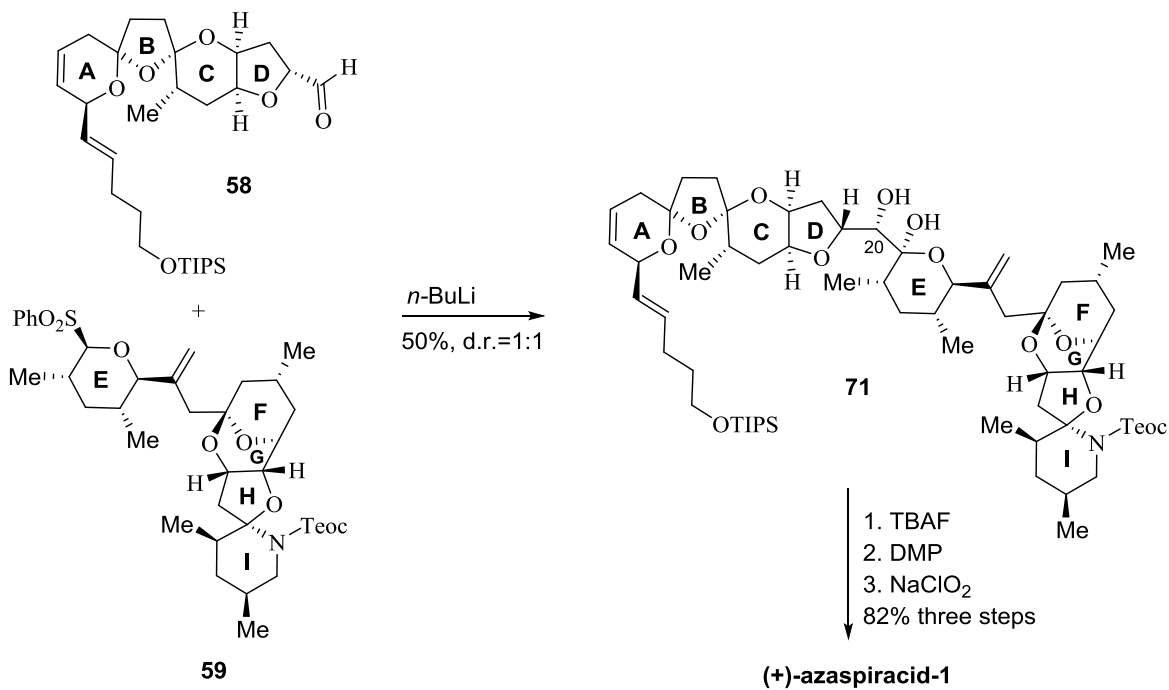
Scheme 13 shows the EFGHI synthetic work. A chelation-controlled Mukaiyama aldol reaction between aldehyde **64** and silyl enol ether **65** was planned to produce a C27-C40 linear precursor **66**. After screening reaction conditions, the freshly prepared $\text{MgBr}_2 \cdot \text{OEt}_2$ was found to be superior to other Lewis acids such as TiCl_4 , SnCl_4 , MgI_2 , MgBr_2 and commercial $\text{MgBr}_2 \cdot \text{OEt}_2$. The E ring domain **67** was then incorporated into **66** through a boron mediated aldol coupling to deliver **68** in quantitative yield. Upon exposure of **68** to aqueous HF, the TBS group was removed and the resulting triol cyclized to form the FG bridged ketal spontaneously. The C26 secondary alcohol was then converted to ketone **69** under DMP conditions. The PMB moiety in **69** was oxidatively removed and the azide functionality was then reduced using palladium, which also induced the thermodynamically favored spiroaminal formation to afford **70**. The spiroaminal nitrogen was protected as Teoc carbamate. To avoid C36 epimerization, a buffered Tebbe reagent was applied to convert C26 ketone to an olefin. The sulfide was then oxidized to sulfone **59** as the coupling partner of **58**. The synthesis of the EFGHI domain was achieved in 22 linear steps and 10% overall yield.



Scheme 13. Evans' EFGHI Domain Synthesis

After extensive study, the sulfone anion derived from **59** generated from *n*-BuLi, was added to aldehyde **58**. The reaction was quenched by pH = 5 aqueous buffer at $-78\text{ }^\circ\text{C}$ (Scheme 14). The products were separable C20 epimers (1:1) a 50% combined yield. The

undersired C20 isomer could be converted into the desired isomer **71** in an oxidation/reduction sequence. The two silyl protecting groups were then removed with buffered TBAF. A two-step oxidation of resultant C1-C40 alcohol delivered the unnatural azaspiracid-1.

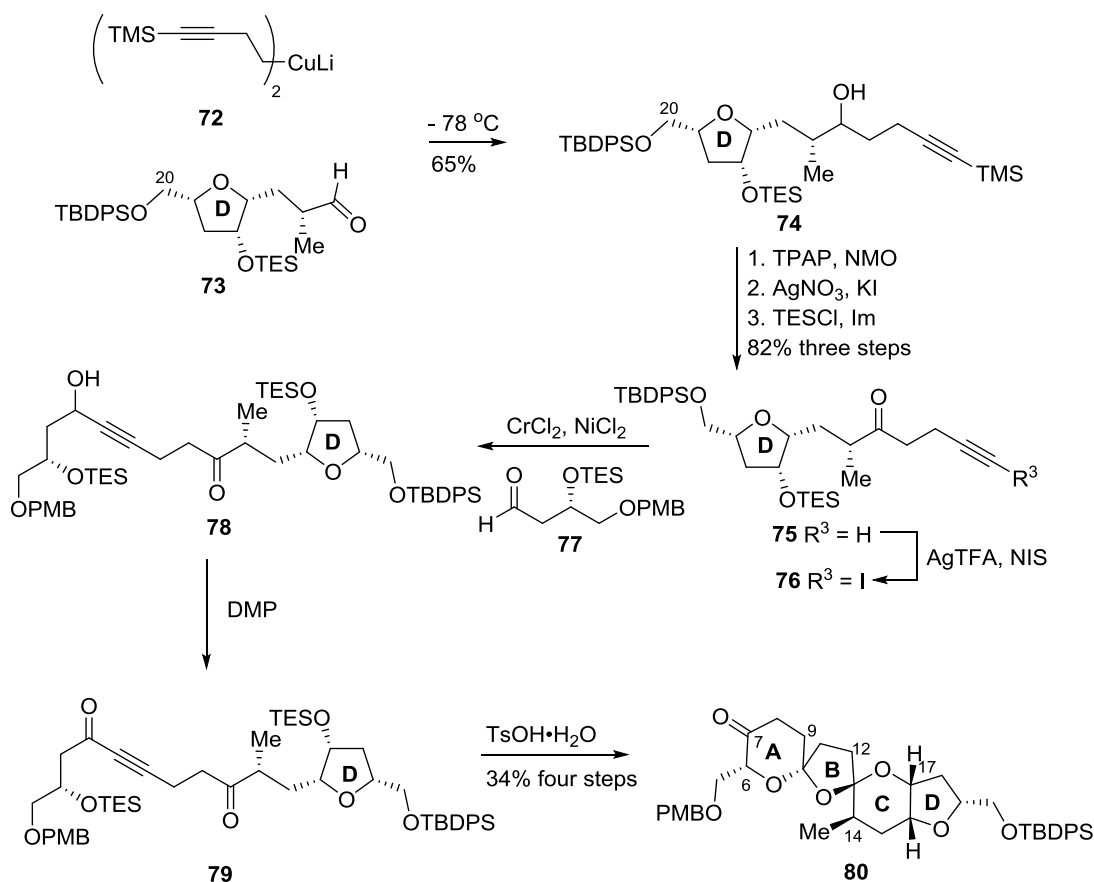


Scheme 14. Evans' Total Synthesis of (+)-Azaspiracid-1

2.2.3 Forsyth's Approach

In 2004, the Forsyth group reported the independent analysis of the relative stereochemistry of the A-D ring system through extensive NMR study and developed a revised structure model.⁴⁰ As shown in Scheme 15, the model was then confirmed through synthesis. For convenience, the C19 epimer **73** was used for the later synthesis.

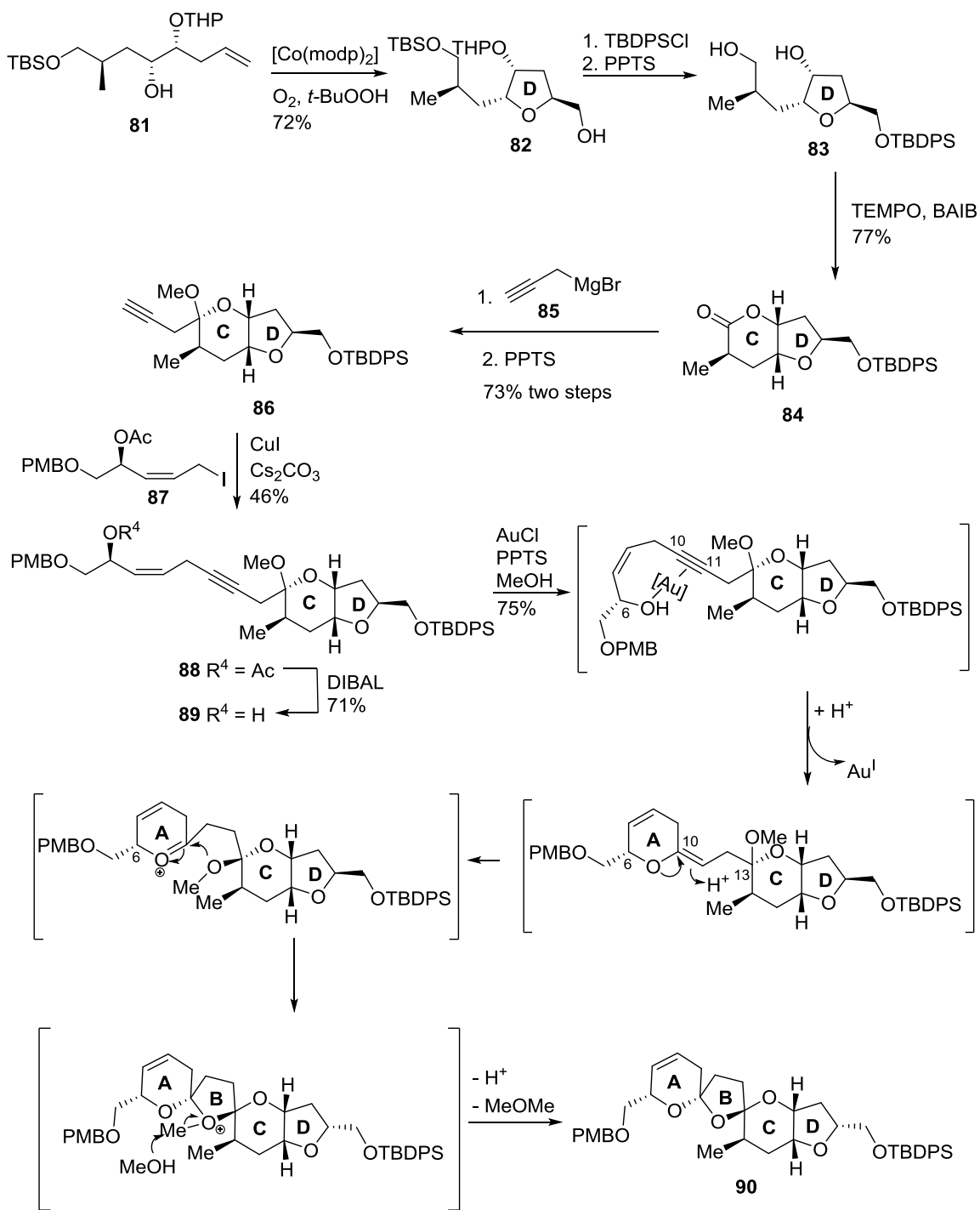
Addition of Gilman reagent **72** to aldehyde **73** provided secondary alcohol **74**, which was then oxidized to a ketone intermediate. Removal of the TMS group with AgNO₃/KI resulted in partial cleavage of the TES ether, which was then re-protected to give **75**. Iodination of the free alkyne was achieved with AgTFA/NIS at low temperature (0 °C). An organochromium-mediated coupling between alkynyl iodide **76** and aldehyde **77** efficiently delivered propargylic alcohols **78**, which were then oxidized to ynone **79** as the precursor of the DIHMA process. Exposure of **79** to TsOH·H₂O promoted selective cleavage of the C6 and C17 silyl ethers and subsequent trioxadispiroketal formation. The structure of the thermodynamic product **80** was then established on the basis of MS and extensive NMR studies. More importantly, the NMR analysis showed the correlation of the synthetic compound **80** with the corresponding fragment of natural product, which validated the model proposed by the authors.



Scheme 15. Forsyth's Synthesis of Trioxadispiroketal **80**

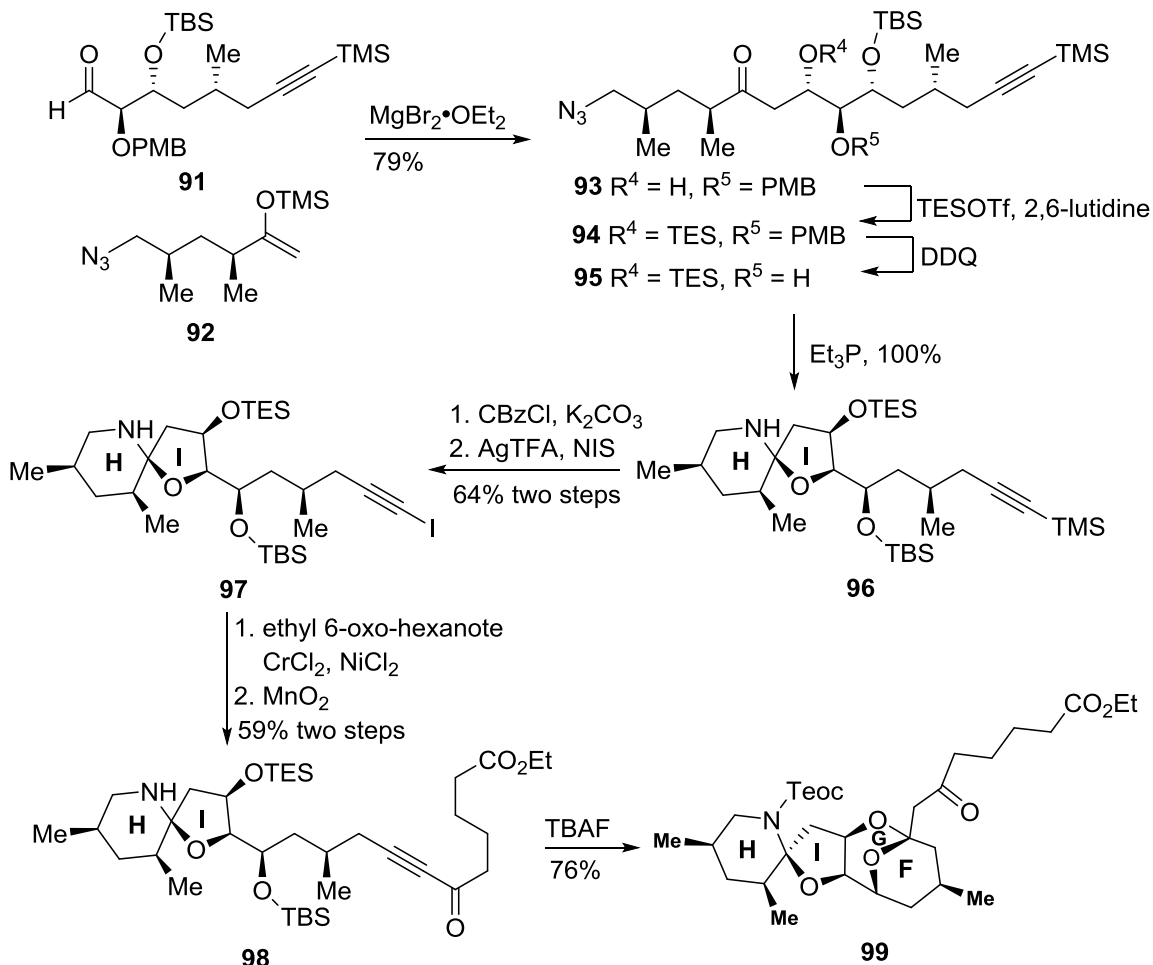
In 2007, the Forsyth group reported another novel synthesis of the C5-C20 domain of azaspiracid-1, which featured a gold(I)-catalyzed bis-spiroketalization.⁴¹ As shown in Scheme 16, the construction of the trisubstituted 2,5-*trans* tetrahydrofuran ring (D ring) was achieved through a cobalt-catalyzed oxyetherification methodology. A two-step protecting group manipulation converted **82** to **83**, which was then oxidized to lactone **84** using TEMPO/BAIB. Lactone **84** was then treated with a Grignard reagent followed by PPTS/MeOH to deliver alkynyl ketal **86** as a CD ring precursor. A copper-mediated coupling between A ring precursor **87** and **86** was applied to give enyne **88** with

moderate yield. The acetate was reductively removed to afford the allylic alcohol **89**. After screening various metal salts, it was found that enyne **89** was cleanly converted into desired trioxadispiroketal **90** in excellent yield under gold (I) conditions. The authors also proposed the plausible mechanism for this efficient transformation. A *syn* addition of the C6 free hydroxyl to gold(I) activated C10-C11 alkyne initiated the whole process to form the pyran ring. The following protiodeauration liberated the catalyst and protonated the resulting enol ether. The C13 methoxy oxygen then nucleophilically attacked C10 to furnish the B ring. Transfer of the methyl group would quench the resulting oxocarbenium species and delivered the final product. The highlighted gold chemistry was one of the earliest applications in complex molecule synthesis.



Scheme 16. Forsyth's Gold-Catalyzed ABCD Domain Synthesis

The Forsyth group also reported synthetic work on the FGHI domain of azaspiracids, which were used as synthetic haptens for biological studies.⁴² A chelate-controlled Mukaiyama aldol reaction coupled the FG aldehyde **91** and HI ketone **92**, delivering FGHI linear precursor **93** (Scheme 17). A two-step protecting group manipulation converted **93** to **95**, involving C34 silyl protection and C33 oxidative PMB cleavage. The resultant azido-keto-alcohol **95** was transformed to spiroaminal **96** through a one-pot Staudinger reduction/intramolecular aza-Wittig reaction. The spiroaminal amine was then protected as a carbamate and the TMS-alkyne was then converted into iodo alkyne **97**. An NHK reaction was applied to couple **97** and ethyl 6-oxo-hexanoate. The resultant α,ω -propargylic alcohols were then oxidized into ynones **98** under MnO_2 conditions. The bridged ketal **99** was constructed by exposure of **98** to TBAF.

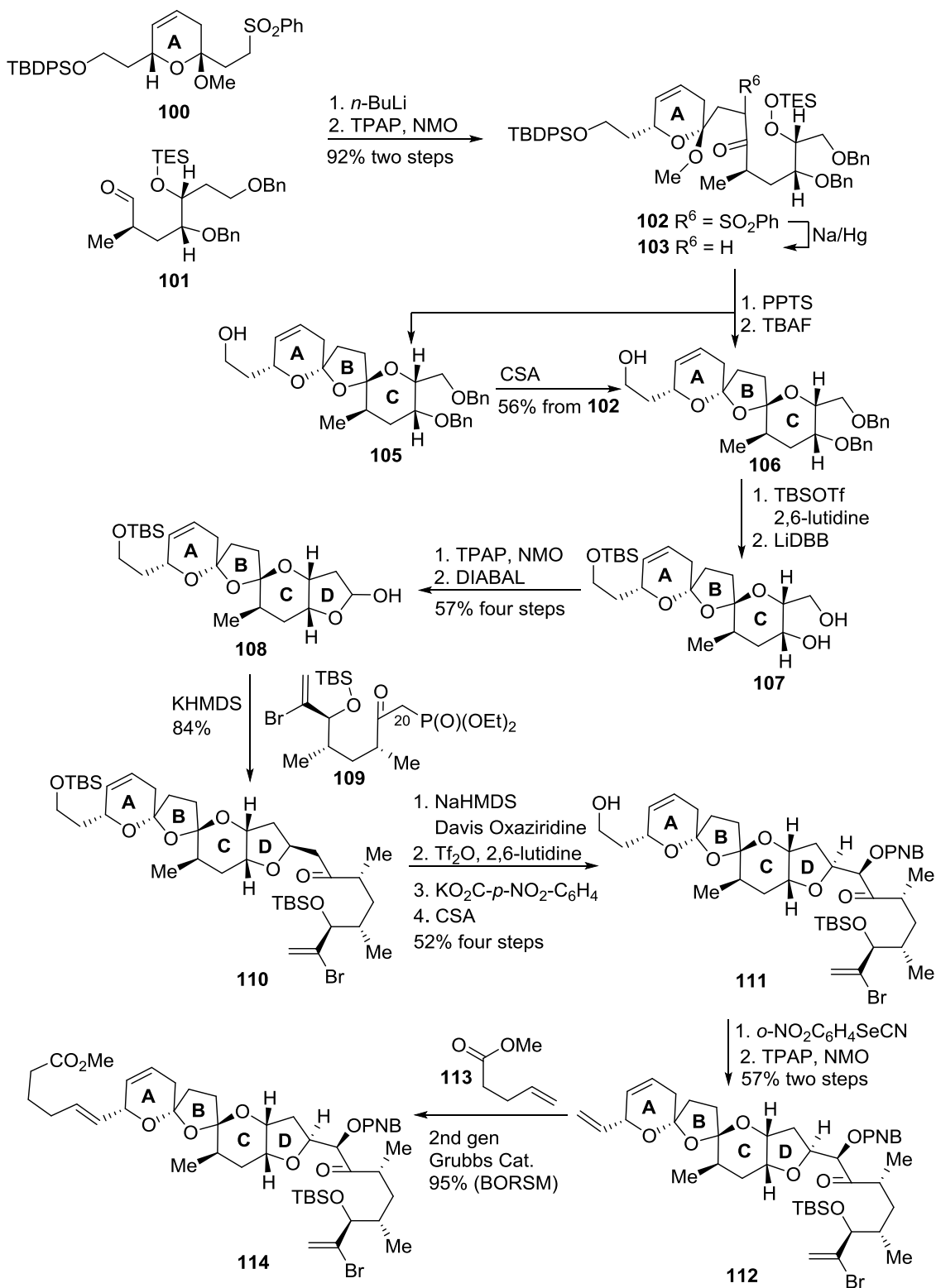


Scheme 17. Forsyth's FGHI Synthesis

2.3 Carter's approach

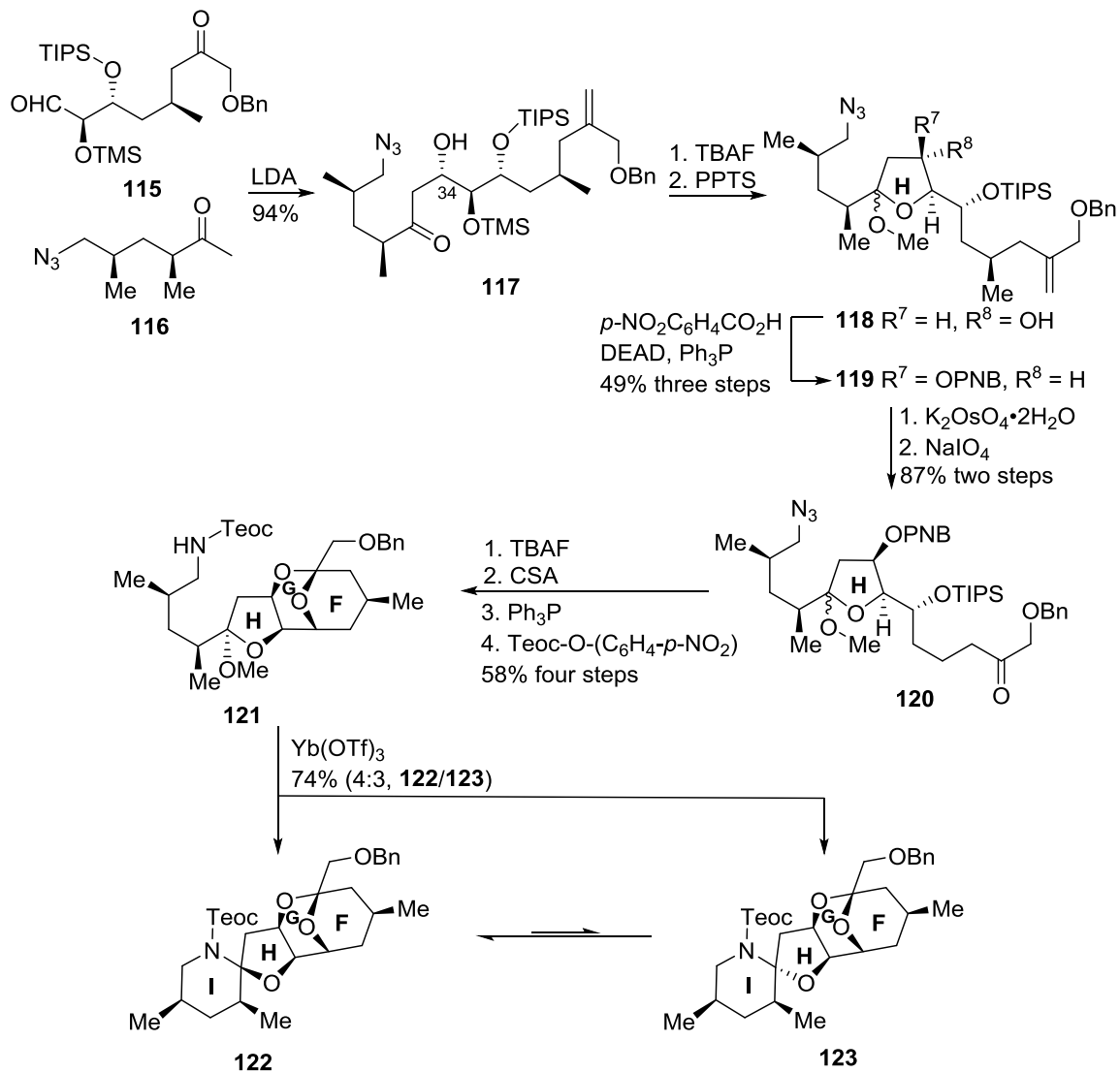
In 2006, the Carter group reported their initial synthetic study on the ABCDE domain.⁴³ A sulfone derived anion from **100** under the influence of *n*-BuLi and 2,2,6,6-tetramethylpiperidine nucleophilically attacked aldehyde **101**, yielding the C4-C19 domain of AZA1 (Scheme 18). The resultant secondary hydroxyl was then oxidized to a ketone. Exposure of ketone **103** to PPTS in THF/H₂O cleaved the *O*-TES ether and initiated the spiroketalization process. Unfortunately, both of the thermodynamic and

kinetic dispiroketal were obtained. It was found that a free C4 hydroxyl would facilitate a clean conversion of the undesired kinetic product *cis*-dispiroketal **105** into the desired *trans*-dispiroketal **106** under CSA conditions. The C4 hydroxyl was then reprotected as TBS ether, and debenzylation with LiDBB provided diol **107**. An oxidation/reduction sequence was then applied to produce lactol **108** as the ABCD domain of AZA1. A Wadsworth-Emmons coupling between **108** and E ring precursor **109** with in situ, intramolecular hetero-Michael addition yielded **110** with the correct stereochemistry at C19 of the D ring. The C20 secondary hydroxyl was set up through treatment with NaHMDS and a large excess of Davis oxaziridine, which gave the undesired isomer based on Mosher ester analysis. A two-step sequence successfully inverted the C19 stereocenter, while a direct one-step Mitsunobu reaction proved to be problematic. The C4 *O*-TBS ether was cleaved with CSA to provide **111**, which was prepared to set up the C1-C4 side chain of the ABCD domain. Selenation and oxidation/elimination with unusual TPAP/NMO conditions yielded the reactive bisallylic pyran **112**. Finally, selective olefin metathesis using the 2nd generation of Grubbs catalyst with **113** delivered C1-C26 domain of AZA1.



Scheme 18. Carter's C1-C26 Domain Synthesis

In the same year, the Carter group also reported a synthetic route to the FGHI domain.⁴⁴ Similar to Forsyth's 1st generation FGHI synthesis,³⁵ Felkin aldol reaction was applied to couple FG precursor **115** and HI precursor **116**. The H ring methoxy ketal was formed in a two-step sequence, involving C32-*O* desilylation and acid-catalyzed ketalization. The undesired C34 stereocenter was inverted under Mitsunobu conditions. The C28 alkene was cleaved upon treatment with K₂OsO₄·2H₂O, followed by NaIO₄. Exposure of **120** to TBAF resulted in removal of the C32 TIPS ether as well as the C34 *p*-nitrobenzoate. After screening a variety of solvents, the CSA/MeOH was found to be optimal for the construction of FG bridged ketal. Azide reduction and Teoc protection provided **121**. The I ring was finally closed under the influence of Yb(OTf)₃, which gave both the thermodynamic product **122** and kinetic product **123** in a 4:3 ratio. The minor product **123** was recycled by resubmission to the identical conditions to generate **122** and **123** with the same 4:3 ratio.



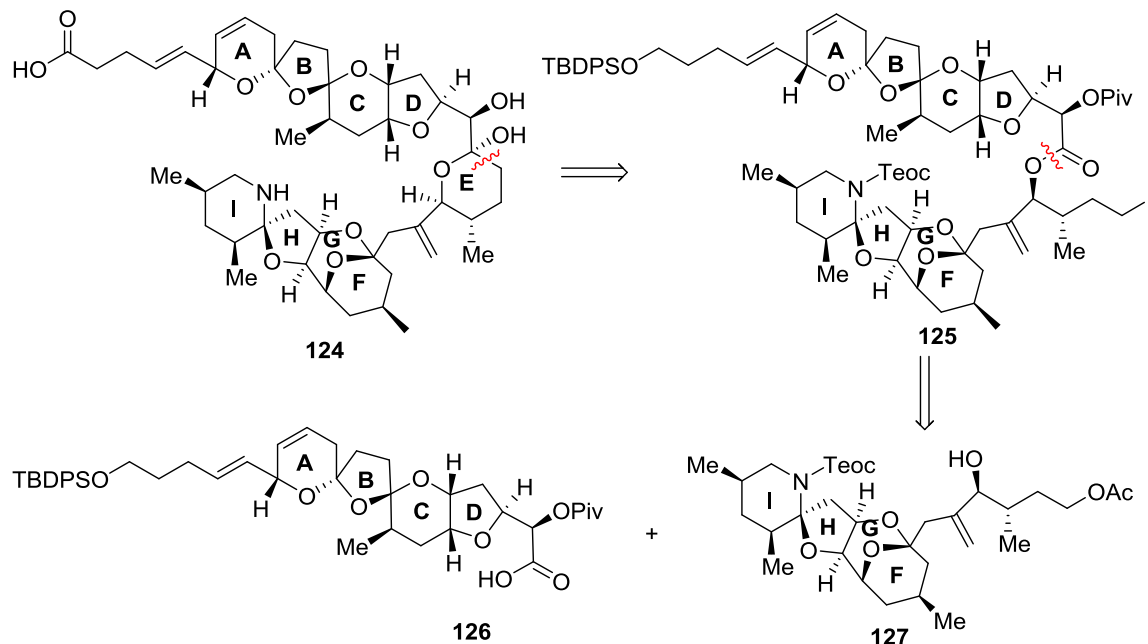
Scheme 19. Carter's FGHI Domain Synthesis

Chapter 3: Research Progress and Discussion

In our group, we had previously synthesized both the ABCD and EFGHI domains. The current research mainly focuses on how to complete the total synthesis of natural products, exploring a reliable and efficient coupling strategy between corresponding ABCD and EFGHI domains. With this purpose, the author's contributions to this research project are mainly in three parts: (1) A-I fragment synthesis in the Yamaguchi esterification route; (2) efforts on the optimization of the FGHI synthetic route highlighting gold-catalyzed spiroaminal and bridged ketal formation; (3) a new generation of the EFGHI domain for a Nozaki-Hiyama-Kishi (NHK) coupling route.

3.1 Yamaguchi Esterification Route

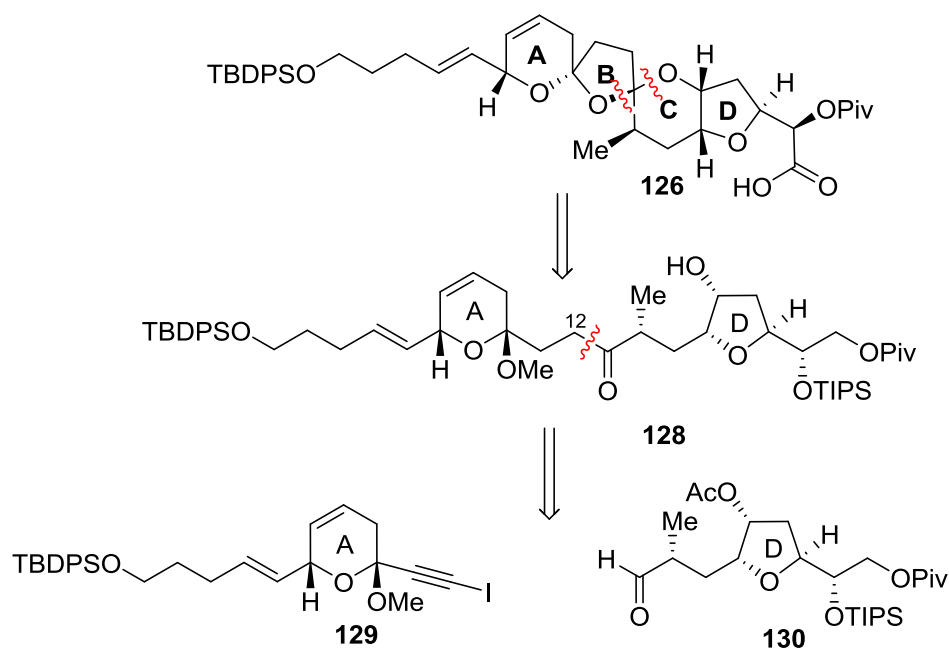
As show in Scheme 20, our current synthetic target is azaspiracid-3 (AZA3). The strategic disconnection is at the C21-C22 linkage to yield intermediate **125** (Scheme 20). An intramolecular Babier-type reaction⁴⁵ was planned to form the hemi-ketal moiety. To avoid potential C26 alkene migration, a lithium-halogen exchange was preferred using the samarium conditions. Disconnection at the ester bond divided the molecule into two parts: the C1-C21 domain **126** and C22-C40 domain **127**.⁴⁶



Scheme 20. Retrosynthetic Analysis

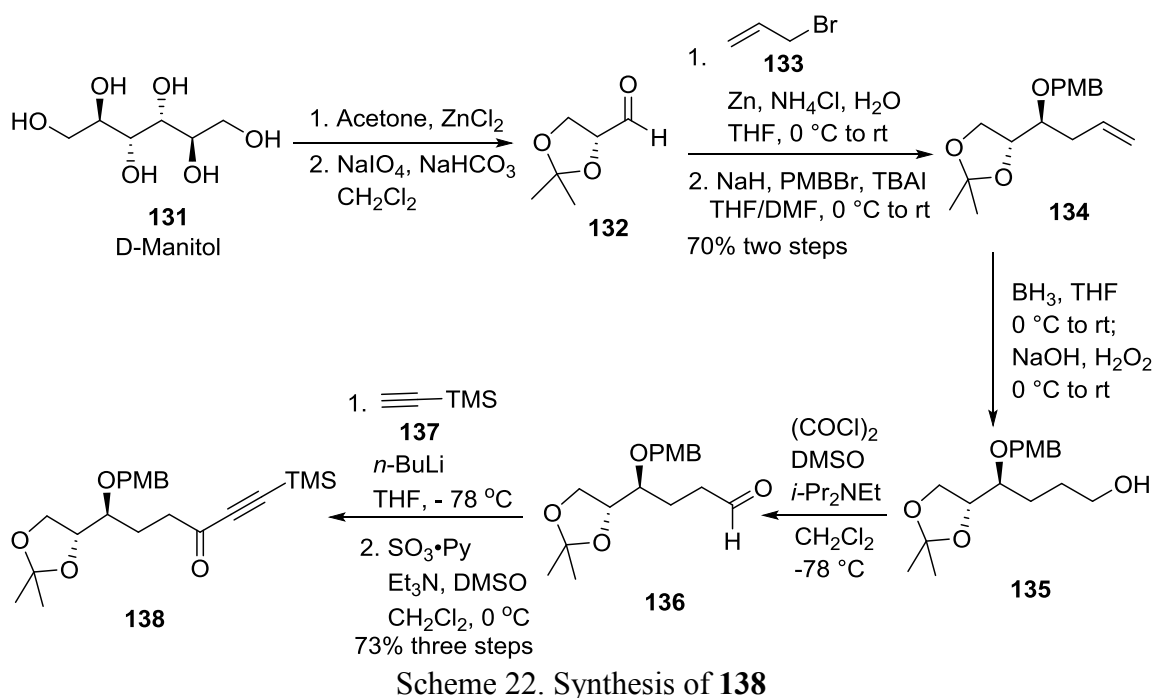
3.1.1 ABCD Domain Synthesis

Compared with previous C1-C20 domain syntheses, the current ABCD target contains one more carbon, that represents C1-C21 part of azaspiracid-3. So our synthetic plan was also revised, especially on the CD ring fragment synthesis. With this in mind, the construction of the trioxadispiroketal, as shown in Scheme 21, relied on an acid-catalyzed spiroketalization of hydroxy ketone **128**. Disconnection of C12-C13 linkage gave a chance to utilize a reliable and efficient NHK coupling reaction⁴⁷ between C1-C12 iodide **129** and C13-C21 aldehyde **130**. It is worth to mention that the C1-C5 side chain was set up prior to the NHK coupling reaction. The trisubstituted *trans*-tetrahydrofuran ring was functionalized through a Kishi protocol.⁴⁸

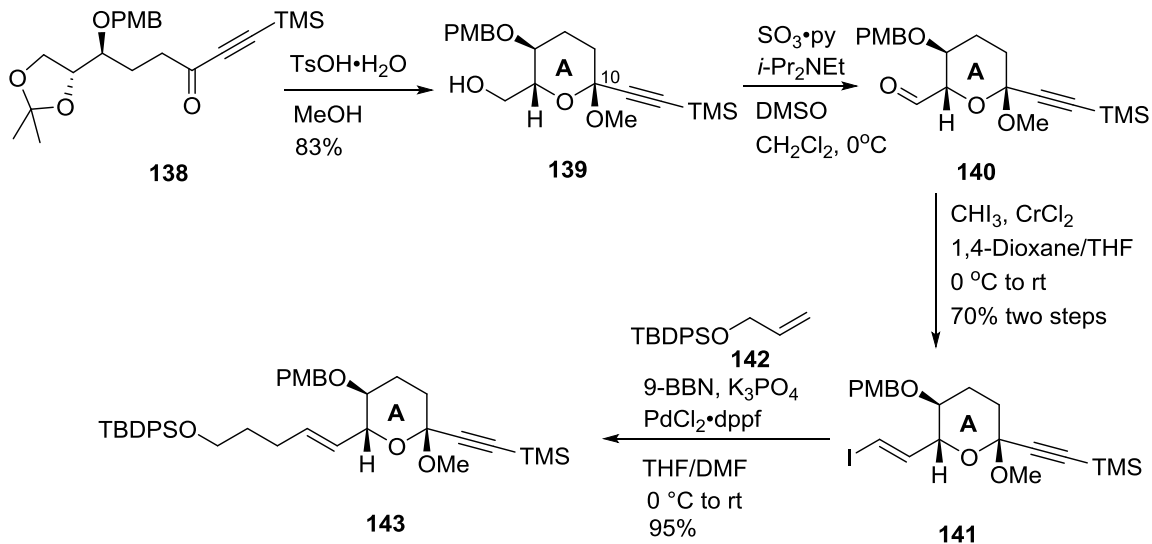


Scheme 21. Retrosynthetic Analysis of the ABCD Domain

Starting from D-mannitol, glyceraldehyde **132** was synthesized in two steps (Scheme 22). A mild Reformatsky reaction was preferred over the Grignard reaction, providing exclusive *S*-homo allylic alcohol, which was then protected as PMB ether **134**. The following hydroboration and oxidation process transformed the terminal olefin into primary alcohol **135**. A Swern oxidation⁴⁹ was applied to produce aldehyde **136**. Addition of TMS acetylide to aldehyde **136** delivered a mixture of propargylic alcohols, which was then oxidized into ketone **138** under the Parikh-Doering conditions.⁵⁰

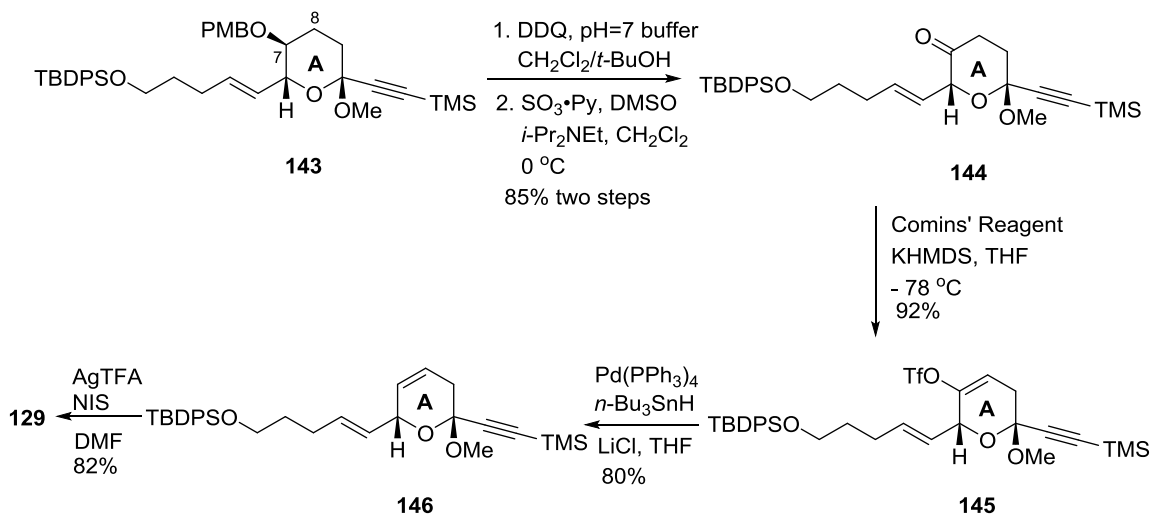


Once having ynone **138**, a short sequence was allowed to construct the A ring skeleton (Scheme 23). Exposure of ynone **138** to TsOH•H₂O/MeOH triggered the removal of the acetonide moiety and cyclization to form ketal **139** as a major product. The anomeric unfavored C10-*S* ketal was separable from **139** through flash chromatography and could be transformed to the thermodynamic product **139** on resubmission to the same acid conditions. The C5 primary alcohol was then oxidized to aldehyde **140**. Because of the instability of the α -H, the resultant aldehyde was quickly converted into vinyl iodide **141** under Takai olefination conditions.⁵¹ A co-solvent of 1,4-dioxane and THF was used to increase the E/Z ratio up to above 15:1. A sp³-sp² Suzuki coupling⁵² was then applied to install the C1-C4 side chain, efficiently delivering C1-C12 domain of azaspiracid-3.



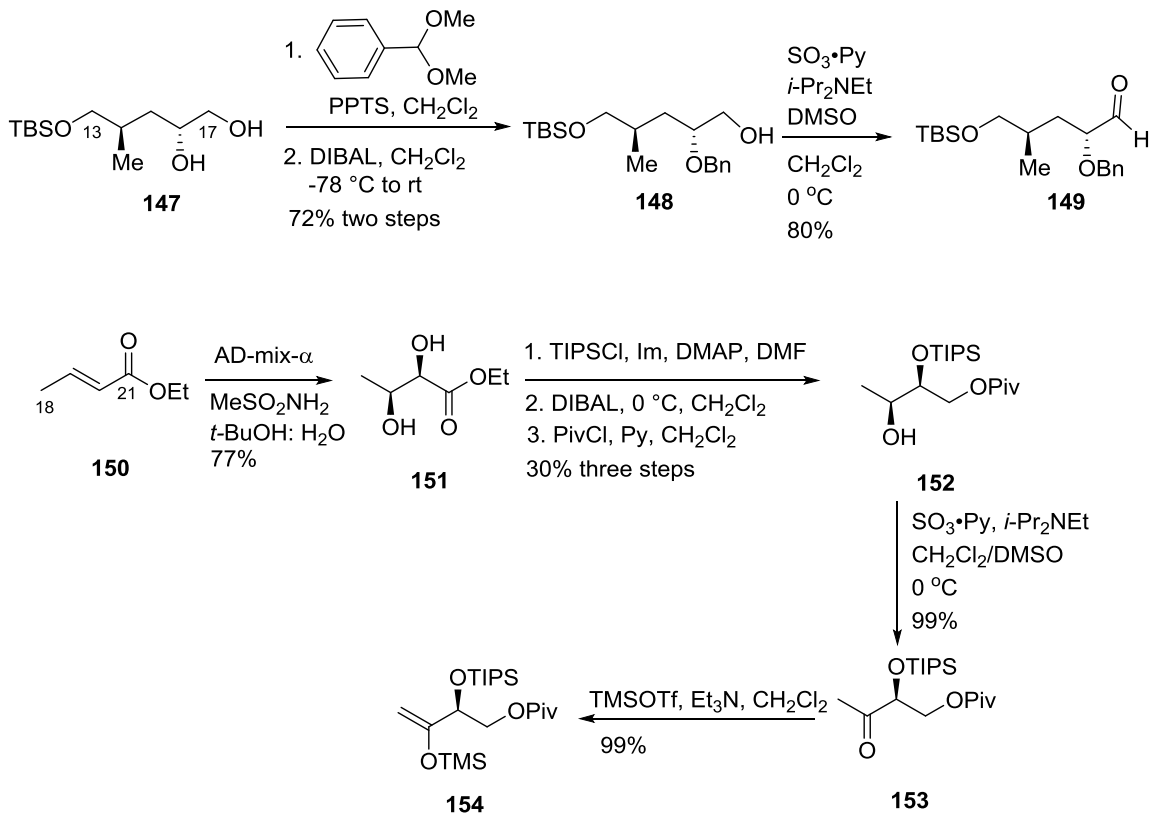
Scheme 23. Synthesis of **143**

As shown in Scheme 24, the installation of the C7-C8 double bond was then addressed. Oxidative removal of the C7-O-PMB group resulted in the corresponding secondary alcohol, which was then oxidized into a ketone. Under the influence of kinetic conditions, the ketone moiety **144** was then functionalized into vinyl triflate **145** with Comins' reagent.⁵³ It is worth mentioning that no epimerization was found at the C6-bis allylic position during the oxidation and the vinyl triflate formation process. A Stille reduction⁵⁴ with LiCl additive was then applied to fully set up the endocyclic double bond with excellent yield. The TMS-alkyne was then converted into iodide **129** under AgTFA/NIS conditions.



Scheme 24. Synthesis of the Iodide **129**

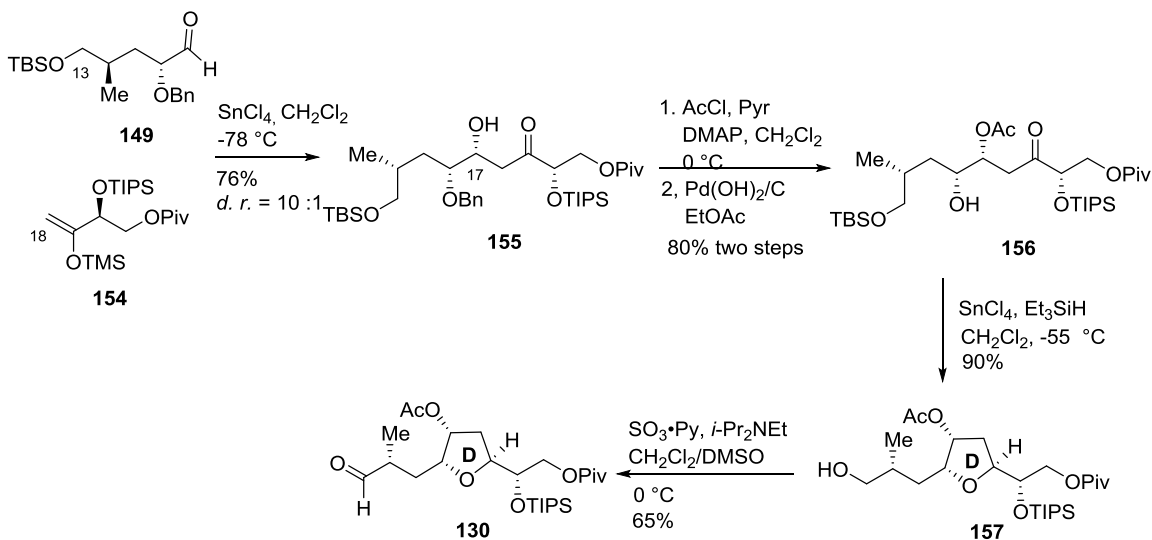
Scheme 25 summarized the synthesis of CD ring precursor aldehyde **149** and silyl enol ether **154**. The synthesis of the C13-C17 segment started with the known compound **147**.⁵⁵ The alcohol functionality in **147** was first protected as a benzylidene acetal, which was then kinetically opened to afford primary alcohol **148**. The resultant alcohol was oxidized to aldehyde **149**. The C18-C21 segment synthesis started with the commercially available ester **150**. The Sharpless asymmetric dihydroxylation (SAD)⁵⁶ of ethyl crotonate **150** produced diol **151** with excellent yield. Due to being slightly more accessible than the β -hydroxyl, the α -hydroxyl in **151** was selectively protected as its triisopropylsilyl ether. The ethyl ester was reduced by DIBAL to afford a diol which was then selectively protected as a pivaloate ester. The C19 secondary alcohol was oxidized to ketone **153**, which was then converted into silyl enol ether **154** under $\text{Et}_3\text{N/TMSOTf}$ conditions.



Scheme 25. Synthesis of the Aldehyde **149** and the Silyl Enol Ether **154**

Once we had aldehyde **149** and silyl enol ether **154** in hand, we started to address the combination of the two segments into our planned CD fragment **130** (Scheme 26). A chelate controlled Mukaiyama aldol reaction⁵⁷ was applied to couple **149** and **154**. After screening a variety of Lewis acids and chelation groups on the α -position of the carbonyl,⁵⁸ it was found that the combination of SnCl₄ and *O*-Bn provided the best result with 76% yield and 10:1 diastereoselectivity. A two-step protecting group manipulation converted the resultant α -hydroxy ketone **155** into β -hydroxy ketone **156**. Upon purification, **156** was obtained as an equilibrium mixture of hydroxyl ketone and hemiketal. A Kishi reduction was then planned to deliver the trisubstituted *trans*-

tetrahydrofuran.⁴⁸ The typical conditions ($\text{BF}_3 \cdot \text{OEt}_2 / \text{Et}_3\text{SiH}$, at $-78\text{ }^\circ\text{C}$) could afford the desired product and the C13 *O*-TBS was concomitantly cleaved. But a significant amount of side products were also detected. Different Lewis acids were screened, providing SnCl_4 as the best choice for the Kishi reduction. The *trans*-selectivity of Kishi reduction could be explained in terms of stereoelectronic effect (Figure 10). Mechanistically, the initially formed oxocarbenium ion would adopt a half envelop conformation, in which the large alkyl side chain is in a pseudo equatorial position. Based on Woerpel's research,⁵⁹ the hydride would have the "inside attack" to yield the *trans* product with lowest energy conformation. The C13 primary alcohol was oxidized to aldehyde **130** as the NHK coupling partner.



Scheme 26. CD Fragment Synthesis

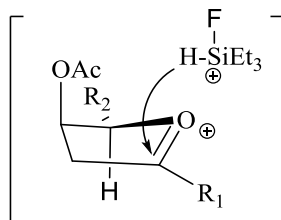
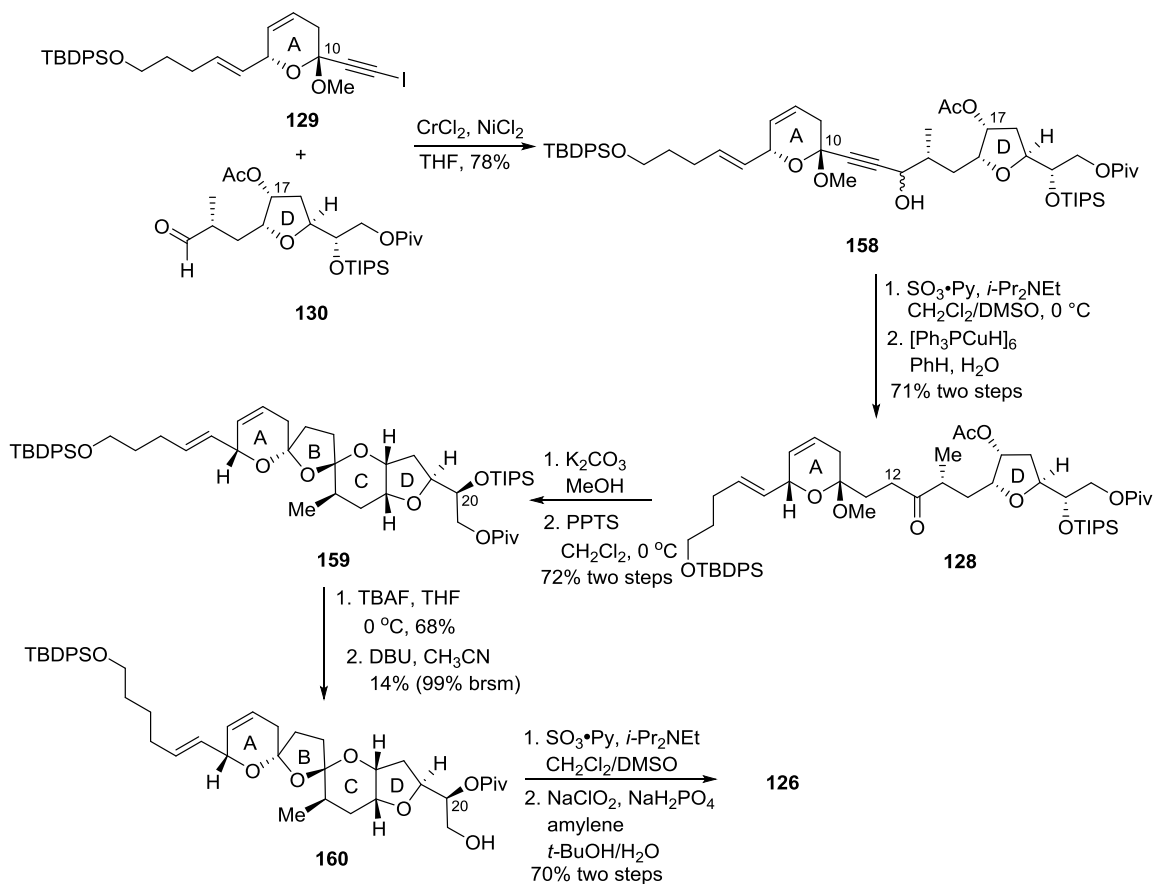


Figure 10. Explanation of the Stereoselectivity

The advanced stage of the ABCD domain synthesis is illustrated in Scheme 27. The NHK reaction was applied to couple the iodide **129** and the aldehyde **130**. The resultant mixture of propargylic alcohols **158** was oxidized into an ynone, which was then reduced to ketone **128** with the Stryker's reagent in degassed solvent.⁶⁰ The C17 *O*-acetate was removed under basic conditions. Exposure of the hydroxy ketone to acid conditions (PPTS, CH₂Cl₂, 0 °C) triggered the formation of the dispiroketal. The C10 and C13 contrathermodynamic dispiroketal were not observed in the cyclization process. To this point, the protected C1-C21 domain of AZA3 was achieved convergently and efficiently. Then protecting group manipulations were investigated for the later Yamaguchi esterification.⁵⁸ A C20 protected alcohol and C21 carboxylic acid was needed. Different α -*O*-protecting groups (PMB, TIPS, etc) were tested, while the electron withdrawing pivaloate (Piv) group at C20 gave the best result for the subsequent esterification coupling process. Selective desilylation was achieved with TBAF at low temperature. A migration process was needed for the installation of C20 pivaloate. After screening a variety of basic conditions,⁵⁸ the combination of DBU/MeCN afforded the optimal result. The yield for pivaloate migration from C21-*O* to C20-*O* could be up to 80% after several recycle process. The resultant primary alcohol **160** was then converted into carboxylic

acid **126** through a two-step sequence: Parikh-Doering oxidation⁵⁰ and Krause-Pinnick oxidation.⁶¹

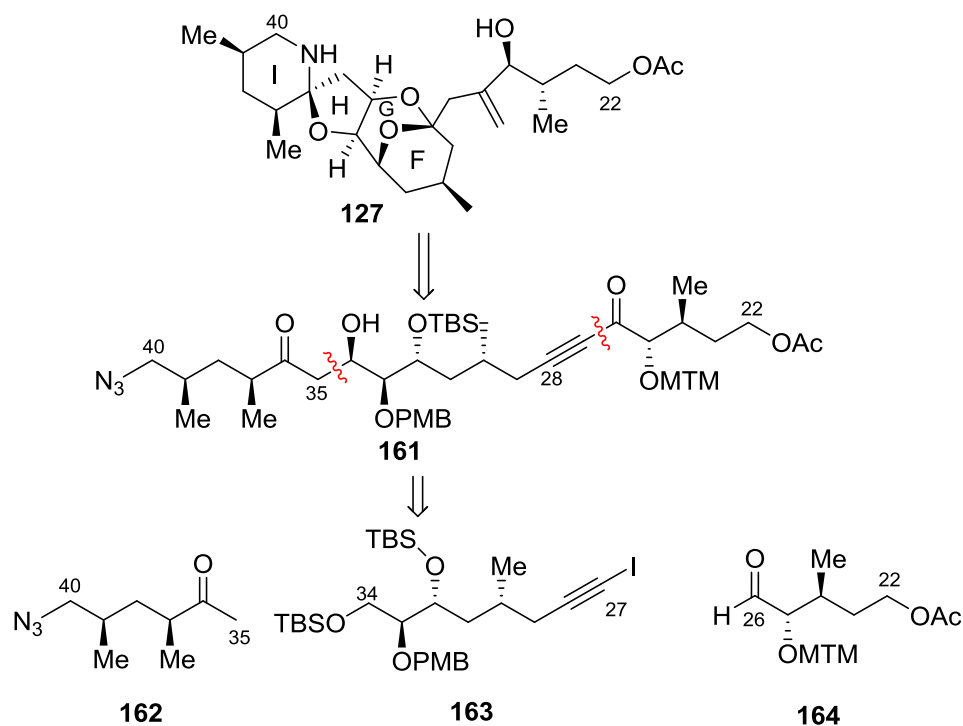


Scheme 27. Synthesis of the C1-C21 Carboxylic Acid **126**

3.1.2 EFGHI Domain Synthesis

The synthetic plan is outlined in Scheme 28. The fully functionalized architecture **127** was planned to be assembled from the linear C22-C40 linear precursor **161**. Disconnection at C26-C27 and C34-C35 linkage gave the E fragment **164**, FG fragment

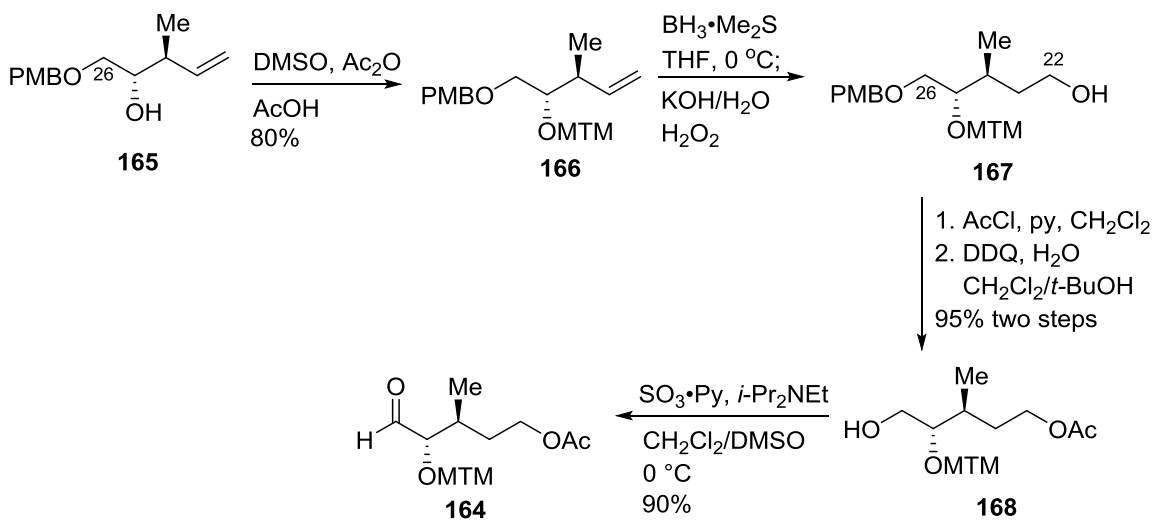
163, and HI fragment **162**. Compared with previous EFGHI domain syntheses,⁶² one less carbon (C21) was cut from the EFGHI domain and incorporated into ABCD carboxylic acid **126**. A newly designed synthesis of **164** was needed, while FG fragment **163** and HI fragment **162** could be prepared from the previously developed synthetic route.⁶² A reliable and efficient NHK reaction was planned to couple aldehyde **164** and iodide **163**. A chelate-controlled Mukaiyama aldol reaction was recognized to yield the β -hydroxy ketone **161** from an EFG ring precursor aldehyde and HI fragment **162**.



Scheme 28. Rerosynthetic Analysis of the EFGHI Domain.

The synthesis of the E fragment aldehyde **164** commenced with the protection of the secondary alcohol as an MTM acetal in **165** (Scheme 29). The MTM protecting group

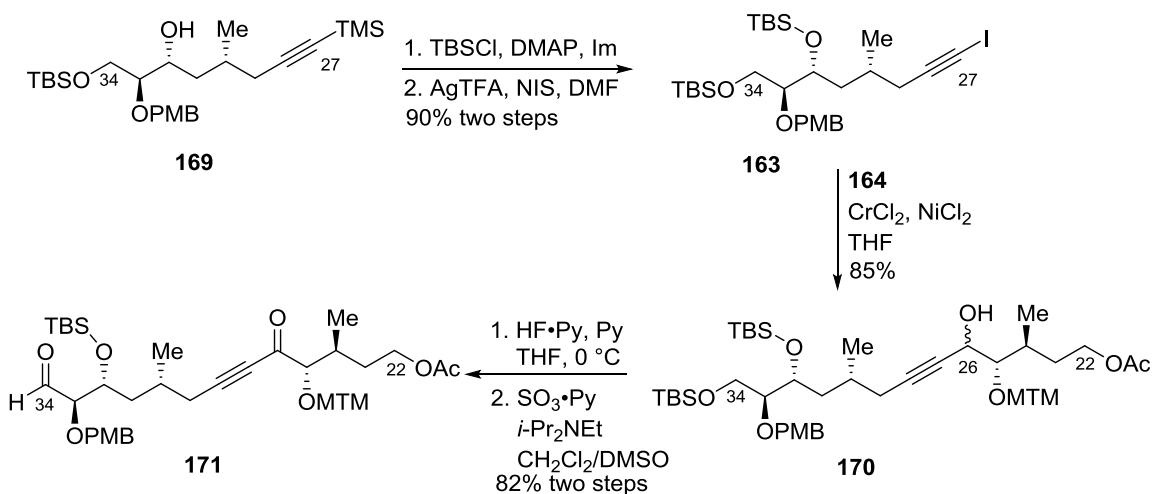
deserves a comment. The C28 ketal in this domain was constructed under TBAF conditions, while silyl protecting groups in the same position consistently gave low yields of desired product.⁶³ Through extensive analysis and experiments, Dr. Ding chose the MTM as the C25 protecting group.⁵⁸ Hydroboration and oxidation of olefin **166** afforded alcohol **167** in moderate yield. Because the MTM group was sensitive to oxidation conditions, the alkyl boron intermediate was treated with care to avoid potential oxidation of the sulfide into a sulfoxide. A two-step protecting group manipulation converted the resultant **167** into C26 primary alcohol **168**. A Parikh-Doering oxidation of **168** efficiently delivered aldehyde **164**.



Scheme 29. Synthesis of the Aldehyde **164**

With aldehyde **164** in hand, the process for the assembly of the EFG linear precursor began (Scheme 30). The secondary alcohol **169**, with 6:1 diastereomeric ratio at C32 stereocenter, could be synthesized by a well-established route.⁴² Alcohol **169** was

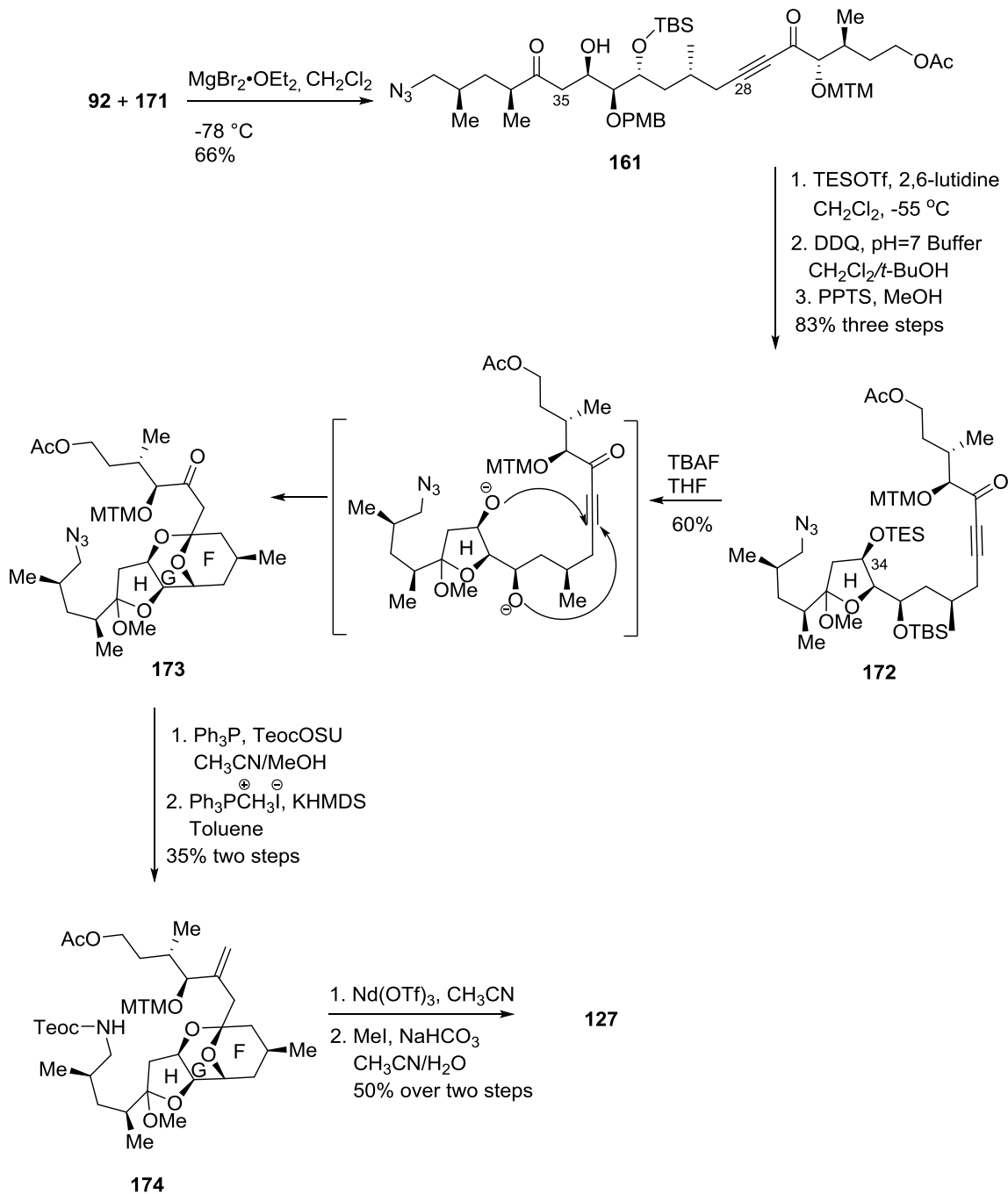
converted into iodide **163** in two steps: silyl protection and conversion of the TMS-alkyne into an iodo-alkyne. During the silyl protection step, it was noticed that the undesired C32 isomer was silylated slower than the desired C32 isomer, due to the steric effect, resulting in increment of the C32 diastereomeric ratio, which could also be considered as a kinetic resolution step. A NHK coupling between resultant iodide **163** and aldehyde **164** efficiently delivered propargylic alcohols **170**. A selective desilylation with HF·Py/Py liberated the C34 alcohol which was then oxidized into aldehyde **171** under Parikh-Doering conditions. The propargylic alcohol moiety was concomitantly converted into an ynone, which acted as a Michael acceptor in the later DIHMA process.



Scheme 30. Synthesis of the EFG aldehyde **171**

The final construction of the complex EFGHI architecture is outlined in Scheme 31. As planned, a chelate-controlled Mukaiyama aldol reaction between silyl enol ether **92** and aldehyde **171** was applied to deliver the C22-C40 domain linear precursor **161** with

excellent yield and high diastereoselectivity.³⁹ Silylation of the resultant β -hydroxy ketone and oxidative cleavage of the C33 PMB ether efficiently afforded a γ -hydroxy ketone intermediate. The H ring was first cyclized as cyclic mixed methyl ketal **172** under acid conditions (PPTS/MeOH). Exposure of resultant methoxy ketal **172** to TBAF conditions initiated the double intramolecular-hetero-Michael addition (DIHMA) process. More specifically, the silyl groups on C32 and C34 were removed to generate the nucleophilic oxygen anions, which attacked the C26-C28 Michael acceptor ynone functionality. Subsequently, the azide functional group was reduced into an amine, by $\text{Ph}_3\text{P}/\text{MeOH}/\text{MeCN}$, and the amine was protected as Teoc carbamate *in-situ*. A Wittig reaction converted the C26 carbonyl into olefin **174** in moderate yield. During the Wittig process, a side product was observed, which was identified as a C22 primary alcohol. Reacylation easily transformed the alcohol into acetate **174**. Treatment of **174** with $\text{Nd}(\text{OTf})_3$ delivered the spiroaminal intermediate, in which a separable C36 epimers with a 3:1 ratio were obtained. The use of the unusual $\text{Nd}(\text{OTf})_3$ was essential for the effective formation of spiroaminal functionality. As aforementioned in Chapter 2, the Forsyth group first discovered $\text{Yb}(\text{OTf})_3$ catalyzed spiroaminal formation in the FGHI domain synthesis of AZA1.³⁵ Following Forsyth's result, Nicolaou and co-workers systematically screened lanthanide Lewis acids to further optimize the ring closure process, which revealed $\text{Nd}(\text{OTf})_3$ to be optimal.⁶⁴ The undesired epimer could be isomerized into desired one when submitted into the same reaction conditions. Finally, the C25 *O*-MTM was cleaved under customized conditions, delivering a fully functionalized C22-C40 domain of AZA3.



Scheme 31. Synthesis of the C21-C40 Domain of AZA3

3.2 Efforts towards FGHI Domain Synthesis with Gold(I) Catalysis

As shown in Scheme 31, several steps in the final stage of the EFGHI domain synthesis consistently gave unacceptably low yields and limited our scale-up process for the total synthesis of target molecule, which made this fragment synthesis route impractical. We then planned to explore an alternative route to construct the same architecture. It was recognized that the oxidation state of a ketone is equivalent to that of an alkyne. As shown in Figure 11, the FGHI domain of AZA3 bears the bridged ketal at C28 and spiroaminal at C36 carbons as ketone oxidation state. It was realized that there were unique opportunities to develop and apply emergent gold chemistry to build the complex architecture of the FGHI domain, based upon intramolecular heteroauration of embedded alkynes.

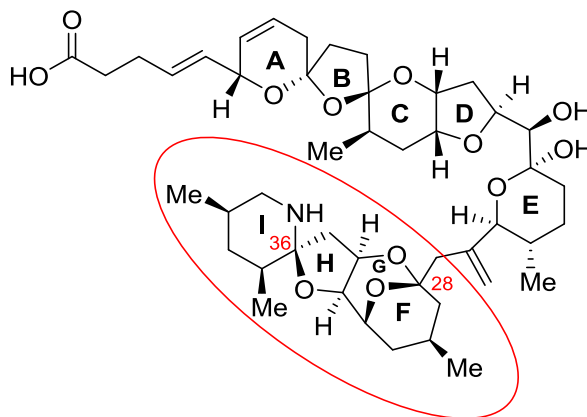
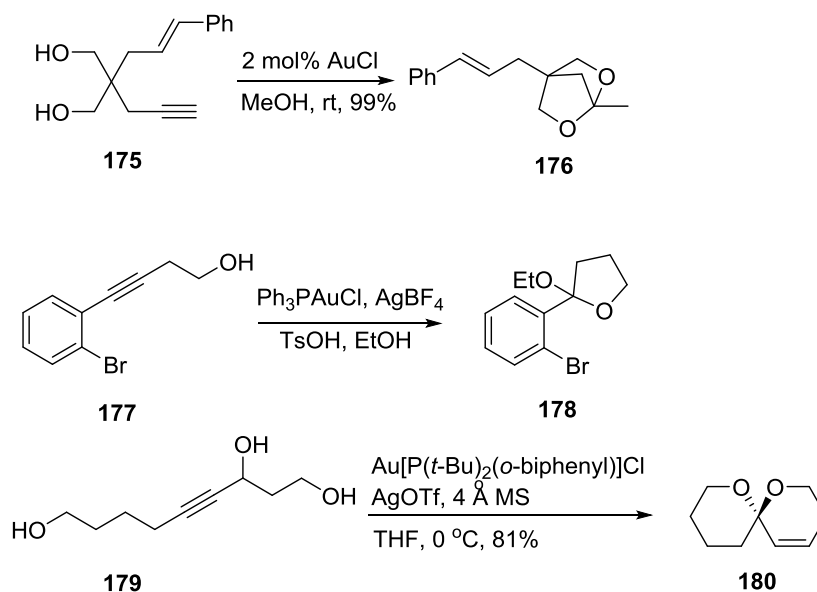


Figure 11. Ketal and Spiroaminal in the FGHI Domain of AZA3

3.2.1 Gold-Catalyzed Ketallizations

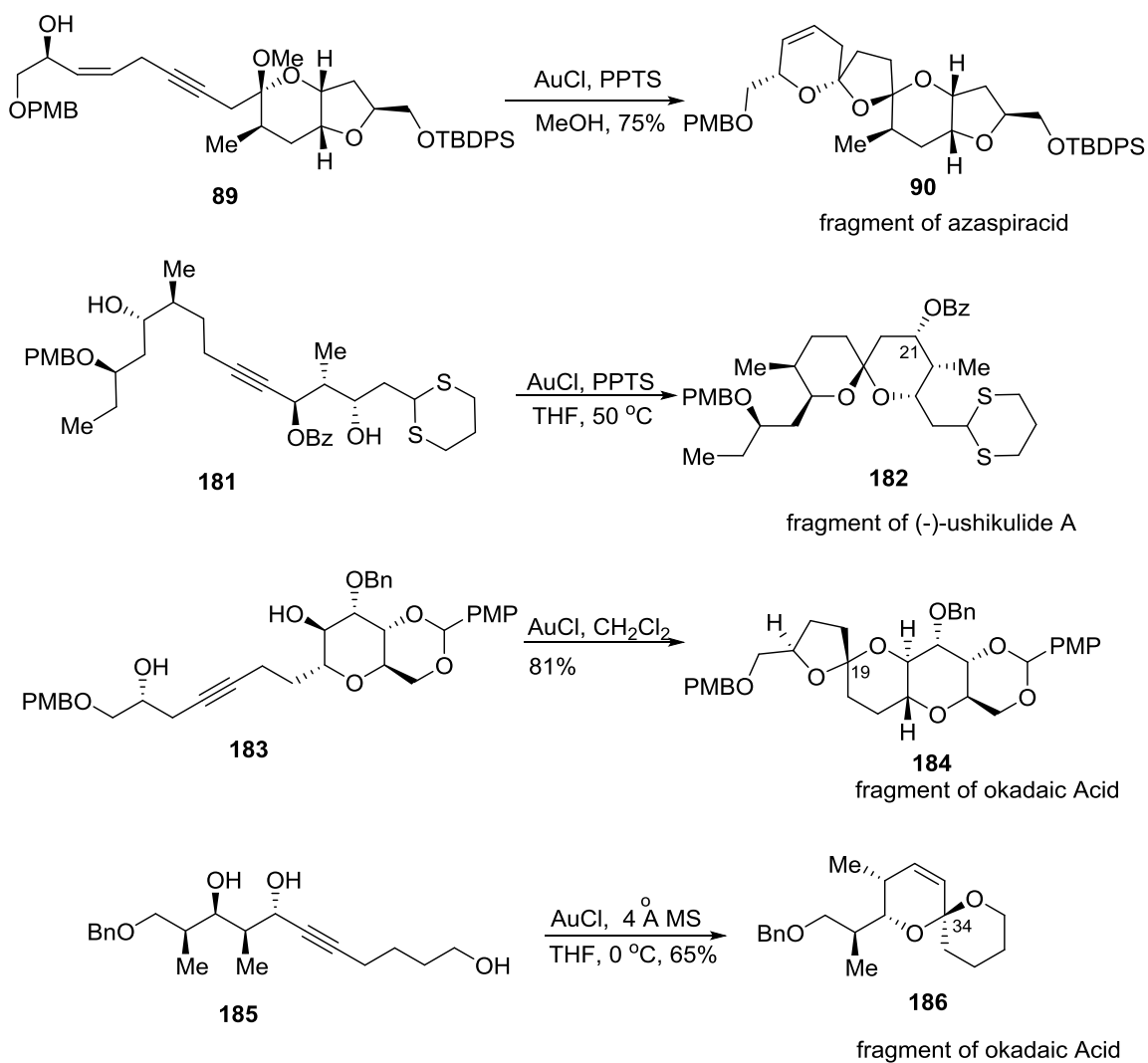
As early as 2005,⁶⁵ Genet and co-workers reported the first example of Au(I) and Au(III) catalyzed cycloisomerization of bis-homopropargylic diols leading to strained dioxabicyclic ketals. Conversion of diol **176** into ketal **177** was achieved efficiently under very mild conditions and in very short time (Scheme 32). The authors also stated that the reaction conditions were compatible with various functional groups. In 2006, the Krause group reported a mild and efficient tandem cycloisomerization-hydroalkoxylation of homopropargylic alcohols to tetrahydrofuranyl ethers.⁶⁶ In presence of gold catalyst, silver additives, and a Brønsted acid, the alcohol **177** cyclized into ethoxy ketal **178**. The reaction could be carried out in various solvents, including alcohols, with both terminal and internal alkynes as the substrates. Recently, the Aponick group at the University of Florida reported an interesting gold-catalyzed isomerization reaction, which is the gold-catalyzed cyclization of monopropargylic triol **179** to produce the unsaturated spiroketal **180**.⁶⁷ The reactions are rapid and high yielding with 2 mole % of gold complex and silver additive at low temperature. Due to the excellent activity of Au(I) and Au(III) catalysts, more gold catalyzed transformations are being developed and designed.



Scheme 32. Examples of Gold-Catalyzed Ketal Formations^{65, 66, 67}

As described above, internal and terminal alkynes provide an ideal platform to construct a variety of ketals under the influence of gold catalysts. Compared to ketalization with hydroxy ketone substrates, gold chemistry was shown to be more atom-economical and reliable, especially when the hydroxy ketone substrate bears an α -stereocenter, there could be potential epimerization problems. As such, gold chemistry has become employed increasingly in natural product syntheses. As shown in Scheme 33, four examples were listed for the applications of gold-catalyzed ketalizations in natural products synthesis. As described in a previous chapter, the Forsyth group reported the construction of trioxadispiroketal system of azaspiracid with the utilization of AuCl/PPTS, which was considered one of the earliest examples for the applications of gold methodology.⁴¹ In the course of the total synthesis of (-)-ushikulide A,⁶⁸ a planned Pd-catalyzed spiroketalization of triol derivative of **181** provided only limited reactivity.

While platinum compounds also failed, Trost and co-workers turned their attention to more versatile gold chemistry. After screening a variety of gold catalysts and protecting groups on the C21 alcohol, it was found that benzoate ester **181** successfully avoided the elimination of the propargylic position under AuCl/PPTS conditions. Recently, the Forsyth group reported a formal total synthesis of okadaic acid, highlighting the regiocontrolled gold-catalyzed spiroketalizations.⁶⁹ Both the C19 and C34 spiroketals of okadaic acid were assembled under gold conditions. More interestingly, exposure of **183** to AuCl at low temperature (0 °C) triggered the ketalization and elimination of the propargylic alcohol functionality, resulting in the C28-C38 fragment of okadaic acid. This was the first application of Aponick's method in the natural product synthesis.

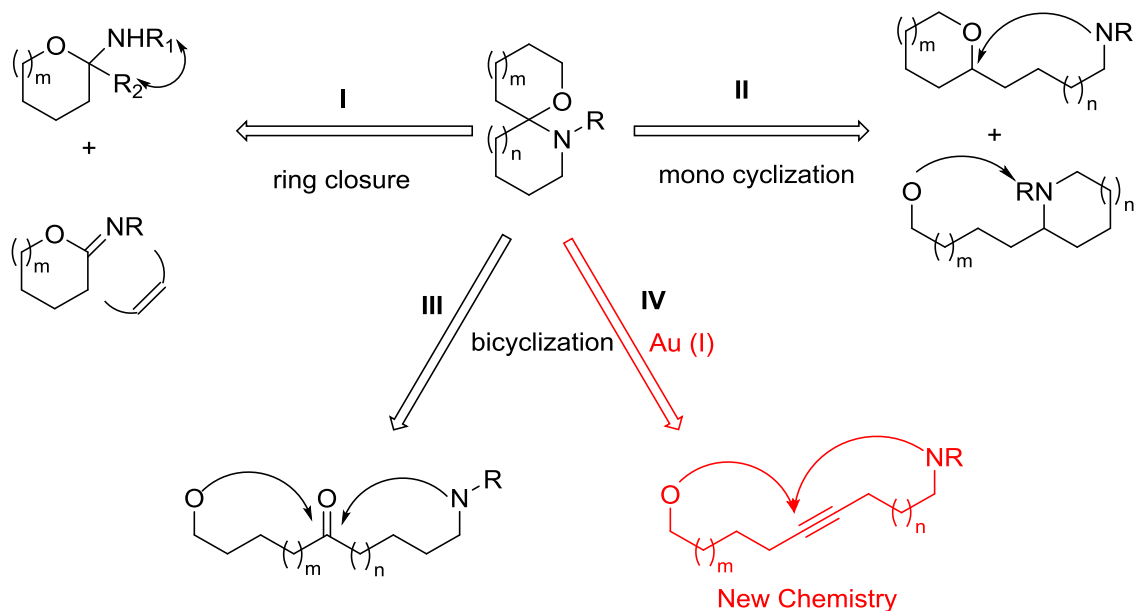


Scheme 33. Examples of Applications of Gold-Catalyzed Transformations in Natural Product Synthesis^{41, 68, 69}

3.2.2 Gold-Catalyzed Spiroaminal Formation

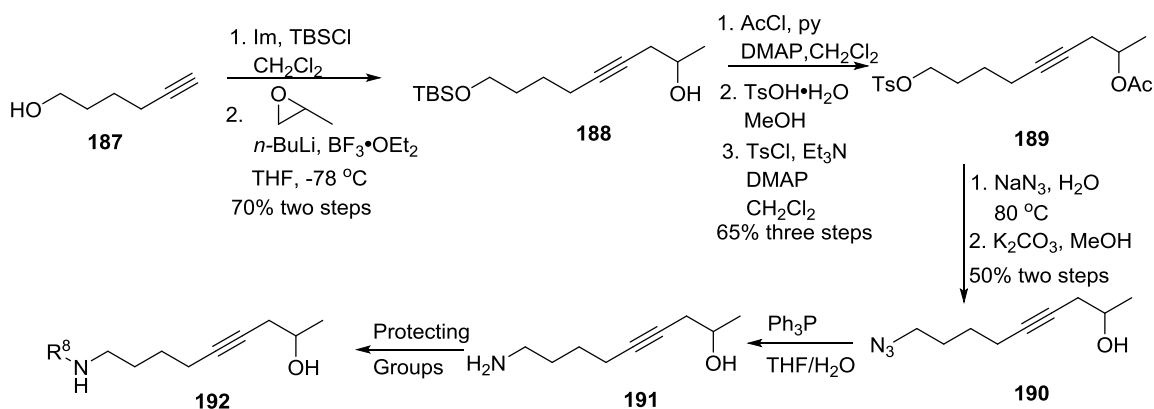
The gold-catalyzed ketalization has been well-established, while little information, could be found for gold-catalyzed spiroaminal formation. Due to the novel and attractive structure, several methods were explored to construct various spiroaminals. The strategies

to construct spiroaminal moieties were summarized by Sinibaldi and Canet⁷⁰ in three different strategies (Scheme 34). Strategy I involves inter- or intra-molecular ring closure reactions from imidate or aminal compounds as precursors. In strategy II, mono-cyclization of piperidine or pyran derivatives could be applied to produce spiroaminal core structures. In strategy III, formation of bicyclic cores could also be achieved through double cyclization, in one step, from a ketone linear precursor. Our proposal to construct the C36 spiroaminal moiety through gold catalysis required an initial investigation of new synthetic route to spiroaminal cores, which is the strategy IV. An internal alkyne, instead of a ketone, was prepared to cyclize into spiroaminals under gold conditions.



Scheme 34. Summary of Synthetic Route for Spiroaminals.

A model compound **191** was synthesized in a short manner. The synthesis commenced with silyl protection of 5-hexyn-1-ol followed by nucleophilic opening of propylene oxide. A three-step sequence converted homopropargylic alcohol **188** into acetate **189**, which involved acylation, desilylation and sulfonylation. Substitution of sulfonate **189** with sodium azide and cleavage of acetate resulted in homopropargylic alcohol **190**. Finally, the azide moiety was reduced to amine **191** in gram scale under Staudinger conditions. Different protecting groups were then tested to modify the nucleophilicity of the nitrogen atom.



Scheme 35. Synthesis of Spiroaminal Model Compound

Once the model compounds were addressed, different conditions were tested to reach the spiroaminal structure. Without protecting groups on nitrogen, Au(III) was initially tested with different temperatures, because it was known that hydroamination of alkynes could be achieved with AuCl $_3$ /MeCN. Only the alkyne hydration product was obtained based under these conditions on NMR spectroscopic analysis, which meant gold catalysis did activate the alkyne functionality, but no cyclization occurred while the addition of

water resulted in hydroxy ketone. Addition of $\text{Nd}(\text{OTf})_3$ into the systems gave the same result. A commonly used Cbz protecting group was incorporated into the substrate. Treatment of the carbamate with Au(I) catalyst activated with silver triflate still gave the hydration product. Based on the Krause's study, the solvent was changed to methanol, and it was found that only a hydration product was obtained after careful flash chromatography. Later study showed that the actual product was cyclic mixed methyl ketal, which could be transformed into a hydroxy ketone upon silica gel chromatography. Nevertheless, a trace amount of the spiroaminal **194** was produced once changing the solvent to CH_2Cl_2 . The product was confirmed by NMR spectroscopic studies, and we also synthesized the same spiroaminal through a known procedure, which was PPTS-catalyzed methoxy ketal formation followed by cyclization under $\text{Nd}(\text{OTf})_3$ conditions. The ^1H - and ^{13}C -NMR of two spiroaminal products were identical! The diastereomeric ratio of the resultant spiroaminals was 3:1, based on NMR spectrum. In contrast to the gold-catalyzed spiroketalization, the anomeric effect between N and O atom could not dominate the diastereoselectivity outcome of spiroaminal formation. A high temperature indeed gave us a slightly higher yield. Finally, the protecting group was changed into sulfonamide which started to give us satisfied yield.

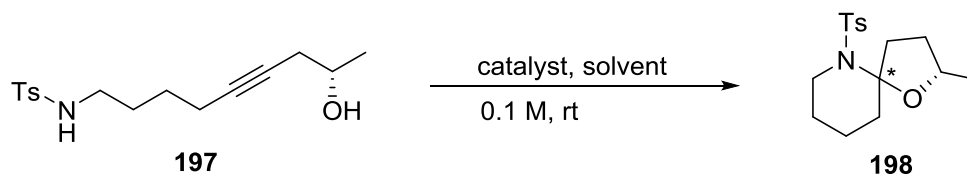


Entry	R ⁸	Conditions	Result
1	H	AuCl ₃ , MeCN	hydration product
2	H	AuCl ₃ , MeCN, 40 °C	hydration product
3	H	AuCl ₃ , Nd(OTf) ₃ , MeCN	hydration product
4	Cbz	AuCl, AgOTf, MeCN	hydration product
5	Cbz	AuCl, AgOTf, MeOH	hydration product
6	Cbz	AuCl, AgOTf, CH ₂ Cl ₂	~ 10% spiroaminal 194
7	Cbz	AuCl, AgOTf, Toluene, 80 °C	30% spiroaminal 195
8	Ts	AuCl, AgOTf, CH ₂ Cl ₂	60% spiroaminal 196

Table 1. Conditions Tested to Construct Spiroaminals

The optimization for this newly discovered gold-catalyzed spiroaminal formation is illustrated in Table 2. Different solvents were screened, which showed that the less polar solvents gave higher yields. An 18% yield was obtained with MeCN, while toluene afforded the spiroaminal in 91%. The nitrile of acetonitrile solvent may chelate with the gold catalyst, resulting in a lower efficiency of the catalyst. Gold (III) chloride could also deliver the spiroaminal in moderate yield. The commonly used gold catalyst Ph₃PAuCl did not promote the cyclization. Once some silver additive (AgOTf) was added, the catalyst system became quite efficient for this transformation, while the combination of AuCl/AgOTf consistently gave a lower yield (67%) than that of AuCl without any silver

additives. These results indicated that it was important to understand the specific details required for the transformation with the specific gold catalyst system.



Entry	Catalyst	Solvent	Time	Yield	<i>d.r.</i>
1	5 mol% AuCl	MeCN	1 h	18%	3 : 1
2	5 mol% AuCl	CH ₂ Cl ₂	1 h	70%	3 : 1
3	5 mol% AuCl	THF	1 h	70%	3 : 1
4	5 mol% AuCl	Toluene	1 h	91%	3 : 1
5	5 mol% AuCl ₃	Toluene	1 h	78%	3 : 1
6	5 mol% Ph ₃ PAuCl	Toluene	1 h	NR	3 : 1
7	5 mol% Ph ₃ PAuCl 5 mol% AgOTf	Toluene	1 h	85%	3 : 1
8	5 mol% AuCl 5 mol% AgOTf	Toluene	1 h	67%	3 : 1

Table 2. Optimization of Gold Conditions

Protic solvents were also tested for this transformation, which gave very interesting results. On submission of substrate **197** to AuCl/MeOH, no spiroaminal could be obtained after several trials. Isolation with neutralized silica gel chromatography gave the major product as a mixed cyclic methyl ketal, which was consistent with Krause's result.⁶⁶ But interestingly, the difference was that no Brønsted acid was used in the present system. It was clear that the formation of the methoxy ketal required an

intermolecular reaction between the organo-gold intermediate and methanol. From this result, two inferences could be made about the mechanism: (1) the oxygen atom has a much greater cyclization rate than the nitrogen atom under the gold conditions; (2) the intramolecular cyclization of spiroaminals requires much higher activation energy than corresponding intermolecular ketalizations. The solvent was then changed to the more bulky alcohol *i*-PrOH, which gave a mixture of products. One was the desired spiroaminal **198**, the other was the corresponding ketal. Thus, the bulky alcohol indeed slowed down the ketalization. The more bulky alcohol *t*-BuOH was then tested. As postulated, no ketal was isolated, and the desired spiroaminal was obtained in 55% yield.

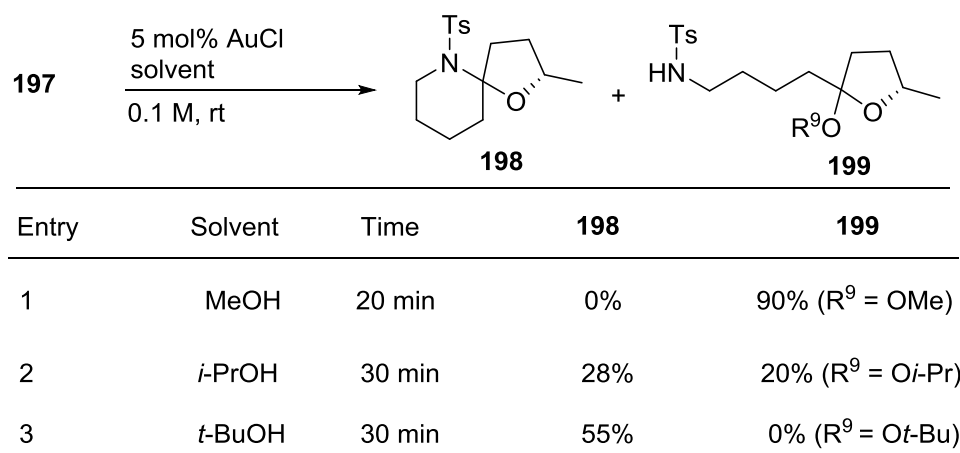


Table 3. Spiroaminal Formation Using Alcohols as Solvent

Different substrates were synthesized by the author and co-worker Mr. Yong Chen. As shown in Figure 12, more than 10 substrates had been tested, among which moderate to excellent yields of spiroaminal moieties could be obtained under gold conditions. The

efficiency of this gold-catalyzed isomerization is dependent on the ring size and the substitution on the nitrogen atoms. It is quite interesting that no (6,6)-spiroaminal could be synthesized under gold (I) conditions. Further study may be required for a more detailed mechanistic study of this transformation.

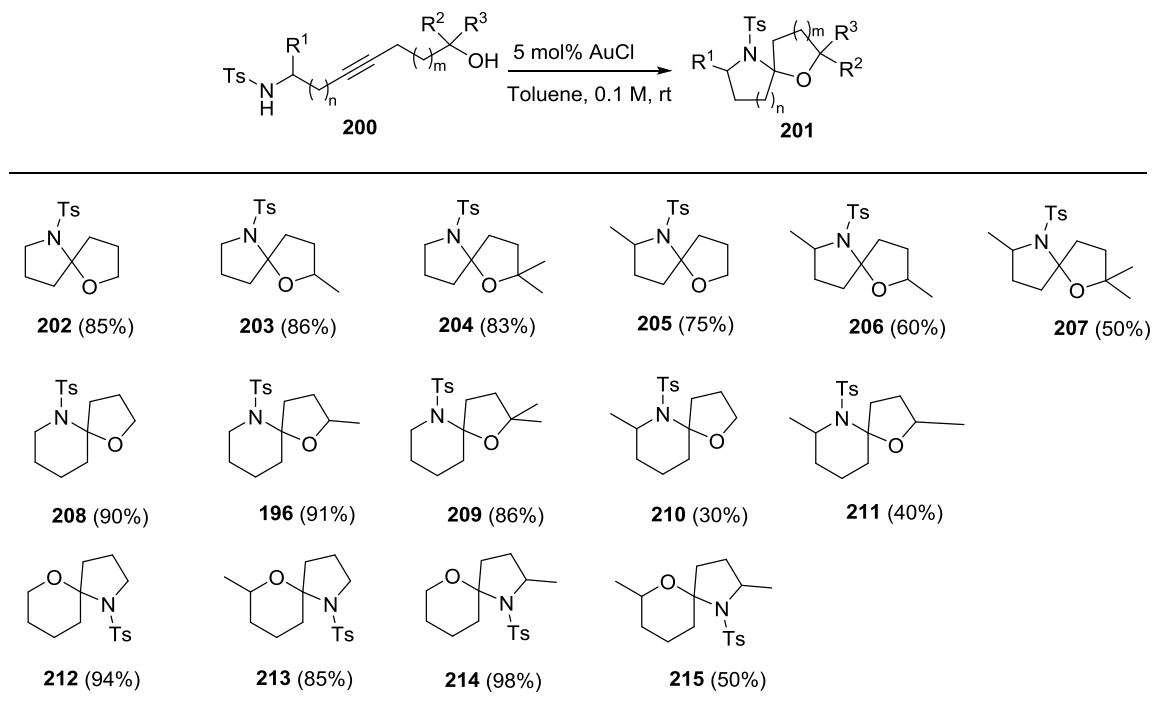
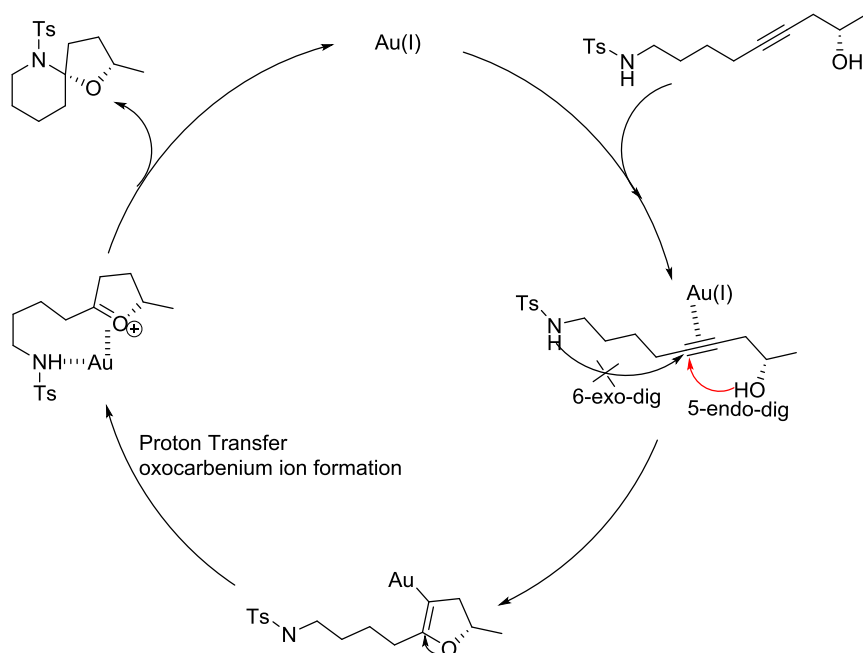


Figure 12. Substrate Scope

A spiroaminal forming mechanism was also proposed based on the experimental data (Scheme 35). The gold (I) catalyst may have a dual role in this cyclization process: (1) to activate the alkyne; (2) to facilitate the second cyclization to furnish the spiroaminal. During this process, the alkyne functionality could initially be more electrophilic under gold activation. Then two nucleophilic additions could be possible, which are the 6-exo-dig of nitrogen and 5-endo-dig of oxygen. Based on the observations, the oxygen atom

first cyclizes to form a vinyl ether intermediate, while the 5-endo-dig mode may not be the kinetically favored pathway in accordance with Baldwin's rules.⁷¹ A following protiodeauration could liberate the gold (I) catalyst and protonation of the resulting enol ether may lead to an oxocarbenium ions. During the gold-catalyzed ketalization, it is believed that oxocarbenium ion would expediently deliver the ketal product, which means that the main function of gold catalyst is to form the oxocarbenium ion intermediate. In this newly discovered gold-catalyzed transformation, gold may have the other function apart from the formation of electrophilic oxocarbenium ion. The Control experiments were also set up for comparison. A corresponding methoxy ketal could not be isomerized into a spiroaminal under PPTS conditions, while it is well known that PPTS can facilitate the formation of oxocarbenium ions. The gold (I) catalyst may act the same way as a lanthanide catalysts⁷² to chelate with an intermediate oxocarbenium ion and nitrogen atom due to the large radius of the gold cation. The catalyst could be finally released to re-enter the next catalytic cycle once the formation of the spiroaminal is complete.

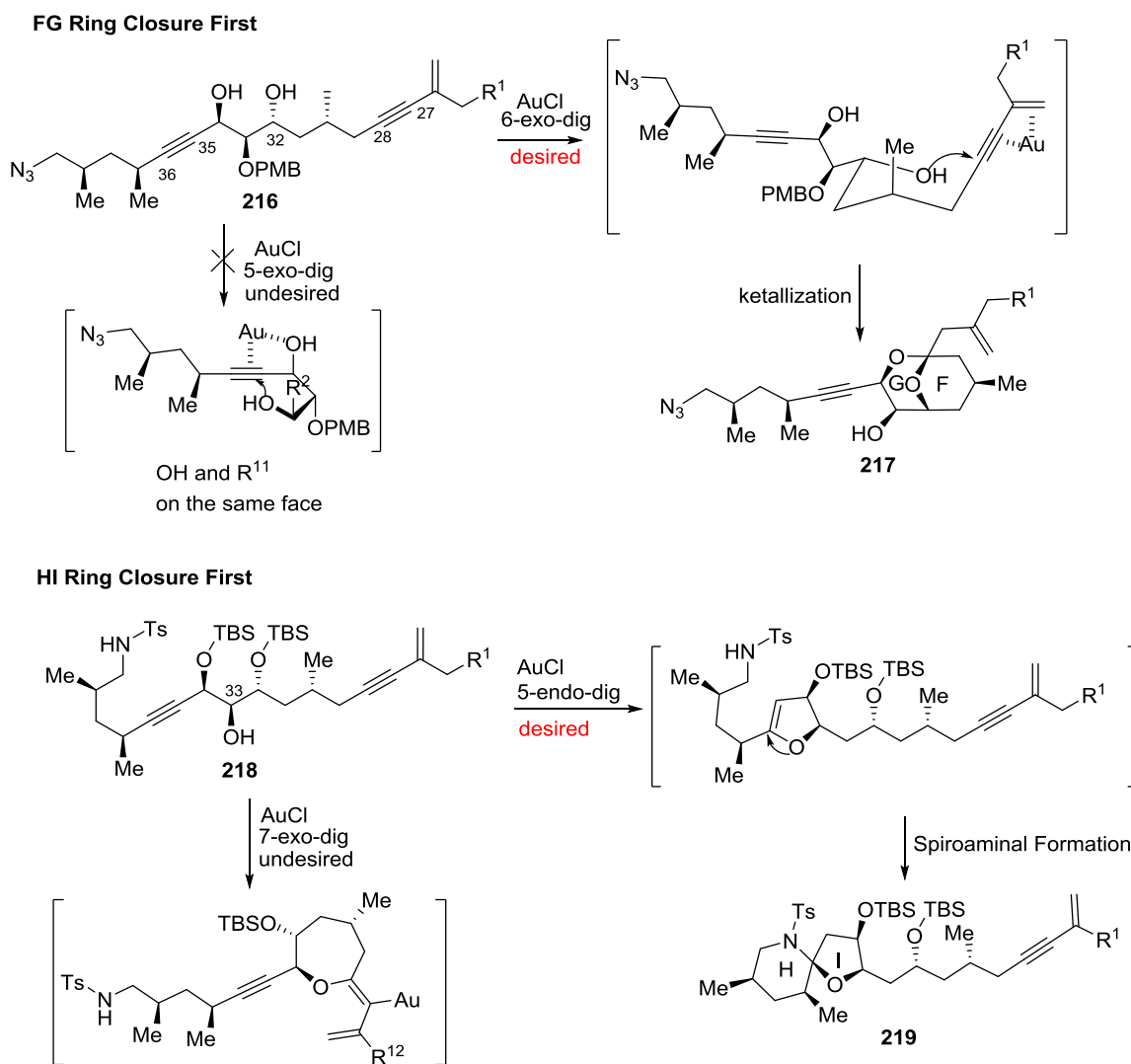


Scheme 36. Proposed Mechanism of Gold-Catalyzed Spiroaminal Formation

3.2.3 Efforts on FGHI Domain Synthesis

Through a systematic study on model compounds, two ideal platforms were prepared for complex molecule synthesis: one is the well-established gold-catalyzed ketalization and the other is the newly developed gold-catalyzed spiroaminal formation. As noticed in Figure 8, both the C28 bridged ketal and C36 spiroaminal could be possibly set up through gold catalysis. The sequence of gold-catalysis should be considered carefully, that is beginning with FG C28 bridged ketal formation or starting with HI spiroaminal formation. Scheme 36 shows the detailed analysis, which led to clear choice of bridged ketal formation at first, followed by spiroaminal formation. The first proposed route is FG ring closure with the requisite diol precursor **216**. Under gold catalysis, there are at least

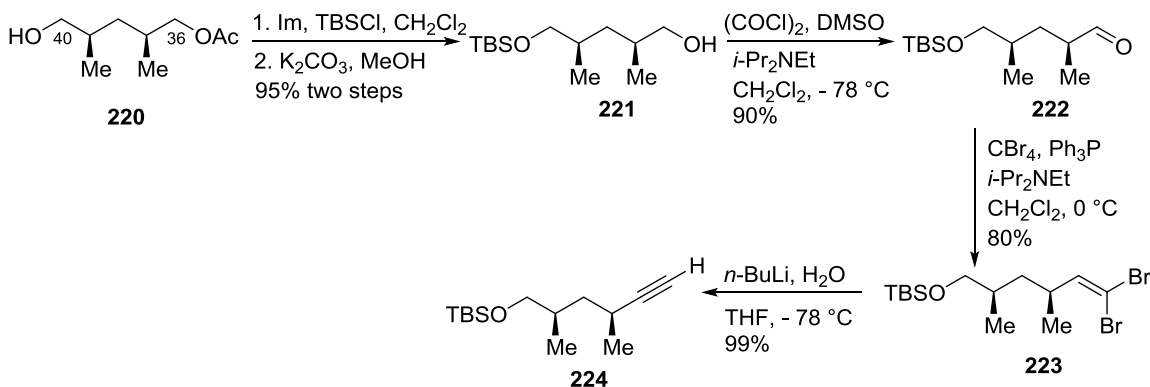
two possible nucleophilic addition pathways. The desired one is the C32 hydroxyl to attack the activated C27-C28 alkyne, while the undesired competing addition is that the same hydroxyl may also attack the C35-C36 alkyne moiety. The anticipated reaction path is 6-exo-dig, while the undesired is 5-exo-dig, which is more kinetically favored. However, after analysis of the intermediate conformation, it was concluded that this route may deliver the desired product **217**. In the transition state, the 6-exo-dig route could adopt the chair-like conformation for the cyclization, while 5-exo-dig may have a five-membered ring intermediate under gold catalysis. From the aforementioned Forsyth's study on the formal total synthesis of okadaic acid,⁶⁹ the propargylic hydroxyl and the bulky R¹¹ may be on the same face of the five-membered ring when the substrate has such 1,3-*anti* hydroxyl functionality. The steric repulsion could slow down the kinetically favored 5-exo-dig cyclization, resulting in the desired 6-exo-dig pathway. The second proposed route is HI ring closure first. The dialkynyl hydroxy sulfonamide **218** was chosen as the precursor of the designed route. Under the gold catalysis, there are also two possible reaction patterns, which are the desired 5-endo-dig and undesired 7-exo-dig. Based on Baldwin's rules, it is difficult to predict which would be preferable. Comparison of the above two synthetic plans clearly showed that the first FG ring closure gives a much higher possibility to reach the final target.



Scheme 37. Synthetic Analysis

The synthesis commenced with the preparation of the alkyne **224** (Scheme 38). The acetyl alcohol **220** was kindly provided by Mr. Yong Chen. Two-step protecting group manipulations efficiently converted **220** into **221**, involving C40-*O*-silylation and removal of the C36-*O*-acetyl group. The resultant C36 primary alcohol **221** was then oxidized into aldehyde **222** under Swern conditions. No epimerization was observed at

the α -position during the oxidation process. Finally, a Corey-Fuchs reaction⁷³ was applied to convert aldehyde **222** into alkyne **224** with excellent yield. Hünig's base was utilized to buffer the acidic environment, since the primary silyl group was clearly cleaved under abasic Corey-Fuchs conditions.



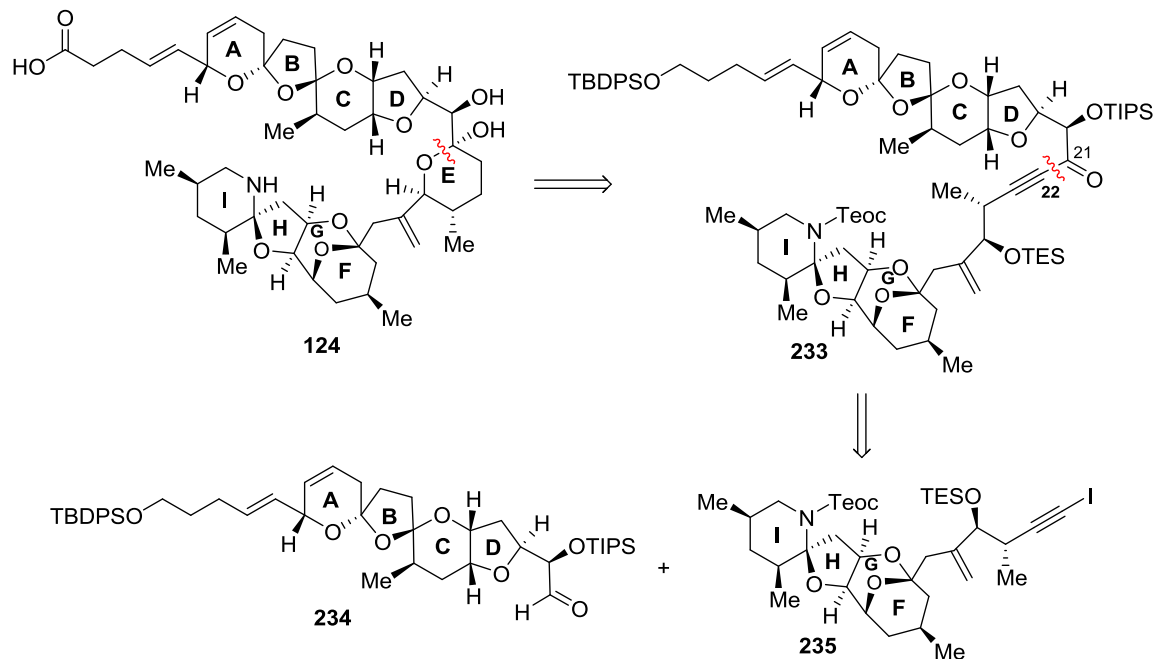
Scheme 38. Synthesis of the Alkyne **224**

Once the HI fragment alkyne **224** was obtained, the assembly of a bridged ketal was addressed (Scheme 39). A mild zinc-mediated coupling between HI alkyne **224** and FG aldehyde **225** stereoselectively produced the propargylic alcohol **226**.⁷⁴ The silyl ethers were cleaved under acid conditions. Treatment of resultant triol with 2,2-dimethoxy propane under acidic conditions resulted in the selective protection of the internal 1,3-*anti*-diol. The ^{13}C -NMR chemical shift difference of the two methyl groups on the acetonide protecting group further confirmed the selectivity of Carreira's protocol.⁷⁵ A Mitsunobu condition⁷⁶ was applied to convert the C40 hydroxyl moiety into a sulfonyl amide functionality. The acetonide was removed under acidic conditions. Exposure of the resultant diol to TBAF solution delivered the free alkyne **228**. The following key step for

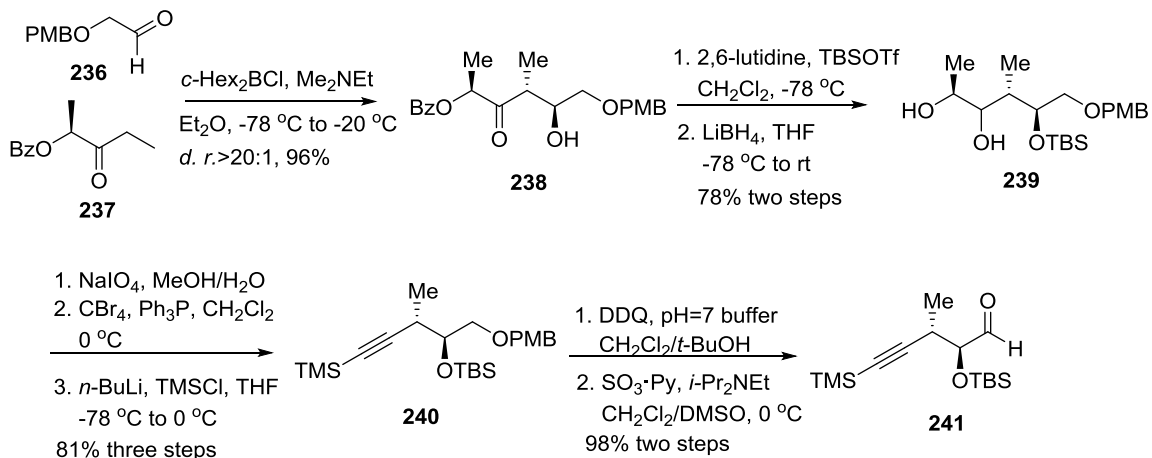
the construction of the bridged ketal actually successfully delivered the anticipated product with AuCl/PPTS. Here, PPTS bears comment of its importance. Two separable products with 2:1 ratio were initially isolated from flash chromatography without PPTS. Through our analysis, the minor portion should be the kinetic ketalization product. Fortunately, the undesired portion could be cleanly isomerized into the desired thermodynamically favored ketal **222**. Finally, the combination of catalytic AuCl and PPTS efficiently delivered **222** as the only ketalization product.

3.3 NHK Route for the Total Synthesis of AZA3

Due to the problems with protecting group manipulations met after the Yamaguchi coupling reactions between carboxylic acid **126** and hydroxyl **127**,⁵⁸ a new synthetic route was proposed (Scheme 41). The hemiketal E ring moiety could also be synthesized from ynone **233**. A copper-mediated reduction and global silyl deprotection is planned to assemble the skeleton of AZA3. A well-known NKH coupling between C1-C21 aldehyde **234** and alkynyl iodide **235** was taken advantage of to deliver the propargylic alcohols, which could be oxidized into ynone **233**. Compared with the previous route, only one slight change has been inserted into the C1-C21 domain, changing the C20 *O*-Piv to *O*-TIPS, which virtually would not affect the aforementioned ABCD domain synthesis. Based on this revised route, we also have opportunities to access the AZA1 and AZA2 through ultimate alkylation of the C22 α -position of ynone **233**. With knowledge of Evans' and Nicolau's late stage syntheses of AZA1, this newly proposed synthetic plan could provide easier manipulations to achieve the total synthesis, especially after the coupling between **234** and **235**.

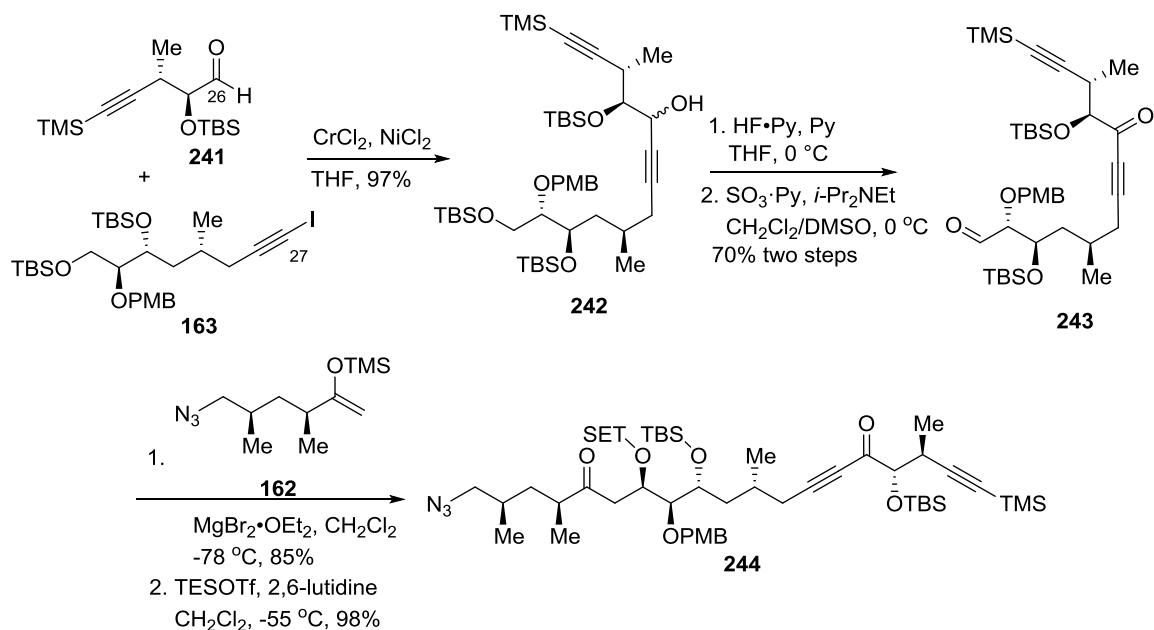


Based on the revised synthetic plan, an alternative synthesis to the E fragment has been achieved. As shown in Scheme 42, the fragment synthesis commences with a Paterson *anti*-aldol reaction⁷⁸ between the aldehyde **236** and lactate derived ketone **237**, yielding the β -hydroxy ketone **238** with excellent yield and stereoselectivity. Silylation of the resultant hydroxyl group followed by reduction of the ketone and benzoate ester functionality delivered the mixture of diols **239**. Sodium periodate efficiently cleaved the diol into an aldehyde intermediate, which was then converted into the TMS-alkyne under Corey-Fuchs conditions. The PMB protecting group was then oxidatively removed with the influence of DDQ. The resultant primary alcohol was then oxidized into aldehyde **241** under Parikh-Doering conditions.



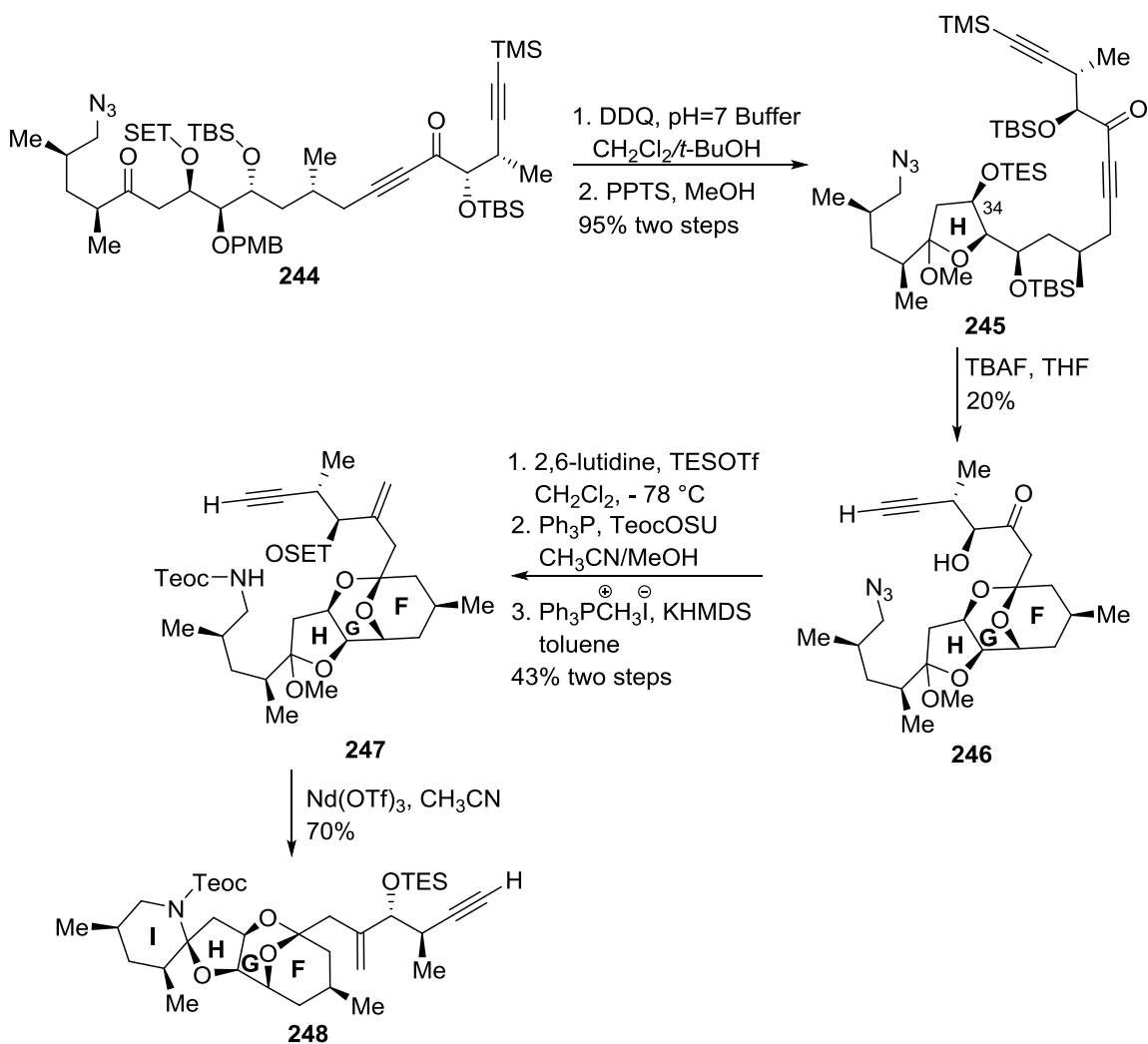
Scheme 42. Revised Synthesis of the E Fragment

Once the aldehyde **241** was obtained, the synthesis of the EFGHI linear precursor **244** was then addressed (Scheme 43). A reliable NHK reaction was applied to couple the aldehyde **241** and the alkynyl iodide **163**, producing mixture of propargylic alcohols **242**. The C34 TBS groups was then selectively removed under buffered HF•Py conditions. The resultant diol was then oxidized into aldehyde **243**. The MgBr₂•OEt₂ chelate-controlled Mukaiyama aldol reaction gave an excellent yield and high stereoselectivity. The resultant β-hydroxy ketone was then silylated into **244**.



Scheme 43. Synthesis of the C22-C40 Linear Precursor

Once the EFGHI linear precursor **244** was efficiently synthesized, the assembly of the C22-C40 complex architecture followed (Scheme 44). The C33 *O*-PMB group was removed under DDQ conditions. Treatment of the resultant γ -hydroxy ketone with PPTS/MeOH resulted in the cyclization to deliver the cyclic methyl ketal. It is worth mentioning that the products after this cyclization step are extremely sensitive to acidic conditions, including the chromatography. A DIHMA reaction was applied to construct the bridged ketal **246**, which consistently gave low yields after different forms of TBAF and temperature were screened. The resultant free C25 hydroxyl was then silylated. The azide group was reduced under modified Staudinger conditions and *in-situ* protected as a Teoc Carbamate. The spiroaminal ring was cyclized with $\text{Nd}(\text{OTf})_3$ to furnish the fully functionalized C22-C40 domain of AZA3.



Scheme 44. Synthesis of the C22-C40 Domain of AZA3

Figure 13 shows a possible reason for the low yield from the key DIHMA process. Under the fluoride conditions, four silyl groups in the **245** were quickly removed. Due to the full dissociation of fluoride with ammonium ion, the strong silicon and fluoride bond would force the desilylation with no selectivity, resulting in a possible tetra anion in the anhydrous THF environment. Because of the repulsion between the same charges, the low yield would result from the DIHMA reactions. Based on this analysis, a modification

on the silyl groups is being tested. A free alkyne is planned to be obtained under the Corey-Fuchs conditions in the E ring fragment synthesis. A smaller TES group was selected for the C32 position, and a more bulky TBS group is chosen to replace the labile TES group at the C34 position.

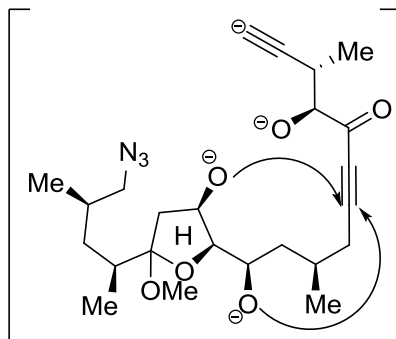


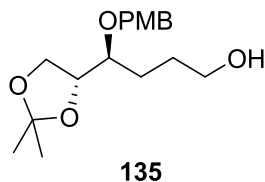
Figure 13. DIHMA Process

Experimental Data

General Methods:

Unless otherwise noted, all reactions were carried out under an argon atmosphere in over-dried glassware using standard syringe, cannula, and septa techniques. Dichloromethane, tetrahydrofuran, diethyl ether, toluene, and dimethylformamide were purified with a Pure Solv. MD-6 solvent purification system. Triethylamine, diisopropylethylamine, acetonitrile, methanol were distilled from calcium hydride under nitrogen. All other solvents were used as received.

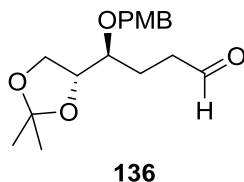
Analytical thin layer chromatography (TLC) was performed using 0.25 mm Silicycle silica gel 60 F₂₅₄ plates. Solvents for chromatography are listed as volume: volume ratios. Optical rotations were measured on a Perkin-Elmer polarimeter. Nuclear magnetic resonance (NMR) spectra were recorded on a Bruker DPX 400 spectrometer, operating at 400 MHz for ¹H NMR and 100 MHz for ¹³C NMR. Chemical shifts were reported in ppm on the δ scale relative to residual CHCl₃ (δ = 7.28 for ¹H NMR and δ = 77.2 for ¹³C NMR) as an internal reference. The coupling constant values (*J*) are in Hertz (Hz). The following abbreviations have been used for signal multiplicities: s, singlet; d, doublet; t, triplet; q, quartet; m, multiplet; and br, broad. ESI mass spectra were measured on a Bruker MicroOTOF instrument.



(S)-4-((R)-2,2-Dimethyl-1,3-dioxolan-4-yl)-4-((4-methoxybenzyl)oxy)butan-1-ol (135)

To a solution of olefin **134** (10.8 g, 37 mmol) in THF (200 mL) at 0 °C was added dropwise BH_3 (37.0 mL, 1 M in THF, 37 mmol). After 2 h at rt, the reaction mixture was cooled to 0 °C. Water (4.0 mL), 3 M aqueous NaOH (13.2 mL) and 30% aqueous H_2O_2 (8.7 mL) were successively added. The mixture was stirred for 2 h at rt and was then diluted with water (200 mL). The pH was adjusted to 6-7 with 10% aqueous HCl. The aqueous phase was extracted with diethyl ether (3 x 200 mL) and the combined organic phases were washed with saturated aqueous NaHCO_3 and brine. The organic phases were dried over anhydrous Na_2SO_4 , filtered, and concentrated. The residue was purified by flash chromatography (hexanes-ethyl acetate, 3:1, v/v) to provide alcohol **135** (7.94 g, 26 mmol, 70%) as a colorless oil.

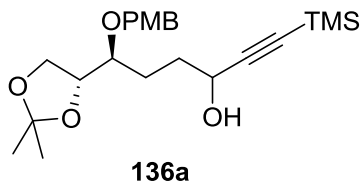
$R_f = 0.33$ (hexanes-ethyl acetate, 1:1, v/v); ^1H NMR (CDCl_3 , 400 MHz): δ 7.26 (d, $J = 8.6$ Hz, 2H), 6.88 (d, $J = 8.6$ Hz), 4.59 (q_{AB}, $\Delta\nu = 16$ Hz, $J_{AB} = 11$ Hz, 2H), 4.12 (q, $J = 6.2$ Hz, 1H), 4.06 (dd, $J = 6.4$ Hz, 1.6 Hz, 1H), 3.88 (dd, $J = 6.4$ Hz, 1.5 Hz, 1H), 3.82 (s, 3H), 3.64 (m, 2H), 3.57 (td, $J = 6.0$ Hz, 3.2 Hz, 1H), 1.72 (m, 3H), 1.63 (m, 3H), 1.44 (s, 3H), 1.37 (s, 3H); ^{13}C NMR (CDCl_3 , 125 MHz): δ 159.3, 130.3, 129.5, 113.8, 109.1, 78.58, 77.5, 72.3, 66.6, 62.9, 55.3, 28.1, 27.4, 26.6, 25.23; IR (neat): 3436, 2935, 1612, 1513, 1454, 1370, 1301, 1248, 1069 cm^{-1} ; $[\alpha]_D^{25} + 17.1$ (c 1.56, CHCl_3); HRMS-ESI(m/z) calculated for $[\text{M}+\text{Na}]^+$ 333.1673, found 333.1687.



(S)-4-((R)-2,2-Dimethyl-1,3-dioxolan-4-yl)-4-((4-methoxybenzyl)oxy)butanal (136)

To a solution of oxalyl chloride (2.3 mL, 26 mmol) in CH₂Cl₂ (100 mL) at -78 °C was added drop-wise DMSO (3.6 mL, 52 mmol). After 20 min at -78 °C, a solution of **135** (4.0 g, 13 mmol) in CH₂Cl₂ (30 mL) was added, then the solution was warmed to -60 °C. After 1 h at -60 °C, *i*-Pr₂NEt (13.5 mL, 77.4 mmol) was added. The mixture was stirred for 10 min at -60 °C and 10 min at 0 °C. Cold 1 M aqueous HCl solution (48 mL) was added. The organic phase was mixed with pH = 7 aqueous buffer solution. The aqueous phase was extracted with CH₂Cl₂ (3 x 50 mL). The combined organic phases were washed with brine and dried over anhydrous Na₂SO₄, filtered, and concentrated. The residue was purified by flash chromatography (hexanes-ethyl acetate, 5:1, v/v) to provide aldehyde **136** (3.92 g, 12.7 mmol, 99%) as a colorless oil.

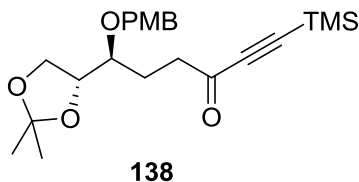
$R_f = 0.8$ (hexanes-ethyl acetate, 1:1, v/v); ¹H NMR (CDCl₃, 400 MHz): δ 9.75 (t, $J = 1.44$ Hz, 1H), 7.26 (d, $J = 8.7$ Hz, 2H), 6.90 (d, $J = 8.6$ Hz, 2H), 4.54 (q_{AB}, $\Delta v = 19$ Hz, $J_{AB} = 11.1$ Hz, 2H), 4.08 (m, 2H), 3.86 (m, 1H), 3.82 (s, 3H), 3.54 (m, 1H), 2.55 (t, $J = 7.2$ Hz, 2H), 2.01 (m, 1H), 1.85 (m, 1H), 1.42 (s, 3H), 1.36 (s, 3H); ¹³C NMR (CDCl₃, 125 MHz): 202.1, 159.4, 130.1, 129.6, 113.9, 109.2, 77.7, 72.2, 66.6, 55.3, 39.3, 26.6, 25.2, 23.3; IR (neat): 2984.3, 2930.1, 2883.6, 1721.5, 1613.0, 1512.3, 1307.7, 1248.7, 1070.7, 1032.0, 846.0; $[\alpha]_D^{25} + 8.14$ (*c* 1.5, CHCl₃); HRMS-ESI(*m/z*) calculated for [M+Na]⁺: 331.1516, found 331.1521.



(6S)-6-((R)-2,2-Dimethyl-1,3-dioxolan-4-yl)-6-((4-methoxybenzyl)oxy)-1-(trimethylsilyl)hex-1-yn-3-ol (136a)

To a solution of trimethylsilylacetylene **137** (6.22 mL, 43.8 mmol) in THF (130 mL) at $-78\text{ }^{\circ}\text{C}$ was added dropwise *n*-BuLi (15.7 mL, 2.5 M in THF, 40 mmol). After 30 min in $-78\text{ }^{\circ}\text{C}$, a solution of aldehyde **136** (4.5 g, 15 mmol) in THF (16 mL) was added slowly. The solution was allowed to stir 1 h before saturated aqueous NH_4Cl was added. The aqueous phase was extracted with diethyl ether (3 x 80 mL). The combined organic phases were washed with brine, dried over anhydrous Na_2SO_4 , filtered, and concentrated. The residue was purified by flash chromatography (hexanes-ethyl acetate, 4:1, v/v) to provide alcohol **136a** (5.0 g, 13 mmol, 87%) as a colorless oil.

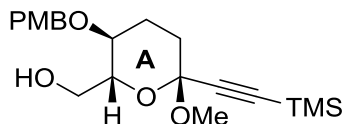
$R_f = 0.43$ (hexanes-ethyl acetate, 3:1 v/v); $^1\text{H NMR}$ (CDCl_3 , 400 MHz): δ 7.29 (m, 2H), 6.90 (d, $J = 8.5$ Hz, 2H), 4.57 (m, 2H), 4.40 (q, 1H), 4.08 (m, 2H), 3.88 (m, 1H), 3.82 (s, 3H), 3.57 (m, 1H), 1.90 (m, 5H), 1.43 (d, 3H), 1.36 (d, 3H), 0.19 (d, 9H); $^{13}\text{C NMR}$ (CDCl_3 , 125 MHz): δ 159.33, 159.27, 130.30, 130.06, 129.66, 129.51, 113.84, 113.82, 109.12, 109.09, 106.76, 106.61, 89.52, 89.42, 78.35, 78.32, 77.29, 71.99, 71.85, 66.86, 66.62, 62.70, 62.55, 55.23, 32.87, 32.44, 26.66, 26.60, 26.23, 25.66, 25.28, 25.26, -0.12, -0.15; IR (neat): 3441.4(broad), 2937.9, 1613.6, 1514.0, 1249.4, 1073.8, 843.5; HRMS-ESI(m/z) calculated for $[\text{M}+\text{Na}]^+$: 429.2068, found 429.2060.



(S)-6-((R)-2,2-Dimethyl-1,3-dioxolan-4-yl)-6-((4-methoxybenzyl)oxy)-1-(trimethylsilyl)hex-1-yn-3-one (138)

To a solution of **12a** (4.5 g, 11 mmol) in CH₂Cl₂ (100 mL) and DMSO (20 mL) at 0 °C was added Et₃N (9.2 mL, 67 mmol) and SO₃·Py (7.6g, 48 mmol) successively. After 2 h at 0 °C, saturated aqueous NH₄Cl (100 mL) was added. The aqueous phase was extracted with diethyl ether (3 x 80 mL). The combined organic phases were washed with brine, dried over anhydrous Na₂SO₄, filtered, and concentrated. The residue was purified by flash chromatography (hexanes-ethyl acetate, 5:1, v/v) to provide ketone **13** (3.7 g, 9.2 mmol, 83%) as colorless oil.

R_f = 0.57 (hexanes-ethyl acetate, 3:1, v/v); ¹H NMR (CDCl₃, 400 MHz): δ 7.27 (d, *J* = 8.6 Hz, 2H), 6.90 (d, *J* = 8.6 Hz, 2H), 4.53 (s, 2H), 4.07 (m, 2H), 3.85 (m, 1H), 3.82 (s, 3H), 3.53 (m, 1H), 2.71 (m, 2H), 2.06 (m, 1H), 1.87 (m, 1H), 1.43 (s, 3H), 1.36 (s, 3H), 0.26 (s, 9H); ¹³C NMR (CDCl₃, 125 MHz): δ 187.3, 159.3, 130.3, 129.5, 113.9, 109.2, 102.0, 97.8, 77.6, 72.2, 66.7, 55.3, 40.5, 26.6, 25.3, 24.8, -0.8; IR(neat): 2957.5, 2945.6, 2899.2, 1676.8, 1612.3, 1513.8, 1250.7, 1072.8, 847.1, 761.5; [α]_D²⁵ + 9.56 (*c* 0.5, CHCl₃); HRMS (ESI+) calculated for [M+Na]⁺: 427.1911, found 427.1903.

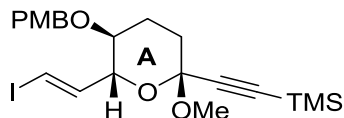


139

**((2*R*,3*S*,6*R*)-6-Methoxy-3-((4-methoxybenzyl)oxy)-6-
((trimethylsilyl)ethynyl)tetrahydro-2*H*-pyran-2-yl)methanol (139)**

To a solution of **138** (3.58 g, 8.86 mmol) in MeOH (30 mL) was added TsOH·H₂O (0.17 g, 0.89 mmol). After 2 h, the solution was diluted by diethyl ether before saturated aqueous NaHCO₃ was added. The aqueous phase was extracted with diethyl ether (3 x 50 mL). The combined organic phases was washed with brine, dried over anhydrous Na₂SO₄, filtered, and concentrated. The residue was purified by flash chromatography (hexanes-ethyl acetate, 8:1, v/v) to provide alcohol **139** (2.2 g, 5.8 mmol, 65%) as a colorless oil.

R_f = 0.37 (hexanes-ethyl acetate, 3:1, v/v); ¹H NMR (CDCl₃, 400 MHz): δ 7.26 (d, *J* = 8.5 Hz, 2H), 6.88 (d, *J* = 8.5 Hz, 2H), 4.43 (q_{AB}, Δ*v* = 64 Hz, *J*_{AB} = 11.2 Hz, 2H), 3.82 (s, 3H), 3.75 (m, 2H), 3.57 (m, 1H), 3.44 (td, *J* = 10.0 Hz, 4.4 Hz, 1H), 3.38 (s, 3H), 3.10 (m, 3H), 1.91 (m, 2H), 0.21 (s, 9H); ¹³C NMR (CDCl₃, 100 MHz): δ 159.3, 130.1, 129.3, 113.9, 101.9, 94.1, 89.0, 73.2, 72.5, 70.3, 62.7, 55.2, 50.4, 35.6, 24.3, -0.27; IR (neat): 3502(broad), 2957, 2899, 1612, 1513, 1250, 1152, 1089, 1040, 846, 760; [α]_D²⁵ + 6.84 (*c* 2.1, CHCl₃); HRMS-ESI(*m/z*) calculated for [M+Na]⁺: 401.1755, found 401.1763.



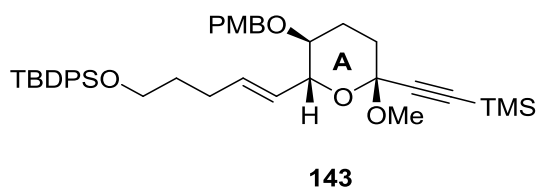
141

(((2*R*,5*S*,6*R*)-6-((*E*)-2-Iodovinyl)-2-methoxy-5-((4-methoxybenzyl)oxy)tetrahydro-2*H*-pyran-2-yl)ethynyl)trimethylsilane (141)

To a solution of **139** (1.0 g, 2.7 mmol) in CH₂Cl₂ (30mL) and DMSO (6 mL) at 0 °C was added *i*-Pr₂NEt (2.78 mL, 15.9 mmol), SO₃·Py (1.8 g, 11.4 mmol) sequentially. After 5 min at 0 °C, cold 1M aqueous HCl (10 mL) was added. The organic phase was neutralized by pH = 7 aqueous buffer. The aqueous phase was extracted with CH₂Cl₂ (3 x 30 mL). The combined organic phase was washed with brine, dried over anhydrous Na₂SO₄, filtered, and concentrated. The residue was purified by flash chromatography (hexanes-ethyl acetate, 4:1, v/v) to provide the aldehyde **140** as a colorless oil (0.99 g, 2.6 mmol, 96%).

A suspension of powdered anhydrous CrCl₂ (1.95 g, 15.9 mmol) was stirred in THF (24 mL) at 0 °C. A solution of the aldehyde **140** (0.99 g, 2.64 mmol) and CHI₃ (1.56 g, 3.96 mmol) in 1,4-dioxane (4 mL) was added drop-wise via cannula. The solution was allowed to warm to rt in 3 h. Then after stirring for 9 h, saturated aqueous NaHCO₃ was added. The aqueous phase was extracted with diethyl ether (3 x 30 mL). The combined organic phases were washed with brine, dried over anhydrous Na₂SO₄, filtered and concentrated. The residue was purified by flash chromatography (hexanes-ethyl acetate, 40:1, v/v) to provide vinyl iodide **141** (0.8 g, 2 mmol, 75%) as a colorless oil.

$R_f = 0.60$ (hexanes-ethyl acetate, 5:1, v/v); $^1\text{H NMR}$ (CDCl_3 , 400 MHz): δ 7.25 (d, $J = 8.6$ Hz, 2H), 6.92 (d, $J = 8.6$ Hz, 2H), 6.65 (dd, $J = 14.8$ Hz, 6.4 Hz, 1H), 6.51 (dd, $J = 14.8$ Hz, 1.2 Hz, 1H), 4.53 (q_{AB}, $\Delta\nu = 54$ Hz, $J_{AB} = 11.3$ Hz, 2H), 3.91 (ddd, $J = 6.2$ Hz, 3.3 Hz, 1.1 Hz, 1H), 3.83 (s, 3H), 3.36 (s, 3H), 3.21 (td, $J = 10$ Hz, 4.4 Hz, 1H), 2.11 (m, 1H), 1.91 (m, 3H), 0.20 (s, 9H); $^{13}\text{C NMR}$ (CDCl_3 , 100 MHz): δ 159.3, 143.2, 130.1, 129.4, 113.9, 101.7, 94.1, 89.1, 79.8, 75.2, 75.1, 70.8, 55.3, 50.5, 35.5, 24.8, -0.03; IR (neat): 2955, 1513, 1249, 1085, 1043, 944, 859, 844, 760; $[\alpha]_D^{25} + 6.57$ (c 1.6, CHCl_3); HRMS-ESI(m/z) calculated for $[\text{M}+\text{Na}]^+$: 523.0772, found 523.0765.

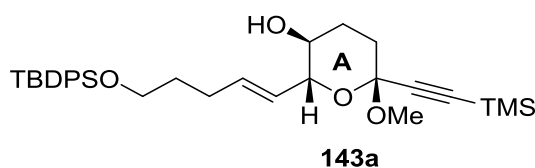


***tert*-Butyl(((*E*)-5-((2*R*,3*S*,6*R*)-6-methoxy-3-((4-methoxybenzyl)oxy)-6-((trimethylsilyl)ethynyl)tetrahydro-2*H*-pyran-2-yl)pent-4-en-1-yl)oxy)diphenylsilane (143)**

To a solution of allyl TBDPS ether **142** (720 mg, 2.4 mmol) in THF (13 mL) at 0 °C was slowly added 9-BBN (6.4 mL, 0.5 M in THF, 3.2 mmol). The solution was slowly warmed to rt and then stirred at rt for 2 h. To this solution was added solution of 3 M aqueous K_3PO_4 (1.06 mL, 1.2 mmol) in DMF (1.1 mL). After 30 min at rt, the above solution was added to a solution of vinyl iodide (600 mg, 1.2 mmol) and $\text{PdCl}_2(\text{dppf})\cdot\text{CH}_2\text{Cl}_2$ (98 mg, 0.12 mmol) via cannula. After 5 min stirring, the solution

was diluted with diethyl ether (10 mL) and H₂O (10 mL). The aqueous phase was extracted with diethyl ether (3 x 10 mL). The combined organic phases were washed with brine, dried over anhydrous Na₂SO₄, filtered and concentrated. The residue was purified by flash chromatography (hexanes-ethyl acetate, 40:1, v/v) to provide **143** (760 mg, 1.16 mmol, 95%) as a colorless oil.

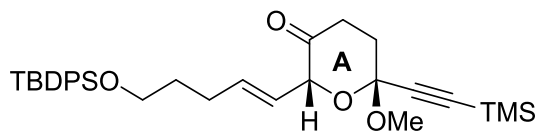
$R_f = 0.62$ (hexanes-ethyl acetate, 5:1, v/v); ¹H NMR (CDCl₃, 400 MHz): δ 7.69 (dd, $J = 7.8$ Hz, 1.6 Hz, 4H), 7.42 (m, 6H), 7.22 (d, $J = 8.6$ Hz, 2H), 6.86 (d, $J = 8.6$ Hz, 2H), 5.85 (dt, $J = 15.4$ Hz, 6.8 Hz, 1H), 5.52 (dd, $J = 15.2$ Hz, 7.6 Hz 1H), 4.50 (q_{AB}, $\Delta\nu = 25$ Hz, $J_{AB} = 11.3$ Hz, 2H), 3.88 (t, $J = 8.1$ Hz, 1H), 3.79 (s, 3H), 3.71 (t, $J = 6.3$ Hz, 2H), 3.38 (s, 3H), 3.20 (td, $J = 9.5$ Hz, 4.5 Hz, 1H), 2.22 (q, $J = 6.4$ Hz, 2H), 2.10 (m, 1H), 1.97 (m, 2H), 1.87 (m, 1H), 1.71 (m, 2H), 1.08 (s, 9H), 0.20 (s, 9H); ¹³C NMR (CDCl₃, 100 MHz): δ 159.1, 135.6, 134.9, 134.0, 130.5, 129.5, 129.3, 127.9, 127.6, 113.7, 102.3, 94.0, 88.5, 75.7, 74.6, 70.9, 63.5, 55.2, 50.4, 35.9, 31.9, 28.9, 26.9, 25.1, 19.2, -0.2; IR (neat): 2933.1, 2856.8, 1612.0, 1513.0, 1249.5, 1109.9, 844.2, 702.5; $[\alpha]_D^{25} + 4.32$ (c 1.6, CHCl₃); HRMS-ESI(m/z) calculated for $[M+Na]^+$: 693.3402, found 693.3434.



(2*R*,3*S*,6*R*)-2-((*E*)-5-((*tert*-Butyldiphenylsilyloxy)pent-1-en-1-yl)-6-methoxy-6-((trimethylsilyl)ethynyl)tetrahydro-2*H*-pyran-3-ol (143a)

To a solution of **143** (406 mg, 0.6 mmol) in CH₂Cl₂ (10 mL), pH = 7 aqueous buffer (1 mL), and *t*-BuOH (0.5 mL) was added DDQ (412 mg, 1.8 mmol). After stirring 10 min at rt, the solution was diluted with diethyl ether (10 mL) and saturated aqueous NaHCO₃ (15 mL). The aqueous phase was extracted with diethyl ether (3 x 15 mL). The combined organic phases were washed with brine, dried over anhydrous Na₂SO₄, filtered and concentrated. The residue was purified by flash chromatography (hexanes-ethyl acetate, 20:1, v/v) to provide **143a** (299 mg, 0.54 mmol, 90%) as a colorless oil.

R_f = 0.62 (hexanes-ethyl acetate, 3:1, v/v); ¹H NMR (CDCl₃, 400 MHz): δ 7.69 (dd, *J* = 7.7 Hz, 1.6 Hz, 4H), 7.42 (m, 6H), 5.87 (dt, *J* = 15.4 Hz, 6.6 Hz, 1H), 5.50 (dd, *J* = 15.6 Hz, 8.4 Hz, 1H), 3.71 (m, 1H), 3.40 (m, 4H), 2.23 (q, *J* = 6.8 Hz 2H), 2.12 (m, 1H), 2.06 (td, *J* = 13 Hz, 4.3 Hz, 1H), 1.94 (m, 1H), 1.85 (m, 1H), 1.70 (m, 2H), 1.54 (d, *J* = 3.0 Hz, 1H), 1.07 (s, 9H), 0.21 (s, 9H); ¹³C NMR (CDCl₃, 125 MHz): δ 137.2, 135.6, 134.0, 129.6, 127.6, 127.2, 102.1, 94.1, 88.8, 76.7, 68.6, 63.2, 50.5, 35.9, 31.7, 28.8, 26.9, 26.8, 19.2, -0.2; IR (neat): 3420.1 (broad), 3070.8, 2933.8, 2858.0, 1428.2, 1251.1, 1111.3, 1049.6, 944.6, 860.0, 702.1; [α]_D²⁵ + 5.48 (*c* 1.07, CHCl₃); HRMS-ESI(*m/z*) calculated for [M+Na]⁺: 573.2852, found 573.2827.

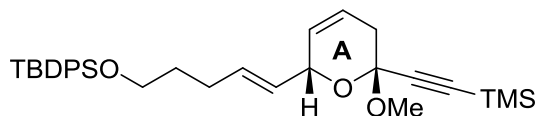


144

(2*R*,6*R*)-2-((*E*)-5-((*tert*-Butyldiphenylsilyloxy)pent-1-en-1-yl)-6-methoxy-6-((trimethylsilyl)ethynyl)dihydro-2*H*-pyran-3(4*H*)-one (144)

To a solution of **143a** (410 mg, 0.75 mmol) in CH₂Cl₂ (6 mL) and DMSO (2 mL) at 0 °C was added *i*-Pr₂NEt (0.77 mL, 4.5 mmol) and SO₃·Py (510 mg, 3.2 mmol) successively. After 10 min at 0 °C, cold 1M aqueous HCl (3 mL) was added. The organic phase was separated and neutralized with pH=7 aqueous buffer. Then the aqueous solution was extracted with CH₂Cl₂ (3 x 10 mL). The combined organic phases were washed with brine, dried over anhydrous Na₂SO₄, filtered and concentrated. The residue was purified by flash chromatography (hexanes-ethyl acetate, 15:1, v/v) to provide **144** (400 mg, 0.72 mmol, 96%) as a colorless oil.

R_f = 0.72 (hexanes-ethyl acetate, 5:1, v/v); ¹H NMR (CDCl₃, 500 MHz): δ 7.69 (dd, *J* = 7.7 Hz, 1.4 Hz, 4H), 7.42 (m, 6H), 5.78 (dt, *J* = 12.3 Hz, 5.3 Hz, 1H), 5.56 (dd, *J* = 12.4 Hz, 5.4 Hz, 1H), 4.44 (d, *J* = 6.9 Hz, 1H), 3.69 (t, *J* = 6.3 Hz, 2H), 3.49 (s, 3H), 2.59 (m, 3H), 2.31 (m, 1H), 2.23 (q, *J* = 5.6 Hz, 2H), 1.71 (m, 2H), 1.07 (s, 9H), 0.23 (s, 9H); ¹³C NMR (CDCl₃, 125 MHz): δ 207.6, 136.7, 135.5, 134.0, 129.5, 127.6, 122.8, 101.0, 94.8, 90.0, 77.1, 63.2, 51.4, 35.6, 33.7, 31.6, 28.8, 26.8, 19.2, -0.3; IR (neat): 3048.1, 2957.1, 2856.7, 1733.7, 1471.8, 1427.7, 1250.9, 1110.8, 1048.2, 932.3, 844.4, 702.5; [α]_D²⁵ + 10.8 (*c* 0.59, CHCl₃); HRMS-ESI(*m/z*) calculated for [M+Na]⁺: 571.2666, found 571.2670.



146

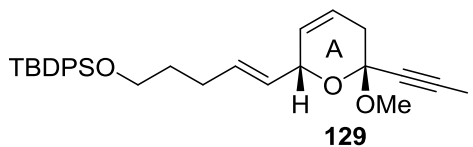
***tert*-Butyl(((*E*)-5-((2*R*,6*R*)-6-methoxy-6-((trimethylsilyl)ethynyl)-5,6-dihydro-2*H*-pyran-2-yl)pent-4-en-1-yl)oxy)diphenylsilane (**146**)**

To a solution of **17** (420 mg, 0.76 mmol) in THF (8 mL) at -78 °C was added Comins' reagent (450 mg, 1.14 mmol) and KHMDS (2.3 mL, 0.5 M in THF, 1.14 mmol) sequentially. After 10 min at -78 °C, pH = 7 aqueous buffer (8 mL) was added. The aqueous phase was extracted with diethyl ether (3 x 15 mL). The combined and organic phases were washed with brine, dried over anhydrous Na₂SO₄, filtered and concentrated. The residue was purified by flash chromatography (hexanes + 0.3% Et₃N, v/v) to provide crude product vinyl triflate **145** (477 mg, 0.70 mmol, 92%) as a pale yellow oil.

To a solution of the vinyl triflate **145** (477 mg, 0.70 mmol) in THF (7 mL) was added LiCl (294 mg, 7 mmol) and *n*Bu₃SnH (0.55 mL, 2.1 mmol). To the mixture was slowly added Pd(PPh₃)₄ (81 mg, 0.07 mmol). After stirring 10 min at rt, saturated aqueous NaHCO₃ (8 mL) was added. The aqueous phase was extracted with diethyl ether (3 x 10 mL). The combined organic phases were washed with brine, dried over Na₂SO₄, filtered and concentrated. The residue was purified by flash chromatography (hexanes-ethyl acetate, 200:1, v/v) to provide **146** (289 mg, 0.54 mmol, 77%) as a colorless oil.

R_f = 0.58 (hexanes-ethyl acetate, 10:1, v/v); ¹H NMR (CDCl₃, 400 MHz): δ 7.69 (dd, *J* = 7.7 Hz, 1.5 Hz, 4H), 7.42 (m, 6H), 5.73 (m, 2H), 5.62 (dt, *J* = 10.5 Hz, 1.3 Hz, 1H), 5.48 (dd, *J* = 15.3 Hz, 7.8 Hz, 1H), 4.50 (s-broad, 1H), 3.69 (t, *J* = 6.3 Hz, 2H), 3.52 (s, 3H), 2.72 (m, 1H), 2.34 (m, 1H), 2.18 (q, *J* = 7 Hz, 2H), 1.69 (m, 2H), 1.07 (s, 9H), 0.21 (s, 9H); ¹³C NMR (CDCl₃, 100 MHz): δ 135.6, 134.0, 133.9, 129.5, 128.6, 127.6, 127.5, 120.1, 102.2, 94.0, 89.2, 71.0, 63.3, 51.3, 36.1, 31.7, 28.6, 26.9, 19.2, -0.2; IR (neat):

3042.9, 2956.4, 1659.9, 1471.7, 1250.3, 1182.5, 1110.8, 1016.6, 863.5, 701.9, 613.4; $[\alpha]_D^{25} + 3.5$ (c 1.5, CHCl_3); HRMS-ESI(m/z) calculated for $[\text{M}+\text{Na}]^+$: 555.2727, found 555.2726.



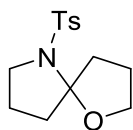
***tert*-Butyl(((*E*)-5-((2*R*,6*R*)-6-(iodoethynyl)-6-methoxy-5,6-dihydro-2*H*-pyran-2-yl)pent-4-en-1-yl)oxy)diphenylsilane (**129**)**

To a solution of **146** (87 mg, 0.16 mmol) in DMF (1.5 mL) at rt was added NIS (47 mg, 0.21 mmol) and AgOTf (36.1 mg, 0.16 mmol) sequentially. After stirring at rt, diethyl ether (3 mL) and saturated aqueous $\text{Na}_2\text{S}_2\text{O}_3$ (3 mL) was added. The aqueous phase was extracted with diethyl ether (3 x 5 mL). The combined organic phases were washed with brine, dried over Na_2SO_4 , filtered and concentrated. The residue was purified by flash chromatography (hexanes-ethyl acetate, 40:1, v/v) to provide **129** (79 mg, 0.13 mmol, 82%) as a colorless oil.

$R_f = 0.42$ (hexanes-ethyl acetate, 10:1, v/v); ^1H NMR (CDCl_3 , 400 MHz): δ 7.69 (dd, $J = 7.7$ Hz, 1.5 Hz, 4H), 7.42 (m, 6H), 5.73 (m, 2H), 5.62 (dt, $J = 10.4$ Hz, 1.2 Hz, 1H), 5.48 (dd, $J = 15$ Hz, 7.8 Hz, 1H), 4.49 (s-broad, 1H), 3.69 (t, $J = 6.3$ Hz, 2H), 3.52 (s, 3H), 2.72 (m, 1H), 2.39 (m, 1H), 2.18 (q, $J = 7.2$ Hz, 2H), 1.70 (m, 2H), 1.07 (s, 9H); ^{13}C NMR (CDCl_3 , 100 MHz): δ 135.6, 134.2, 134.0, 129.5, 128.3, 127.6, 127.5, 120.6, 95.0, 92.6, 71.1, 63.2, 51.6, 36.1, 31.7, 28.6, 26.9, 19.2, 3.8; IR (neat): 3069.7, 3042.9, 2930.9, 2855.5, 2180.9, 1660.0, 1588.9, 1470.6, 1427.2, 1232.0, 1182.4, 1110.2, 1016.2, 1036.6,

967.1, 822.9, 702.2, 505.5; $[\alpha]_D^{25} + 10.4$ (c 0.85, CHCl_3); HRMS-ESI(m/z) calculated for $[\text{M}+\text{Na}]^+$: 609.1298, found 609.1294.

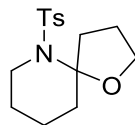
A typical procedure of gold-catalyzed spiroaminal formation: To a flask of gold (I) chloride (2 mg, 8 μmol) was added the solution of hydroxy sulfonamide **197** (45 mg, 0.16 mmol) in toluene (1.5 mL) through cannula. The reaction was stirred for 1 h before Et_3N (0.1 mL). The reaction mixture was directly separated by flash chromatography (hexanes-ethyl acetate, 40:1, v/v) to provide spiroaminal **198** (40 mg, 0.15 mmol, 91%) as colorless oil.



202 (85%)

6-Tosyl-1-oxa-6-azaspiro[4.4]nonane (202)

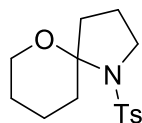
$R_f = 0.80$ (hexanes-ethyl acetate, 1:1, v/v); ^1H NMR (CDCl_3 , 400 MHz): δ 7.81 (d, $J = 8.3$ Hz, 2H), 7.27 (d, $J = 7.9$ Hz, 2H), 4.18 (q_{AB}, $J = 6.8$ Hz, 1H), 3.77 (m, 1H), 3.46 (m, 1H), 3.31 (m, 1H), 2.93 (m, 1H), 2.43 (s, 3H), 2.27 (m, 1H), 2.05 (m, 3H), 1.78 (m, 2H); ^{13}C NMR (CDCl_3 , 100 MHz): δ 142.8, 137.6, 129.2, 127.8, 103.5, 68.5, 49.1, 41.9, 37.0, 25.6, 22.1, 21.5; HRMS-ESI (m/z) calculated for $[\text{M}+\text{Na}]^+$: 304.0978, found: 304.0979



208 (90%)

6-Tosyl-1-oxa-6-azaspiro[4.5]decane (208)

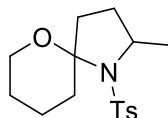
$R_f = 0.47$ (hexanes-ethyl acetate, 3:1, v/v); $^1\text{H NMR}$ (CDCl_3 , 400 MHz): δ 7.78 (d, $J = 8.3$ Hz, 2H), 7.27 (d, $J = 8.0$ Hz, 2H), 4.04 (m, 1H), 3.72 (m, 1H), 3.56 (m, 1H), 3.36 (m, 1H), 2.54 (m, 1H), 2.41 (s, 3H), 1.72 (m, 5H), 1.51 (m, 4H); $^{13}\text{C NMR}$ (CDCl_3 , 100 MHz): δ 142.3, 140.8, 129.1, 127.0, 97.8, 68.2, 45.6, 36.7, 35.8, 25.0, 24.6, 22.5, 21.4; HRMS-ESI (m/z) calculated for $[\text{M}+\text{Na}^+]$: 318.1134, found: 318.1132



212 (94%)

1-Tosyl-6-oxa-1-azaspiro[4.5]decane (212)

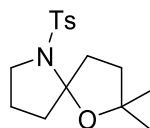
$R_f = 0.43$ (hexanes-ethyl acetate, 3:1, v/v); $^1\text{H NMR}$ (CDCl_3 , 400 MHz): δ 7.85 (d, $J = 8.3$ Hz, 2H), 7.27 (d, $J = 8.0$ Hz, 2H), 3.82 (m, 1H), 3.50 (m, 2H), 3.35 (m, 1H), 2.88 (td, $J = 13.2$ Hz, 4.4 Hz, 1H), 2.42 (s, 3H), 2.25 (m, 1H), 1.89 (m, 1H), 1.76 (m, 3H), 1.67 (m, 2H), 1.54 (m, 2H); $^{13}\text{C NMR}$ (CDCl_3 , 100 MHz): δ 142.6, 137.8, 128.9, 128.3, 96.3, 64.6, 49.4, 34.7, 34.5, 25.0, 22.1, 21.5, 21.3; HRMS-ESI (m/z) calculated for $[\text{M}+\text{Na}^+]$: 318.1134, found: 318.1135



214 (98%)

7-Methyl-1-tosyl-6-oxa-1-azaspiro[4.5]decane (214)

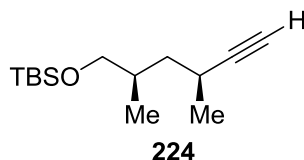
$R_f = 0.50$ (hexanes-ethyl acetate, 3:1, v/v); $^1\text{H NMR}$ (CDCl_3 , 400 MHz): δ 7.87 (d, $J = 8.2$ Hz, 2H), 7.23 (d, $J = 8.1$ Hz, 2H), 3.56 (m, 1H), 3.49 (m, 1H), 3.31 (m, 1H), 2.76 (td, $J = 13.3$ Hz, 4.6 Hz, 1H), 2.41 (s, 3H), 2.15 (m, 1H), 1.86 (m, 2H), 1.78 (m, 2H), 1.67 (m, 1H), 1.51 (m, 2H), 1.05 (d, $J = 6.1$ Hz, 3H); $^{13}\text{C NMR}$ (CDCl_3 , 100 MHz): δ 142.4, 137.6, 128.7, 128.5, 96.7, 70.5, 49.3, 35.2, 34.1, 32.4, 22.2, 21.8, 21.5, 21.4; HRMS-ESI (m/z) calculated for $[\text{M}+\text{Na}^+]$: 332.1291, found: 332.1293



204 (83%)

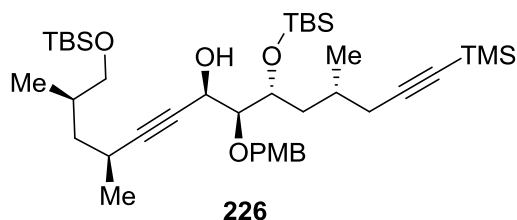
2,2-Dimethyl-6-tosyl-1-oxa-6-azaspiro[4.4]nonane (204)

$R_f = 0.75$ (hexanes-ethyl acetate, 2:1, v/v); $^1\text{H NMR}$ (CDCl_3 , 400 MHz): δ 7.88 (d, $J = 8.3$ Hz, 2H), 7.26 (d, $J = 8.0$ Hz, 2H), 3.38 (m, 1H), 3.27 (m, 1H), 3.02 (m, 1H), 2.41 (s, 3H), 2.19 (m, 2H), 2.02 (m, 2H), 1.82 (m, 3H), 1.40 (s, 3H), 1.21 (s, 3H); $^{13}\text{C NMR}$ (CDCl_3 , 100 MHz): δ 142.7, 137.8, 129.1, 127.7, 103.1, 82.3, 49.0, 43.5, 37.3, 37.1, 28.9, 28.3, 21.9, 21.5; HRMS-ESI (m/z) calculated for $[\text{M}+\text{Na}^+]$: 332.1291, found: 332.1290



***tert*-Butyl(((2*R*,4*S*)-2,4-dimethylhex-5-yn-1-yl)oxy)dimethylsilane (224)**

To a solution of vinyl bromide **223** (1.6 g, 4.0 mmol) in THF (50 mL) at - 78 °C was added drop-wise *n*-BuLi (3.3 mL, 2.5 M in Hexane, 8.1 mmol). After 30 min, water (0.7 mL, 40 mmol) was added drop-wise. The mixture was allowed to stir for 30 min before saturated aqueous NH₄Cl (40 mL) was added. The aqueous was extracted with diethyl ether (3 x 40 mL). The combined organic phases were dried over anhydrous Na₂SO₄, filtered, and concentrated. The residue was purified by flash chromatography (hexanes-ethyl acetate, 80:1, v/v) to provide alkyne **217** (0.96 g, 4.0 mmol, 99%) as a colorless oil. *R*_f = 0.85 (Hexanes-Ethyl acetate, 10:1, v/v); ¹H NMR (CDCl₃, 400 MHz): δ 3.47 (m, 2H), 2.54 (m, 1H), 2.04 (d, *J* = 2.4 Hz, 1H), 1.88 (m, 1H), 1.62 (m, 1H), 1.22 (d, *J* = 6.8 Hz, 3H), 1.15 (m, 1H), 0.92 (m, 12H), 0.06 (s, 6H); ¹³C NMR (CDCl₃, 100 MHz): δ 88.89, 68.61, 68.20, 40.57, 33.88, 25.95, 23.46, 21.69, 18.35, 16.17, -5.36; IR (neat): 3312, 2929, 2856, 1471, 1255, 1093, 836, 774, 628; [α]_D²⁵ + 16.4 (c 1.91, CHCl₃); HRMS-ESI (*m/z*) calculated for [M+ Na⁺]: 263.1802, found: 263.1801.

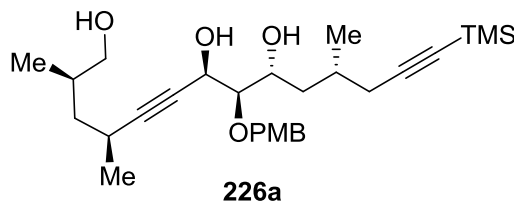


(5*R*,6*S*,7*R*,10*S*,12*R*)-6-((4-methoxybenzyl)oxy)-2,2,3,3,10,12,15,15,16,16-decamethyl-5-((*R*)-2-methyl-5-(trimethylsilyl)pent-4-yn-1-yl)-4,14-dioxo-3,15-disilaheptadec-8-yn-7-ol (226)

To a flask of Zn(OTf)₂ (0.8 g, 2.2 mmol, pre-dried overnight 120 °C under house vacuum) was added ligand (0.37 g, 2.2 mmol). The mixture was then dried under house vacuum at rt for 30 min before toluene (3 mL) and Et₃N (0.3 mL, 2.2 mmol) was added. The resulting slurry was then stirred for 2 h. The solution of Alkyne **224** (0.49 g, 2.2 mmol) in toluene (1 mL) was added drop-wise. The mixture was allowed to stirred for 1 h before the solution of aldehyde **225** (0.17 g, 0.42 mmol) in toluene (1 mL) was added through cannula. The mixture was stirred for 48 h before saturated aqueous NaHCO₃ (5 mL) was added. The aqueous phase was extracted with diethyl ether (3 x 5 mL). The combined organic phases were dried over anhydrous Na₂SO₄, filtered, and concentrated. The residue was purified by flash chromatography (hexanes-ethyl acetate, 20:1, v/v) to provide alkyne **226** (0.2 g, 0.28 mmol, 69%) as a colorless oil.

R_f = 0.4 (Hexanes-Ethyl acetate, 5:1, v/v); ¹H NMR (CDCl₃, 400 MHz): δ 7.34 (d, *J* = 8.6 Hz, 2H), 6.90 (d, *J* = 8.6 Hz, 2H), 4.86 (q_{AB}, Δ*v* = 72 Hz, *J* = 10.8 Hz, 2H), 4.39 (m, 1H), 4.05 (m, 1H), 3.83 (s, 3H), 3.55 (dd, *J* = 6.3 Hz, 3.1 Hz, 1H), 3.47 (m, 2H), 2.90 (d, *J* = 3.8 Hz, 1H), 2.63 (m, 1H), 2.24 (m, 2H), 1.91 (m, 1H), 1.61 (m, 3H), 1.24 (d, *J* = 6.7 Hz, 3H), 1.17 (m, 1H), 1.04 (d, *J* = 6.7 Hz, 3H), 0.92 (m, 21H), 0.16 (m, 15H), 0.06 (s, 6H); ¹³C NMR (CDCl₃, 100 MHz): δ 159.35, 130.46, 129.61, 113.86, 113.81, 105.41, 90.79, 85.89, 78.94, 74.26, 71.29, 68.56, 62.02, 55.25, 40.67, 39.26, 33.72, 28.67, 26.53, 25.95, 25.91, 23.67, 21.61, 20.42, 18.33, 17.98, 16.32, 0.15, -4.03, -4.60, -5.39; IR (neat): 3460,

2956, 1514, 1462, 1249, 1097, 1035, 839, 775; $[\alpha]_D^{25}$ - 1.68 (c 1.41, CHCl₃); HRMS-ESI (m/z) calculated for $[M+Na^+]$: 739.4580, found: 739.4578.

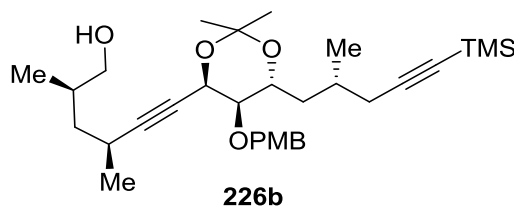


(2*R*,4*S*,7*R*,8*R*,9*R*,11*R*)-8-((4-Methoxybenzyl)oxy)-2,4,11-trimethyl-14-(trimethylsilyl)tetradeca-5,13-diyne-1,7,9-triol (226a**)**

To a solution of **226** (120 mg, 0.16 mmol) in MeOH (1 mL) was added TsOH•H₂O (3 mg, 0.02 mmol). The mixture was allowed to stir 3.5 h before diethyl ether (4 mL) and saturated aqueous NaHCO₃ (4 mL) was added. The aqueous phase was extracted by diethyl ether (3 x 5 mL). The combined organic phases were dried over anhydrous Na₂SO₄, filtered, and concentrated. The residue was purified by flash chromatography (hexanes-ethyl acetate, 1:1, v/v) to provide triol **226a** (72 mg, 0.15 mmol, 90%) as a colorless oil.

R_f = 0.5 (Hexanes-Ethyl acetate, 1:1, v/v); ¹H NMR (CDCl₃, 400 MHz): δ 7.31 (d, J = 8.6 Hz, 2H), 6.89 (d, J = 8.6 Hz, 2H), 4.78 (q_{AB}, $\Delta\nu$ = 52 Hz, J = 11.1 Hz, 2H), 4.46 (br, 1H), 4.06 (m, 1H), 3.81 (s, 3H), 3.61 (m, 4H), 3.03 (br, 1H), 2.61 (m, 3H), 1.97 (m, 1H), 1.69 (m, 2H), 1.41 (m, 1H), 1.21 (d, J = 6.8 Hz, 3H), 1.13 (m, 1H), 1.04 (d, J = 6.7 Hz, 3H), 0.91 (d, J = 6.7 Hz, 3H), 0.16 (s, 9H); ¹³C NMR (CDCl₃, 100 MHz): δ 159.40, 130.07, 129.64, 113.86, 106.22, 90.65, 85.90, 83.69, 79.60, 73.61, 69.69, 68.11, 62.68, 55.26, 40.72, 39.59, 34.26, 29.12, 25.97, 24.05, 21.75, 20.79, 16.30, 0.11; IR (neat): 3373, 2956,

2872, 2171, 1514, 1458, 1247, 1089, 1035, 842; $[\alpha]_D^{25} + 28.1$ (c 1.0, CHCl₃); HRMS-ESI (m/z) calculated for $[M+Na]^+$: 511.2850, found: 511.2851.

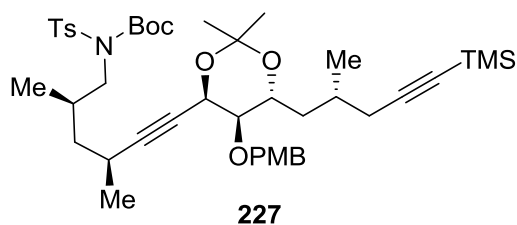


(2*R*,4*S*)-6-((4*R*,5*R*,6*R*)-5-((4-methoxybenzyl)oxy)-2,2-dimethyl-6-((*R*)-2-methyl-5-(trimethylsilyl)pent-4-yn-1-yl)-1,3-dioxan-4-yl)-2,4-dimethylhex-5-yn-1-ol (226b)

To a solution of **226a** (0.18 g, 0.37 mmol) in CH₂Cl₂ (4 mL) was added PPTS (2 mg, 3.7 μmol) and Dimethoxy propane (0.45 mL, 3.7 mmol). The mixture was allowed to stir 12 h before saturated aqueous NaHCO₃ (4 mL) was added. The aqueous phase was extracted by diethyl ether (3 x 5 mL). The combined organic phases were dried over anhydrous Na₂SO₄, filtered, and concentrated. The residue was dissolved in MeOH (1 mL), and the solution was added PPTS (2 mg, 3.7 μmol). The mixture was stirred 5 min before saturated aqueous NaHCO₃ (4 mL) was added. The aqueous phase was extracted by diethyl ether (3 x 5 mL). The combined organic phases were dried over anhydrous Na₂SO₄, filtered, and concentrated. The residue was purified by flash chromatography (hexanes-ethyl acetate, 8:1, v/v) to provide **226b** (160 mg, 0.31 mmol, 83%) as a colorless oil.

$R_f = 0.3$ (Hexanes-Ethyl acetate, 3:1, v/v); ¹H NMR (CDCl₃, 400 MHz): δ 7.26 (d, $J = 8.6$ Hz, 2H), 6.87 (d, $J = 8.6$ Hz, 2H), 4.75 (q_{AB}, $\Delta\nu = 105$ Hz, $J = 11.4$ Hz, 2H), 4.73 (m, 1H), 3.84 (m, 1H), 3.79 (s, 3H), 3.42 (d, $J = 5.9$ Hz, 2H), 3.32 (dd, $J = 8.1$ Hz, 4.7 Hz, 1H), 2.59

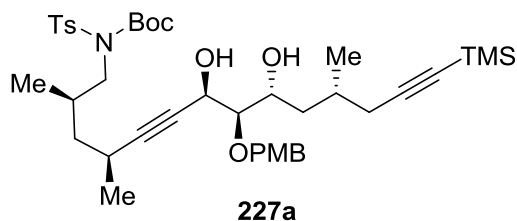
(m, 1H), 2.25 (m, 2H), 1.87 (m, 1H), 1.63 (m, 3H), 1.54 (s, 3H), 1.32 (s, 3H), 1.28 (m, 1H), 1.21 (d, $J = 6.8$ Hz, 3H), 1.13 (m, 1H), 1.01 (d, $J = 6.7$ Hz, 3H), 0.91 (d, $J = 6.7$ Hz, 3H), 0.13 (s, 9H); ^{13}C NMR (CDCl_3 , 100 MHz): δ 159.23, 130.18, 129.38, 113.66, 105.95, 100.49, 92.37, 85.60, 78.64, 76.75, 72.07, 68.74, 68.05, 63.60, 55.22, 40.33, 38.75, 34.23, 29.01, 27.10, 26.17, 24.10, 23.41, 21.54, 20.12, 16.33, 0.13; IR (neat): 3464, 2958, 2171, 1610, 1514, 1458, 1379, 1247, 1037, 842; $[\alpha]_{\text{D}}^{25} + 68.7$ (c 1.0, CHCl_3); HRMS-ESI (m/z) calculated for $[\text{M} + \text{Na}^+]$: 551.3163, found: 551.3162.



***tert*-Butyl((2*R*,4*S*)-6-((4*R*,5*R*,6*R*)-5-((4-methoxybenzyl)oxy)-2,2-dimethyl-6-((*R*)-2-methyl-5-(trimethylsilyl)pent-4-yn-1-yl)-1,3-dioxan-4-yl)-2,4-dimethylhex-5-yn-1-yl)(tosyl)carbamate (**227**)**

To a solution of **226b** (0.16 g, 0.31 mmol) in THF (4 mL) was added Ph_3P (357 mg, 1.4 mmol), NHTsBoc (328 mg, 1.24 mmol), and DIAD (0.2 mL, 1.1 mmol) sequentially. The mixture was allowed to stir 1h before saturated aqueous NH_4Cl (4 mL) was added. The aqueous phase was extracted by diethyl ether (3 x 5 mL). The combined organic phases were dried over anhydrous Na_2SO_4 , filtered, and concentrated. The residue was purified by flash chromatography (hexanes-ethyl acetate, 15:1, v/v) to provide **227** (210 mg, 0.31 mmol, 89%) as a colorless oil.

$R_f = 0.6$ (Hexanes-Ethyl acetate, 3:1, v/v); $^1\text{H NMR}$ (CDCl_3 , 400 MHz): δ 7.81 (d, $J = 8.3$ Hz, 2H), 7.31 (m, 4H), 6.88 (d, $J = 8.6$ Hz, 2H), 4.81 (q_{AB}, $\Delta\nu = 122$ Hz, $J = 11.4$ Hz, 2H), 4.77 (m, 2H), 3.80 (m, 4H), 3.73 (m, 2H), 3.33 (dd, $J = 7.9$ Hz, 4.6 Hz, 1H), 2.66 (m, 1H), 2.43 (s, 3H), 2.34 (m, 1H), 2.23 (m, 1H), 2.07 (m, 1H), 1.85 (m, 1H), 1.62 (m, 2H), 1.54 (s, 3H), 1.33 (m, 13H), 1.23 (d, $J = 6.8$ Hz, 3H), 1.01 (d, $J = 6.7$ Hz, 3H), 0.95 (d, $J = 6.7$ Hz, 3H), 0.15 (s, 9H); $^{13}\text{C NMR}$ (CDCl_3 , 100 MHz): δ 159.22, 151.26, 143.90, 137.53, 130.33, 129.55, 129.21, 127.92, 113.66, 106.05, 100.56, 91.80, 85.52, 83.95, 79.08, 76.96, 72.29, 69.06, 63.55, 55.24, 52.49, 41.09, 38.91, 31.72, 31.55, 29.15, 27.82, 26.74, 26.29, 23.81, 23.52, 21.54, 21.31, 20.12, 16.90, 14.08, 0.16; IR (neat): 2960, 1728, 1514, 1355, 1249, 1155, 1089, 842; $[\alpha]_D^{25} + 20.1$ (c 1.33, CHCl_3); HRMS-ESI (m/z) calculated for $[\text{M} + \text{Na}^+]$: 804.3936, found: 804.3938.

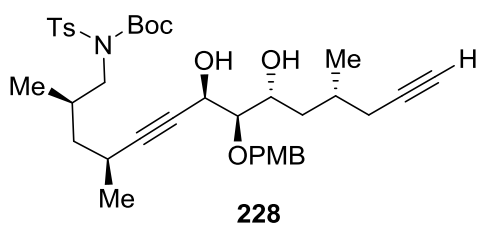


***tert*-Butyl((2*R*,4*S*,7*R*,8*R*,9*R*,11*R*)-7,9-dihydroxy-8-((4-methoxybenzyl)oxy)-2,4,11-trimethyl-14-(trimethylsilyl)tetradeca-5,13-diyn-1-yl)(tosyl)carbamate (**227a**)**

To a solution of **227** (60 mg, 76 μmmol) in MeOH (1.5 mL) was added TsOH \cdot H₂O (1.2 mg, 7.6 μmmol). The mixture was allowed to stir 10 min before diethyl ether (4 mL) and saturated aqueous NaHCO₃ were added. The aqueous phase was extracted by diethyl ether (3 x 5 mL). The combined organic phases were dried over anhydrous Na₂SO₄,

filtered, and concentrated. The residue was purified by flash chromatography (hexanes-ethyl acetate, 8:1, v/v) to provide **227a** (60 mg, 7.6 μ mol, 99%) as a colorless oil.

R_f = 0.44 (Hexanes-Ethyl acetate, 2:1, v/v); ^1H NMR (CDCl_3 , 400 MHz): δ 7.79 (d, J = 8.4 Hz, 2H), 7.32 (m, 4H), 6.88 (d, J = 8.6 Hz, 2H), 4.74 (q_{AB}, $\Delta\nu$ = 24 Hz, J = 11.2 Hz, 2H), 4.54 (m, 1H), 4.01 (m, 1H), 3.81 (s, 3H), 3.73 (m, 2H), 3.47 (t, J = 5.2 Hz, 1H), 3.18 (br, 1H), 2.88 (br, 1H), 2.59 (m, 1H), 2.44 (s, 3H), 2.38 (m, 2H), 2.27 (m, 1H), 2.18 (m, 1H), 1.97 (m, 1H), 1.61 (m, 2H), 1.48 (m, 1H), 1.33 (s, 9H), 1.25 (d, J = 6.8 Hz, 3H), 1.03 (d, J = 6.8 Hz, 3H), 0.98 (d, J = 6.8 Hz, 3H), 0.15 (s, 9H); ^{13}C NMR (CDCl_3 , 100 MHz): δ 159.32, 151.31, 144.15, 137.38, 130.33, 129.66, 129.24, 127.82, 113.83, 106.09, 90.14, 85.73, 84.36, 84.10, 79.71, 73.69, 69.91, 62.78, 55.24, 52.98, 41.59, 39.19, 32.20, 28.93, 27.82, 26.04, 23.96, 21.68, 21.57, 20.70, 16.77, 0.14; IR (neat): 3527, 2958, 1728, 1514, 1354, 1249, 1153, 1087, 842; $[\alpha]_D^{25}$ + 19.0 (c 1.33, CHCl_3); HRMS-ESI (m/z) calculated for $[\text{M} + \text{Na}^+]$: 764.3623, found: 764.3625.

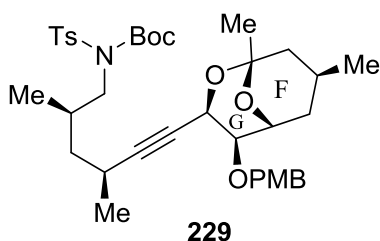


***tert*-Butyl((2*R*,4*S*,7*R*,8*R*,9*R*,11*R*)-7,9-dihydroxy-8-((4-methoxybenzyl)oxy)-2,4,11-trimethyltetradeca-5,13-diyn-1-yl)(tosyl)carbamate (**228**)**

To a solution of **227a** (80 mg, 0.1 mmol) in THF (2 mL) was added TBAF (0.4 mL, 0.3 mmol, 1 M solution in THF). The reaction was allowed to stir 10 min before saturated aqueous NH_4Cl (3 mL) was added. The aqueous phase was extracted by diethyl ether (3 x

5 mL). The combined organic phases were dried over anhydrous Na₂SO₄, filtered, and concentrated. The residue was purified by flash chromatography (hexanes-ethyl acetate, 8:1, v/v) to provide **228** (60 mg, 86 μmol, 86%) as a colorless oil.

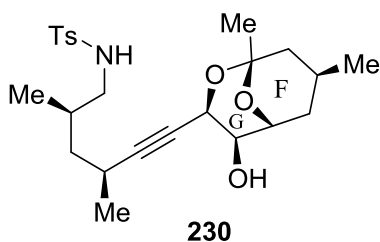
R_f = 0.1 (Hexanes-Ethyl acetate, 3:1, v/v); ¹H NMR (CDCl₃, 400 MHz): δ 7.78 (d, *J* = 8.4 Hz, 2H), 7.31 (m, 4H), 6.88 (d, *J* = 8.6 Hz, 2H), 4.76 (q_{AB}, Δ*v* = 29 Hz, *J* = 11.2 Hz, 2H), 4.53 (d, *J* = 3.5 Hz, 2H), 4.01 (m, 1H), 3.81 (s, 3H), 3.73 (d, *J* = 7.6 Hz, 2H), 3.47 (t, *J* = 5 Hz, 1H), 3.26 (br, 1H), 2.91 (br, 1H), 2.66 (m, 1H), 2.45 (s, 3H), 2.38 (m, 1H), 2.28 (m, 1H), 2.15 (m, 1H), 1.97 (m, 1H), 1.93 (t, *J* = 2.6 Hz, 1H), 1.63 (m, 2H), 1.46 (m, 1H), 1.33 (s, 9H), 1.25 (d, *J* = 6.8 Hz, 3H), 1.05 (d, *J* = 6.8 Hz, 3H), 0.98 (d, *J* = 6.8 Hz, 3H); ¹³C NMR (CDCl₃, 100 MHz): δ 159.3, 151.3, 144.2, 137.4, 130.3, 129.7, 127.8, 113.8, 90.2, 84.4, 83.9, 79.6, 73.6, 70.0, 69.4, 62.9, 55.2, 53.0, 41.6, 38.9, 32.2, 28.6, 27.8, 24.5, 24.0, 21.7, 21.6, 20.6, 16.7; IR (neat): 3527, 2962, 2929, 1728, 1514, 1352, 1249, 1155, 1087, 842; [α]_D²⁵ + 20.0 (c 1.0, CHCl₃); HRMS-ESI (*m/z*) calculated for [M+ Na⁺]: 692.3228, found: 692.3229.



***tert*-butyl((2*R*,4*S*)-6-((1*R*,3*R*,4*R*,5*R*,7*S*)-4-((4-methoxybenzyl)oxy)-1,7-dimethyl-2,9-dioxabicyclo[3.3.1]nonan-3-yl)-2,4-dimethylhex-5-yn-1-yl)(tosyl)carbamate (229)**

To a flask of AuCl (1.4 mg, 6 μ mol) was added the solution of **228** (40 mg, 59 μ mol) and PPTS (1.5 mg, 6 μ mo) in CH₂Cl₂ (2 mL). The mixture was allowed to stir 10 min before Et₃N (0.02 mL) was added. The mixture was purified by flash chromatography (hexanes-ethyl acetate, 8:1, v/v) to provide **229** (34 mg, 51 μ mol, 85%) as a colorless oil.

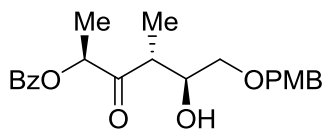
R_f = 0.62 (Hexanes-Ethyl acetate, 3:1, v/v); ¹H NMR (CDCl₃, 400 MHz): δ 7.83 (d, J = 8.4 Hz, 2H), 7.31 (m, 4H), 6.89 (d, J = 8.6 Hz, 2H), 4.88 (dd, J = 6.5 Hz, 1.6 Hz, 1H), 4.45 (q_{AB}, Δv = 80 Hz, J = 11.5 Hz, 2H), 4.19 (t, J = 2.5 Hz, 1H), 3.81 (s, 3H), 3.76 (m, 2H), 3.59 (dd, J = 6.5 Hz, 2.5 Hz, 1H), 2.70 (m, 1H), 2.43 (s, 3H), 2.38 (m, 1H), 1.98 (m, 1H), 1.75 (dd, J = 13.2 Hz, 4.0 Hz, 1H), 1.59 (m, 1H), 1.49 (m, 4H), 1.34 (m, 10H), 1.25 (m, 5H), 0.97 (d, J = 6.7 Hz, 3H), 0.88 (d, J = 6.5 Hz, 3H); ¹³C NMR (CDCl₃, 100 MHz): δ 159.2, 151.3, 143.8, 137.6, 130.2, 129.3, 129.2, 127.9, 113.7, 97.9, 90.0, 83.9, 78.5, 75.9, 73.7, 70.7, 61.4, 55.3, 52.6, 43.3, 41.2, 35.8, 31.8, 28.2, 27.8, 23.8, 22.4, 22.1, 21.6, 21.5, 16.8; IR (neat): 2954, 1726, 1354, 1514, 1249, 1153, 1087, 842; [α]_D²⁵ + 40 (c 0.5, CHCl₃); HRMS-ESI (m/z) calculated for [M+ Na⁺]: 692.3228, found: 692.3226.



***N*-((2*R*,4*S*)-6-((1*R*,3*R*,4*R*,5*R*,7*S*)-4-hydroxy-1,7-dimethyl-2,9-dioxabicyclo[3.3.1]nonan-3-yl)-2,4-dimethylhex-5-yn-1-yl)-4-methylbenzenesulfonamide (230)**

To a cooled (0 °C) solution of **229** (140 mg, 0.21 mmol) in CH₂Cl₂ (3 mL) was added TFA (0.6 mL) slowly. The mixture was allowed to warm up to rt. After stirring 2.5 h, the reaction was added saturated aqueous NaHCO₃ (5 mL) and diethyl ether (5 mL). The aqueous phase was extracted by diethyl ether (3 x 5 mL). The combined organic phases were dried over anhydrous Na₂SO₄, filtered, and concentrated. The residue was purified by flash chromatography (hexanes-ethyl acetate, 3:1, v/v) to provide **230** (90 mg, 190 μmol, 93%) as a colorless oil.

R_f = 0.2 (Hexanes-Ethyl acetate, 2:1, v/v); ¹H NMR (CDCl₃, 400 MHz): δ 7.77 (d, *J* = 8.3 Hz, 2H), 7.34 (d, *J* = 8.0 Hz, 2H), 4.66 (br, 1H), 4.61 (dd, *J* = 9.5 Hz, 1.9 Hz, 1H), 4.34 (t, *J* = 3.7 Hz, 1H), 4.11 (m, 1H), 2.88 (m, 3H), 2.51 (m, 1H), 2.44 (s, 3H), 2.13 (m, 1H), 1.88 (m, 3H), 1.47 (m, 5H), 1.31 (m, 1H), 1.16 (m, 4H), 0.95 (d, *J* = 6.6 Hz, 3H), 0.89 (d, *J* = 6.7 Hz, 3H); ¹³C NMR (CDCl₃, 100 MHz): δ 143.4, 136.9, 129.7, 127.1, 108.8, 90.8, 83.4, 78.1, 76.0, 61.6, 49.3, 43.3, 41.0, 32.7, 31.9, 24.9, 24.7, 23.9, 21.9, 21.54, 21.50, 17.2; IR (neat): 3481, 3410, 2956, 1448, 1327, 1159, 843; [α]_D²⁵ + 38 (c 0.5, CHCl₃); HRMS-ESI (*m/z*) calculated for [M+ Na⁺]: 472.2128, found: 472.2129.

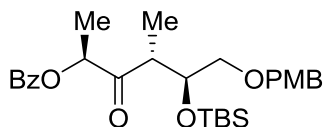


238

(2S,4R,5S)-5-hydroxy-6-((4-methoxybenzyl)oxy)-4-methyl-3-oxohexan-2-yl benzoate (238)

To a cooled (- 78 °C) solution of *c*-Hex₂BCl (0.32 g, 1.5 mmol) in Et₂O (4 ml) was added Me₂Net (0.2 g, 1.8 mmol), followed by ketone **237** (0.2 g, 1.0 mmol) in Et₂O (4 mL). The reaction mixture was warmed to 0 °C and stirred for 2 h before cooling to - 78 °C. The aldehyde **236** (0.7 g, 4.0 mmol) in Et₂O (2 mL) was added and the stirring continued for another 2 h, before being transferred to a freezer (- 20 °C) for 14 h. the reaction was quenched at 0 °C by addition of MeOH (4 mL), and pH = 7 aqueous buffer (4 mL). H₂O₂ (4 mL, 30%) was then added and the stirring continued for 1 h before the addition of H₂O (30 mL) and CH₂Cl₂ (30 mL). The aqueous phase was then extracted by CH₂Cl₂ (3 x 30 mL). The organic phases were dried over anhydrous MgSO₄, filtered, and concentrated. The residue was purified by flash chromatography (hexanes-ethyl acetate, 5:1, v/v) to provide alcohol **238** (0.38 g, 0.98 mmol, 98%) as a colorless oil.

R_f = 0.2 (Hexanes-Ethyl acetate, 3:1, v/v); ¹H NMR (CDCl₃, 400 MHz): δ 8.07 (m, 2H), 7.54 (t, *J* = 7.4 Hz, 1H), 7.42 (t, *J* = 7.8 Hz, 2H), 7.21 (d, *J* = 8.5 Hz, 2H), 6.86 (d, *J* = 8.5 Hz, 2H), 5.43 (q, *J* = 7.0 Hz, 1H), 4.46 (q_{AB}, Δ*v* = 24 Hz, *J* = 11.5 Hz, 2H), 3.95 (m, 1H), 3.75 (s, 3H), 3.50 (m, 2H), 3.32 (br, 1H), 3.09 (m, 1H), 1.54 (d, *J* = 7.0 Hz, 3H), 1.17 (d, *J* = 7.1 Hz, 3H); ¹³C NMR (CDCl₃, 100 MHz): δ 210.3, 165.4, 159.0, 132.9, 129.6, 129.4, 129.2, 129.1, 128.1, 113.5, 74.5, 72.7, 72.0, 71.3, 54.9, 44.4, 15.1, 13.5; IR (neat): 3527, 2935, 1717, 1514, 1250, 1114, 1002, 819, 714; [α]_D²⁵ + 12.1 (c 2.1, CHCl₃); HRMS-ESI (*m/z*) calculated for [M+ Na⁺]: 409.1622, found: 409.1621.

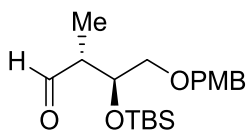


238a

(2S,4R,5S)-5-((tert-butyldimethylsilyl)oxy)-6-((4-methoxybenzyl)oxy)-4-methyl-3-oxohexan-2-yl benzoate (238a)

To a cooled (- 78 °C) solution of β -hydroxy ketone **238** (0.38 g, 0.98 mmol) in CH₂Cl₂ (10 mL) was added 2,6- lutidine (0.46 ml, 3.92 mmol) and TBSOTf (0.68 mL, 2.94 mmol) sequentially. The mixture was allowed to stir 1 h before saturated aqueous NaHCO₃ (10 mL) was added. The aqueous phase was then extracted by diethyl ether (3 x 10 mL). The combined organic phases were washed with brine. The organic phases were dried over anhydrous Na₂SO₄, filtered, and concentrated. The residue was purified by flash chromatography (hexanes-ethyl acetate, 30:1, v/v) to provide **238a** (0.43 g, 0.86 mmol, 89%) as a colorless oil.

R_f = 0.68 (Hexanes-Ethyl acetate, 3:1, v/v); ¹H NMR (CDCl₃, 400 MHz): δ 8.09 (m, 2H), 7.59 (m, 1H), 7.46 (m, 2H), 7.24 (d, *J* = 8.7 Hz, 2H), 6.89 (d, *J* = 8.7 Hz, 2H), 5.48 (q, *J* = 7.0 Hz, 1H), 4.47 (q_{AB}, Δv = 31 Hz, *J* = 11.6 Hz, 2H), 4.14 (m, 1H), 3.82 (s, 1H), 3.48 (m, 2H), 3.24 (m, 1H), 1.52 (d, *J* = 7.0 Hz, 3H), 1.13 (d, *J* = 7.0 Hz, 3H), 0.86 (s, 9H), 0.05 (s, 3H), - 0.01 (s, 3H); ¹³C NMR (CDCl₃, 100 MHz): δ 208.4, 165.7, 159.2, 133.1, 130.2, 129.8, 129.7, 129.3, 128.3, 113.7, 74.7, 73.0, 72.8, 71.7, 55.2, 46.2, 25.8, 18.0, 15.3, 12.9, - 4.7, - 4.9; IR (neat): 2930, 1720, 1612, 1513, 1452, 1249, 1114, 835, 712; $[\alpha]_D^{25}$ - 4.24 (c 2.2, CHCl₃); HRMS-ESI (*m/z*) calculated for [M+ Na⁺]: 523.2486, found: 523.2489.



239a

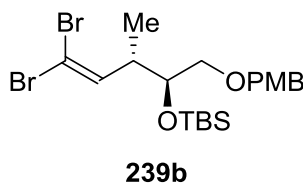
**(2R,3S)-3-((tert-butyldimethylsilyl)oxy)-4-((4-methoxybenzyl)oxy)-2-methylbutanal
(239a)**

To a cooled (-78 °C) solution of ketone **238a** (0.2 g, 0.4 mmol) in THF (5 mL) was added LiBH₄ (176 mg, 8 mmol). The mixture was allowed to warm up to rt slowly and stir 24 h before slow addition of H₂O (5 mL) and diethyl ether (5 mL). The aqueous phase was extracted by diethyl ether (3 x 10 mL). The organic phases were dried over anhydrous MgSO₄, filtered, and concentrated. The residue was purified by flash chromatography (hexanes-ethyl acetate, 4:1, v/v) to provide alcohol **239** (153 g, 0.38 mmol, 96%) as a colorless oil.

To a solution of **239** (110 mg, 0.28 mmol) in MeOH (1.5 mL) and H₂O (0.7 mL) was added NaIO₄ (354 mg, 1.68 mmol). The reaction mixture was stirred at rt for 30 min before the addition of H₂O (5 mL) and diethyl ether (5 mL). The aqueous phase was extracted by diethyl ether (3 x 5 mL). The organic phases were dried over anhydrous MgSO₄, filtered, and concentrated. The residue was purified by flash chromatography (hexanes-ethyl acetate, 12:1, v/v) to provide alcohol **239a** (95 mg, 0.27 mmol, 96%) as a colorless oil.

R_f = 0.61 (Hexanes-Ethyl acetate, 3:1, v/v); ¹H NMR (CDCl₃, 400 MHz): δ 9.75 (d, *J* = 1.9 Hz, 1H), 7.23 (d, *J* = 8.7 Hz, 2H), 6.88 (d, *J* = 8.7 Hz, 2H), 4.44 (s, 2H), 4.14 (m, 1H),

3.81 (s, 3H), 3.48 (dd, $J = 6.2$ Hz, 1.4 Hz, 1H), 2.61 (m, 1H), 1.11 (d, $J = 7.0$ Hz, 3H), 0.89 (s, 9H), 0.09 (s, 3H), 0.08 (s, 3H); ^{13}C NMR (CDCl_3 , 100 MHz): δ 203.7, 159.2, 129.9, 129.3, 113.7, 73.0, 72.6, 71.6, 55.2, 49.9, 25.7, 18.0, 9.9, - 4.5, - 5.1; IR (neat): 2953, 1724, 1612, 1513, 1463, 1249, 1102, 836, 777; $[\alpha]_{\text{D}}^{25} - 43.7$ (c 1.9, CHCl_3); HRMS-ESI (m/z) calculated for $[\text{M} + \text{Na}^+]$: 375.1962, found: 375.1962.

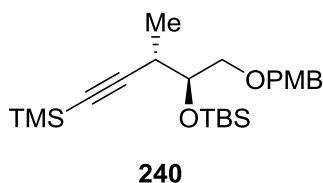


tert-butyl(((2S,3S)-5,5-dibromo-1-((4-methoxybenzyl)oxy)-3-methylpent-4-en-2-yl)oxy)dimethylsilane (239b)

To a cooled (0 °C) solution of CBr_4 (2.51 g, 7.56 mmol) in CH_2Cl_2 (25 mL) was added Ph_3P (3.96 g, 15.1 mmol). The mixture was allowed to stir 30 min before the addition of aldehyde **239a** (1.33 g, 3.77 mmol) and $i\text{-Pr}_2\text{Net}$ (1.32 mL, 7.56 mmol) in CH_2Cl_2 (12 mL). The reaction was stirred another 20 min and was then added saturated aqueous NaHCO_3 (20 mL). The aqueous phase was extracted by CH_2Cl_2 (3 x 5 mL) and the combined organic phases were washed with brine. The organic phases were dried over anhydrous Na_2SO_4 , filtered, and concentrated. The residue was purified by flash chromatography (hexanes-ethyl acetate, 50:1, v/v) to provide alcohol **239b** (1.6 g, 3.16 mmol, 84%) as a colorless oil.

$R_f = 0.37$ (Hexanes-Ethyl acetate, 10:1, v/v); ^1H NMR (CDCl_3 , 400 MHz): δ 7.26 (d, $J = 8.7$ Hz, 2H), 6.91 (d, $J = 8.7$ Hz, 2H), 6.45 (d, $J = 9.5$ Hz, 1H), 4.45 (s, 3H), 3.83 (s,

3H), 3.77 (m, 1H), 3.34 (m, 1H), 2.78 (m, 1H), 1.06 (d, $J = 7.0$ Hz, 2H), 0.91 (s, 9H), 0.08 (s, 3H), 0.07 (s, 3H); ^{13}C NMR (CDCl_3 , 100 MHz): δ 159.2, 140.0, 130.2, 129.3, 113.8, 88.2, 73.8, 73.1, 72.8, 55.3, 41.7, 25.9, 18.1, 16.1, - 4.2, - 4.9; IR (neat): 2953, 1612, 1513, 1620, 1248, 1102, 1035, 837, 776; $[\alpha]_{\text{D}}^{25}$ - 11.6 (c 1.6, CHCl_3); HRMS-ESI (m/z) calculated for $[\text{M} + \text{Na}^+]$: 529.0380, found: 529.0381.

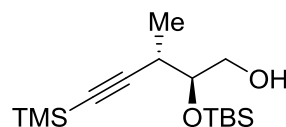


***tert*-butyl(((2*S*,3*S*)-1-((4-methoxybenzyl)oxy)-3-methyl-5-(trimethylsilyl)pent-4-yn-2-yl)oxy)dimethylsilane (**240**)**

To a cooled (- 78 °C) solution of **239b** (1.1 g, 2.2 mmol) in THF (20 mL) was added *n*-BuLi (2.0 mL, 4.8 mmol, 2.5 M in Hexane) slowly. After stirring 30 min, TMSCl (0.85 mL, 6.6 mmol) was added. The mixture was allowed to stir another 1 h before saturated aqueous NH_4Cl (20 mL) was added. The aqueous phase was extracted by diethyl ether (3 x 20 mL) and the combined organic phases were washed with brine. The organic phases were dried over anhydrous Na_2SO_4 , filtered, and concentrated. The residue was purified by flash chromatography (hexanes-ethyl acetate, 100:1, v/v) to provide alcohol **240** (1.0 g, 2.0 mmol, 93%) as a colorless oil.

$R_f = 0.37$ (Hexanes-Ethyl acetate, 10:1, v/v); ^1H NMR (CDCl_3 , 400 MHz): δ 7.27 (d, $J = 8.7$ Hz, 2H), 6.90 (d, $J = 8.7$ Hz, 2H), 4.48 (s, 2H), 3.80 (s, 3H), 3.77 (m, 1H), 3.63 (m, 1h), 3.45 (m, 1H), 2.76 (m, 1H), 1.18 (d, $J = 7.0$ Hz, 2H), 0.92 (s, 9H), 0.15 (s, 9H), 0.08

(s, 3H), 0.07 (s, 3H); ^{13}C NMR (CDCl_3 , 100 MHz): δ 159.3, 130.8, 129.4, 113.9, 108.9, 85.8, 73.9, 73.2, 72.8, 55.5, 31.7, 26.0, 18.3, 16.9, 0.4, - 4.0, - 4.7; IR (neat): 2930, 1612, 1513, 1249, 1096, 840, 776; $[\alpha]_{\text{D}}^{25}$ - 14.6 (c 2.5, CHCl_3); HRMS-ESI (m/z) calculated for $[\text{M} + \text{Na}^+]$: 443.2408, found: 443.2406.



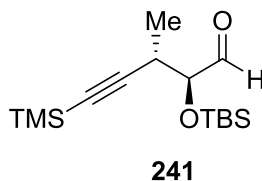
240a

**(2*S*,3*S*)-2-((*tert*-Butyldimethylsilyl)oxy)-3-methyl-5-(trimethylsilyl)pent-4-yn-1-ol
(240a)**

To a solution of **240** (1.4 g, 3.3 mmol) in CH_2Cl_2 (20 mL), *t*-BuOH (4 mL), pH = 7 aqueous buffer (4 mL) was added DDQ (1.52 g, 6.6 mmol). The reaction mixture was allowed to stir 1 h before saturated aqueous NaHCO_3 (20 mL) was added. The aqueous phase was extracted by diethyl ether (3 x 40 mL) and the combined organic phases were washed with brine. The organic phases were dried over anhydrous Na_2SO_4 , filtered, and concentrated. The residue was purified by flash chromatography (hexanes-ethyl acetate, 25:1, v/v) to provide alcohol **240a** (1.0 g, 3.3 mmol, 99%) as a colorless oil.

R_f = 0.5 (Hexanes-Ethyl acetate, 5:1, v/v); ^1H NMR (CDCl_3 , 400 MHz): δ 3.78 (m, 2H), 3.64 (m, 1H), 2.73 (m, 1H), 1.81 (br, 1H), 1.19 (d, J = 7.0 Hz, 3H), 0.93 (s, 9H), 0.16 (s, 9H), 0.14 (s, 3H), 0.13 (s, 3H); ^{13}C NMR(CDCl_3 , 100 MHz): δ 108.83, 86.48, 74.81, 64.20, 31.20, 26.00, 18.30, 16.06, 0.28, -4.34, -4.38; IR (neat): 3426, 2957, 1250, 1097,

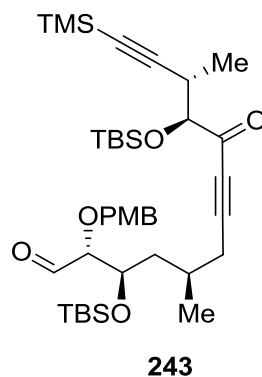
1045, 840, 776; $[\alpha]_D^{25}$ - 3.20 (c 1.86, CHCl₃); HRMS-ESI (m/z) calculated for $[M+ Na^+]$: 323.1833, found: 323.1831.



(2S,3S)-2-((tert-butyldimethylsilyloxy)-3-methyl-5-(trimethylsilyl)pent-4-ynal (241)

To a cooled (0 °C) solution of **240a** (1.0 g, 3.3 mmol) in CH₂Cl₂ (24 mL) and DMSO (6 mL) was added *i*-Pr₂Net (3.5 mL, 19.8 mmol) and SO₃·Py (2.28 g, 14.2 mmol) sequentially. The reaction mixture was allowed to stir 5 min before cold 1 M HCl (14 mL) was added. The aqueous phase was extracted by CH₂Cl₂ (3 x 15 mL) and the combined organic phases were washed with pH = 7 aqueous buffer and brine. The organic phases were dried over anhydrous Na₂SO₄, filtered, and concentrated. The residue was purified by flash chromatography (hexanes-ethyl acetate, 40:1, v/v) to provide alcohol aldehyde **241** (1.0 g, 3.3 mmol, 99%) as a colorless oil.

R_f = 0.7 (Hexanes-Ethyl acetate, 5:1, v/v); ¹H NMR (CDCl₃, 400 MHz): δ 9.69 (d, J = 1.8 Hz, 1H), 3.94 (dd, J = 5.2 Hz, 1.8 Hz, 1H), 2.83 (m, 1H), 1.21 (d, J = 7.0 Hz, 3H), 0.95 (s, 9H), 0.16 (s, 9H), 0.11 (s, 3H), 0.10 (s, 3H); ¹³C NMR (CDCl₃, 100 MHz): δ 202.5, 106.2, 87.4, 79.3, 30.8, 25.7, 18.3, 18.2, - 0.01, - 4.6, - 5.1; IR (neat): 3947, 2857, 1739, 1250, 1215, 841, 758; $[\alpha]_D^{25}$ + 4.42 (c 1.2, CHCl₃); HRMS-ESI (m/z) calculated for $[M+ Na^+]$: 321.1677, found: 321.1675.



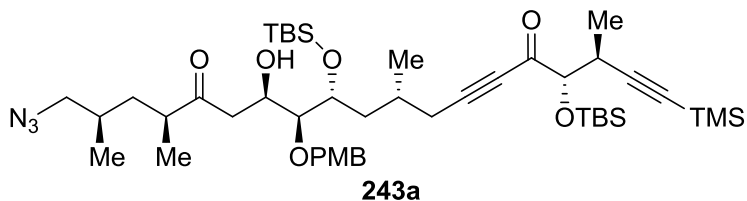
(2R,3R,5R,10S,11S)-3,10-bis((tert-butyldimethylsilyl)oxy)-2-((4-methoxybenzyl)oxy)-5,11-dimethyl-9-oxo-13-(trimethylsilyl)trideca-7,12-diynal
(243)

To a flask of CrCl₂ (1.6 g, 13 mmol) and NiCl₂ (40 mg, 0.31 mmol) was added the solution of alkynyl iodide **163** (2.6 g, 4 mmol) and aldehyde **241** (1.0 g, 3.4 mmol) in THF (40 mL). The reaction was allowed to stir 14 h before 1 M aqueous serine saturated with NaHCO₃ (60 mL) and diethyl ether (60 mL) was added. The mixture was stirred for 2 h to fully separate the aqueous and organic phases. The aqueous phase was then extracted by diethyl ether (3 x 80 mL) and the combined organic phases were washed with brine. The residue was purified by flash chromatography (hexanes-ethyl acetate, 60:1 to 20:1, v/v) to provide alcohol **242** (2.7 g, 3.3 mmol, 97%) as a colorless oil

To a solution of **242** (1.3 g, 1.6 mmol) in THF (8 mL) was added Py (0.6 mL, 7.2 mmol) and HF·Py (0.21 mL, 2.4 mmol) sequentially. The mixture was stirred for 12 h before saturated aqueous NaHCO₃ (10 mL) was slowly added. The aqueous phase was then extracted by diethyl ether (3 x 10 mL) and the combined organic phases were washed with brine. The residue was purified by flash chromatography (hexanes-ethyl acetate, 8:1, v/v) to provide alcohol **242a** (0.85 g, 1.2 mmol, 75%) as a colorless oil.

To a solution of **242a** (0.41 g, 0.58 mmol) in CH₂Cl₂ (6 mL) and DMSO (2 mL) was added *i*-Pr₂NEt (1.2 mL, 7.0 mmol) and SO₃·Py (0.74 g, 4.6 mmol) sequentially. The mixture was stirred 10 min before saturated aqueous NH₄Cl (10 mL) was added. The aqueous phase was then extracted by diethyl ether (3 x 10 mL) and the combined organic phases were washed with brine. The residue was purified by flash chromatography (hexanes-ethyl acetate, 12:1, v/v) to provide aldehyde **243** (0.36 g, 0.51 mmol, 88%) as a colorless oil.

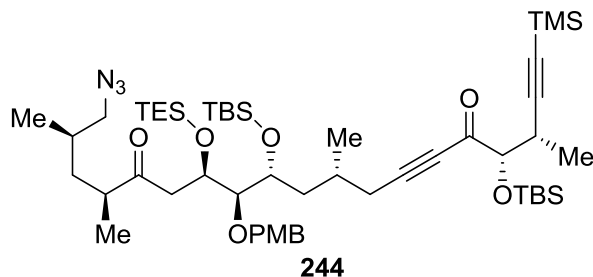
R_f = 0.7 (Hexanes-Ethyl acetate, 5:1, v/v); ¹H NMR (CDCl₃, 400 MHz): δ 9.64 (d, *J* = 2.2 Hz, 1H), 7.27 (d, *J* = 8.7 Hz, 2H), 6.89 (d, *J* = 8.7 Hz, 2H), 4.58 (s, 2H), 4.07 (m, 1H), 3.93 (d, *J* = 7 Hz, 1H), 3.83 (s, 3H), 3.65 (m, 1H), 2.95 (m, 1H), 2.46 (m, 1H), 2.22 (m, 1H), 1.88 (m, 1H), 1.58 (m, 2H), 1.17 (d, *J* = 7.1 Hz, 3H), 1.05 (d, *J* = 6.8 Hz, 3H), 0.95 (s, 9H), 0.89 (s, 9H), 0.15 (s, 9H), 0.11 (m, 12H); ¹³C NMR (CDCl₃, 100 MHz): δ 203.3, 187.9, 159.5, 129.7, 129.2, 113.9, 107.2, 95.8, 86.3, 86.1, 81.8, 80.4, 72.6, 72.0, 55.3, 40.3, 32.1, 28.3, 26.1, 25.8, 25.7, 20.2, 18.3, 18.1, 16.7, 0.1, - 4.4, - 4.7, - 4.8, - 4.9; IR (neat): 2924, 1725, 1612, 1513, 1462, 1250, 1098, 838; [α]_D²⁵ - 20.5 (c 1.2, CHCl₃); HRMS-ESI (*m/z*) calculated for [M+ Na⁺]: 723.3903, found: 723.3905.



(3S,4S,9R,11R,12S,13R,16S,18R)-19-azido-4,11-bis((tert-butyldimethylsilyl)oxy)-13-hydroxy-12-((4-methoxybenzyl)oxy)-3,9,16,18-tetramethyl-1-(trimethylsilyl)nonadeca-1,6-diyne-5,15-dione (243a)

To a flask of $\text{MgBr}_2 \cdot \text{OEt}_2$ (1.4 g, 5.4 mmol) was added the solution of **243** (0.38 g, 0.54 mmol) in CH_2Cl_2 (5 mL) at -78°C . After stirring 15 min, the mixture was added solution of silyl enol ether (1.1 g, 4.3 mmol) in CH_2Cl_2 (3 mL). The reaction was allowed to stir for 5 h, before slowly warming up to -40°C in 1 h. pH = 7 aqueous buffer (10 mL) and diethyl ether (10 mL) was added. The aqueous phase was then extracted by diethyl ether (3 x 10 mL) and the combined organic phases were washed with brine. The residue was purified by flash chromatography (hexanes-ethyl acetate, 10:1, v/v) to provide alcohol **243a** (0.4 g, 0.46 mmol, 85%) as a colorless oil.

$R_f = 0.6$ (Hexanes-Ethyl acetate, 3:1, v/v); ^1H NMR (CDCl_3 , 400 MHz): δ 7.27 (d, $J = 8.6$ Hz, 2H), 6.89 (d, $J = 8.6$ Hz, 2H), 4.68 (q_{AB} , $\Delta\nu = 119$ Hz, $J = 11.5$ Hz, 2H), 4.09 (m, 1H), 3.92 (d, $J = 7.0$ Hz, 1H), 3.82 (s, 3H), 3.59 (br, 1H), 3.31 (t, $J = 2.4$ Hz, 1H), 3.18 (m, 1H), 3.11 (m, 1H), 2.96 (m, 1H), 2.77 (m, 1H), 2.54 (m, 3H), 2.29 (m, 1H), 1.94 (m, 1H), 1.68 (m, 4H), 1.16 (d, $J = 7.0$ Hz, 3H), 1.07 (m, 6H), 0.94 (m, 21H), 0.12 (m, 21H); ^{13}C NMR (CDCl_3 , 100 MHz): δ 213.0, 187.9, 159.4, 130.0, 129.7, 113.9, 107.1, 95.9, 86.4, 81.8, 80.5, 80.4, 72.6, 71.9, 67.0, 57.6, 55.3, 44.6, 44.3, 40.7, 37.1, 32.1, 31.4, 28.6, 25.8, 25.7, 20.1, 18.3, 18.0, 17.9, 17.0, 16.9, 0.1, - 4.3, - 4.6, - 4.7, - 4.9; IR (neat): 3487, 2956, 2098, 1674, 1514, 1462, 1249, 1103, 839, 777; $[\alpha]_{\text{D}}^{25} - 37.5$ (c 1.2, CHCl_3); HRMS-ESI (m/z) calculated for $[\text{M} + \text{Na}^+]$: 892.5118, found: 892.5118.

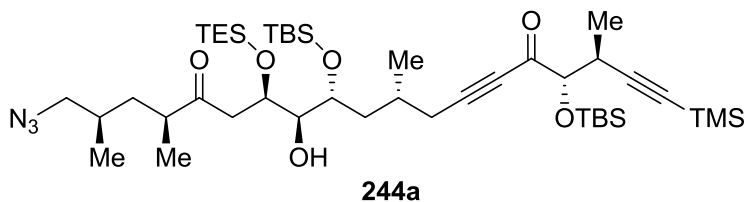


(3S,4S,9R,11R,12R,13R,16S,18R)-19-azido-4,11-bis((tert-butyldimethylsilyl)oxy)-12-((4-methoxybenzyl)oxy)-3,9,16,18-tetramethyl-13-((triethylsilyl)oxy)-1-(trimethylsilyl)nonadeca-1,6-diyne-5,15-dione (244)

To a cooled (- 55 °C) solution of **243a** (0.72 g, 0.83 mmol) in CH₂Cl₂ (10 mL) was added 2,6-lutidine (0.41 mL, 3.3 mmol), TESOTf (0.5 mL, 2.1 mmol) successively. The reaction mixture was allowed to stir 20 min before pH = 7 aqueous buffer (10 mL) and diethyl ether (10 mL) was added. The aqueous phase was then extracted by diethyl ether (3 x 10 mL) and the combined organic phases were washed with brine. The residue was purified by flash chromatography (hexanes-ethyl acetate, 30:1, v/v) to provide alcohol **244** (0.8 g, 0.82 mmol, 98%) as a colorless oil

R_f = 0.63 (Hexanes-Ethyl acetate, 5:1, v/v); ¹H NMR (CDCl₃, 400 MHz): δ 7.27 (d, *J* = 8.6 Hz, 2H), 6.89 (d, *J* = 8.6 Hz, 2H), 4.51 (q_{AB}, Δ*v* = 68 Hz, *J* = 11.3 Hz, 2H), 4.41 (m, 1H), 4.01 (m, 1H), 3.91 (d, *J* = 7.1 Hz, 1H), 3.82 (s, 3H), 3.49 (m, 1H), 3.21 (m, 1H), 3.08 (m, 1H), 2.95 (m, 1H), 2.87 (m, 1H), 2.71 (m, 2H), 2.49 (m, 1H), 2.18 (m, 1H), 1.99 (m, 1H), 1.74 (m, 3H), 1.51 (m, 1H), 1.17 (d, *J* = 7.1 Hz, 3H), 1.07 (d, *J* = 7.1 Hz, 6H), 0.94 (m, 27H), 0.56 (m, 6H), 0.15 (s, 9H), 0.11 (m, 12H); ¹³C NMR(CDCl₃, 100 MHz): δ 212.0, 187.8, 159.1, 130.9, 129.2, 113.6, 107.2, 96.5, 86.3, 83.9, 81.9, 80.2, 73.0, 71.5, 68.4, 57.6, 55.2, 45.6, 44.3, 40.0, 37.0, 32.1, 31.4, 28.8, 26.0, 25.7, 20.8, 18.2, 18.1, 18.0,

17.0, 16.9, 7.0, 4.9, 0.1, - 3.6, - 4.7, - 4.9, -5.0; IR (neat): 2956, 2098, 1716, 1514, 1458, 1249, 1107, 833, 775; $[\alpha]_D^{25}$ - 19.0 (c 1.2, CHCl₃); HRMS-ESI (m/z) calculated for $[M+Na]^+$: 1006.5983, found: 1006.5981.

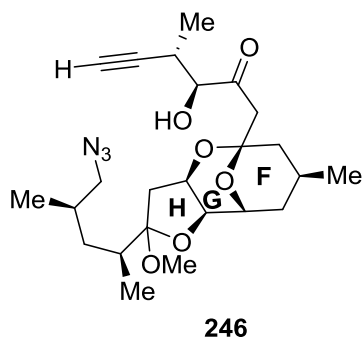


(3S,4S,9R,11R,12R,13R,16S,18R)-19-azido-4,11-bis((tert-butyldimethylsilyloxy)-12-hydroxy-3,9,16,18-tetramethyl-13-((triethylsilyloxy)-1-(trimethylsilyl)nonadeca-1,6-diyne-5,15-dione (244a)

To a solution of **244** (0.16 g, 0.16 mmol) in CH₂Cl₂ (2 mL), pH = 7 aqueous buffer (0.4 mL) and *t*-BuOH (0.2 mL) was added DDQ (93 mg, 0.4 mmol). The reaction was allowed to stir for 10 min before pH = 7 aqueous buffer (4 mL) and diethyl ether (8 mL) was added. The aqueous phase was then extracted by diethyl ether (3 x 8 mL) and the combined organic phases were washed with brine. The residue was purified by flash chromatography (hexanes-ethyl acetate, 30:1, v/v) to provide alcohol **244a** (0.14 g, 0.16 mmol, 98%) as a colorless oil.

R_f = 0.60 (Hexanes-Ethyl acetate, 5:1, v/v); ¹H NMR (C₆D₆, 400 MHz): δ 4.53 (q, J = 5.6 Hz, 1H), 4.06 (d, J = 6.6 Hz, 1H), 3.93 (m, 1H), 3.59 (q, J = 5.4 Hz, 1H), 3.19 (m, 1H), 2.88 (m, 1H), 2.77 (m, 1H), 2.65 (m, 2H), 2.51 (d, J = 6 Hz, 1H), 2.43 (m, 1H), 2.27 (m, 1H), 2.15 (m, 2H), 1.78 (m, 4H), 1.51 (m, 1H), 1.19 (d, J = 7.1 Hz, 3H), 1.05 (m, 24H), 0.93 (m, 3H), 0.73 (m, 9H), 0.15 (m, 27H); ¹³C NMR (C₆D₆, 125 MHz): δ 210.7, 187.0, 109.2, 107.7, 95.5, 86.7, 82.4, 81.1, 77.1, 71.9, 69.3, 57.4, 15.9, 44.8, 39.3, 37.0, 32.6,

31.5, 28.7, 26.1, 26.0, 20.7, 18.6, 18.3, 17.9, 17.3, 17.1, 7.2, 5.6, 0.2, - 3.8, -4.35, - 4.83;
IR (neat): 3487, 2929, 2098, 1676, 1716, 1458, 1249, 1103, 839, 777; $[\alpha]_D^{25}$ - 25.6 (c
1.0, Benzene); HRMS-ESI (m/z) calculated for $[M+Na^+]$: 886.5408, found: 886.5405.



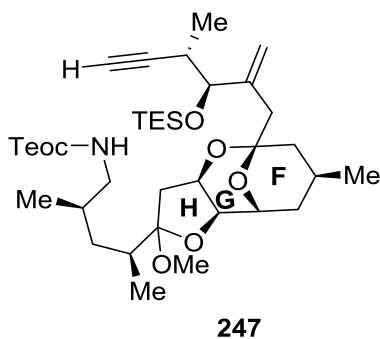
(3R,4R)-1-((2S,3aR,5S,7S,9R,9aR)-2-((2S,4R)-5-azido-4-methylpentan-2-yl)-2-methoxy-7-methyloctahydro-5H-5,9-epoxyfuro[3,2-b]oxocin-5-yl)-3-hydroxy-4-methylhex-5-yn-2-one (246)

To a solution of **244a** (0.11 g, 0.13 mmol) in MeOH (1.5 mmol) was added PPTS (0.3 mg, 1.3 μ mol). The reaction was stirred for 10 min in rt. To the reaction mixture was added pH = 7 aqueous buffer (5 mL) and diethyl ether (3 mL). The aqueous phase was then extracted by diethyl ether (3 x 5 mL) and the combined organic phases were washed with brine. The residue was purified by flash chromatography (hexanes-ethyl acetate, 80:1, v/v) to provide alcohol **245** (0.11 g, 0.13 mmol, 99%) as a colorless oil.

To a solution of **245** (0.11 g, 0.13 mmol) in THF (2 mL) was added TBAF (0.65 mL, 0.65 mmol, 1 M in THF) in rt. The mixture was allowed to stir for 20 min before pH = 7 aqueous buffer (5 mL) and diethyl ether (3 mL) was added. The aqueous phase was then extracted by diethyl ether (3 x 5 mL) and the combined organic phases were washed with

brine. The residue was purified by flash chromatography (hexanes-ethyl acetate, 8:1, v/v) to provide alcohol **246** (12 mg, 26 μ mol, 20%) as a colorless oil.

R_f = 0.4 (Hexanes-Ethyl acetate, 3:1, v/v); ^1H NMR (C_6D_6 , 400 MHz): δ 4.24 (m, 4H), 3.26 (d, J = 3.8 Hz, 1H), 3.13 (s, 3H), 3.11 (m, 1H), 2.92 (s, 2H), 2.84 (m, 1H), 2.71 (m, 1H), 2.11 (m, 1H), 2.01 (m, 2H), 1.78 (m, 2H), 1.64 (m, 3H), 1.43 (m, 1H), 3.38 (d, J = 7.1 Hz, 3H), 1.14 (m, 1H), 1.06 (m, 4H), 0.79 (m, 4H), 0.58 (d, J = 7.1 Hz, 3H); ^{13}C NMR (C_6D_6 , 125 MHz): δ 206.9, 111.2, 95.9, 84.0, 80.1, 75.2, 73.8, 71.3, 70.2, 56.5, 50.9, 47.6, 42.8, 41.8, 36.4, 34.4, 33.1, 31.1, 30.3, 35.1, 23.0, 19.6, 17.8, 15.1; IR (neat): 3466, 2929, 2096, 1701, 1450, 1249, 1103, 1047, 839, 777; $[\alpha]_D^{25}$ + 1.2 (c 0.3, Benzene); HRMS-ESI (m/z) calculated for $[\text{M} + \text{Na}^+]$: 486.2575, found: 486.2573.



2,2,2-trichloroethyl ((2R,4S)-4-((2S,3aR,5S,7S,9R,9aR)-2-methoxy-7-methyl-5-((3R,4R)-4-methyl-2-methylene-3-((triethylsilyl)oxy)hex-5-yn-1-yl)octahydro-2H-5,9-epoxyfuro[3,2-b]oxocin-2-yl)-2-methylpentyl)carbamate (247)

To a cooled (-78 $^{\circ}\text{C}$) solution of **246** (12 mg, 26 μ mol) in CH_2Cl_2 (1 mL) was added 2,6-lutidine (0.01 mL, 78 μ mol) and TESOTf (0.01 mL, 39 μ mol) successively. The reaction was allowed to stir 30 min before pH = 7 aqueous buffer (3 mL) and diethyl ether (2 mL)

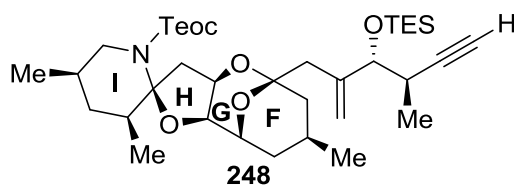
was added. The aqueous phase was then extracted by diethyl ether (3 x 3 mL) and the combined organic phases were washed with brine. The residue was purified by flash chromatography (hexanes-ethyl acetate, 12:1, v/v) to provide alcohol **246a** (14 mg, 20 μ mol, 92%) as a colorless oil.

To a solution of **246a** (35 mg, 61 μ mol) in MeCN (0.2 mL) and MeOH (0.2 mL) was added Ph₃P (48 mg, 0.18 mmol). The mixture was stirred for 12 h before TeocOSU (49 mg, 0.18 mmol) was added. After another 12 h, the reaction mixture was concentrated. The residue was purified by flash chromatography (hexanes-ethyl acetate, 8:1, v/v) to provide alcohol **246b** (37 mg, 53 μ mol, 87%).

To a stirred suspension of methyl triphenyl phosphonium iodide (0.3 g, 0.74 mmol) in PhMe (1 mL) was added KHMS (1.3 mL, 0.67 mmol, 0.5 M solution in PhMe) in rt. The mixture was warmed up to 80 °C. After stirring 30 min, the yellow solution was allowed to slowly cool back to rt. 1 mL of the ylide solution was added to a solution of **246b** (37 mg, 53 μ mol) in PhMe (1 mL). The solution was stirred at rt for 30 min, before pH = 7 aqueous buffer (3 mL) and diethyl ether (2 mL) was added. The aqueous phase was then extracted by diethyl ether (3 x 3 mL) and the combined organic phases were washed with brine. The residue was purified by flash chromatography (hexanes-ethyl acetate-Et₃N, 8:1:0.09, v/v/v) to provide alcohol **247** (20 mg, 28 μ mol, 54%) as a colorless oil

$R_f = 0.4$ (Hexanes-Ethyl acetate, 3:1, v/v); ¹H NMR (C₆D₆, 400 MHz): δ 5.53 (q, $J = 1.2$ Hz, 1H), 5.26 (d, $J = 1.7$ Hz, 1H), 4.51 (t, $J = 6.0$ Hz, 1H), 4.47 (d, $J = 4.3$ Hz, 1H), 4.42 (t, $J = 3.8$ Hz, 1H), 4.43 (m, 3H), 3.39 (d, $J = 3.8$ Hz, 1H), 3.29 (m, 1H), 3.04 (s, 3H), 2.91 (m, 2H), 2.51 (q_{AB}, $J = 14.6$ Hz, 2H), 2.26 (m, 1H), 2.11 (m, 2H), 1.92 (d, $J = 2.5$ Hz, 1H),

1.72 (m, 4H), 1.31 (m, 6H), 1.23 (m, 1H), 1.17 (d, $J = 6.7$ Hz, 3H), 1.08 (t, $J = 8.0$ Hz, 9H), 1.01 (m, 2H), 0.87 (d, $J = 6.5$ Hz, 3H), 0.73 (m, 9H), - 0.05 (s, 9H); ^{13}C NMR (C_6D_6 , 125 MHz): δ 156.9, 145.3, 129.7, 116.2, 115.6, 111.7, 97.0, 86.2, 77.8, 76.2, 73.5, 70.5, 70.1, 62.6, 47.9, 45.9, 42.6, 40.2, 37.0, 34.8, 32.1, 31.8, 25.1, 23.3, 19.6, 18.1, 18.0, 15.7, 7.3, 5.4, - 1.5; IR (neat): 3054, 2955, 1718, 1437, 1189, 1121, 883, 742, 695; $[\alpha]_{\text{D}}^{25}$ - 6.2 (c 0.5, Benzene); HRMS-ESI (m/z) calculated for $[\text{M} + \text{Na}^+]$: 716.4348, found: 716.4349.



2,2,2-trichloroethyl (2S,3S,3a'R,5R,5'S,7'S,9'R,9a'R)-3,5,7'-trimethyl-5'-((3R,4R)-4-methyl-2-methylene-3-((triethylsilyl)oxy)hex-5-yn-1-yl)octahydrospiro[piperidine-2,2'-[5,9]epoxyfuro[3,2-b]oxocine]-1-carboxylate (248)

To a solution of **247** (20 mg, 28 μmol) in MeCN (1 mL) was added $\text{Nd}(\text{OTf})_3$ (0.2 mg). The reaction was allowed to stir 10 min before Et_3N (0.01 mL) was added. The mixture was directly filtered through a pad of silica gel and washed with ethyl acetate (5 mL). The combined organic phase was concentrated. The residue was purified by flash chromatography (hexanes-ethyl acetate- Et_3N , 15:1:0.8, v/v/v) to provide alcohol **248** (13 mg, 20 μmol , 70%) as a colorless oil.

$R_f = 0.4$ (Hexanes-Ethyl acetate, 5:1, v/v); ^1H NMR (C_6D_6 , 400 MHz): δ 5.62 (q, $J = 1.4$ Hz, 1H), 5.17 (d, $J = 1.6$ Hz, 1H), 4.59 (d, $J = 3.2$ Hz, 1H), 4.37 (m, 2H), 4.31 (m, 2H), 4.11 (d, $J = 4.7$ Hz, 1H), 4.05 (dd, $J = 13.2$ Hz, 4.2 Hz, 1H), 3.46 (dd, $J = 13.1$ Hz, 12.0

Hz, 1H), 3.22 (m, 1H), 3.14 (d, $J = 4.6$ Hz, 1H), 2.64 (q_{AB}, $J = 14.1$ Hz, 2H), 2.25 (m, 1H), 1.92 (m, 2H), 1.75 (m, 1H), 1.59 (m, 2H), 1.47 (m, 5H), 1.26 (m, 2H), 1.17 (m, 2H), 1.11 (t, $J = 8.0$ Hz, 9H), 0.84 (m, 6H), 0.75 (m, 9H), - 0.04 (s, 9H); ¹³C NMR (C₆D₆, 125 MHz): δ 156.0, 145.9, 115.5, 97.4, 96.6, 85.9, 78.2, 77.5, 73.8, 70.9, 70.4, 62.9, 49.0, 45.9, 40.8, 39.61, 39.57, 36.3, 34.6, 32.0, 31.8, 24.7, 23.2, 19.1, 18.9, 18.2, 16.7, 7.4, 5.5, - 1.6; IR (neat): 2953, 1697, 1458, 1252, 1169, 1121, 883, 742; $[\alpha]_D^{25} + 9.2$ (c 0.6, Benzene); HRMS-ESI (m/z) calculated for [M+ Na⁺]: 684.4086, found: 684.4084.

References

- (1) Silver, M. W. *American Scientist*, **2006**, *4*, 316.
- (2) Clark, R. F.; Williams, S. R.; Nordt, S. P.; Manoguerra, A. S. *Undersea Hyperbaric Medicine*. **1991**, *38*, 175.
- (3) Botana, L. M.; Rodriguez-Vieytes, M.; Alfonso, A.; Louzao, M. C. *Food Science and Technology*. **1996**, *77*, 1147.
- (4) Watkins, S. M.; Reich, A.; Fleming, L. E.; Hammond, R. *Marine Drugs*. **2008**, *6*, 431.
- (5) Satake, M.; Ofuji, K.; Naoki, H.; James, K. J.; Furey, A.; McMahon, T.; Silke, J.; Yasumoto, T. *J. Am. Chem. Soc.* **1998**, *120*, 9967.
- (6) Quilliam M. A.; Wright J. L. C. *Analytical Chemistry*. **1989**, *61*, 1530A.
- (7) Yasumoto, T.; Oshima, Y.; Yamaguchi, M. *In Toxic Dinoflagellate Blooms*; Taylor, D.; Seliger, H. H. Eds. *Elsevier: Amsterdam*, **1979**, 495.
- (8) Kumagai, M.; Yanagi, T.; Murata, M.; Yasumoto, T.; Kat, M.; Lassus, P.; Rodriguez-Vasquez, J. A. *Agric. Biol. Chem.* **1986**, *50*, 2853-2857.
- (9) Hu, T.; Doyle, J.; Jackson, D.; Marr, J.; Nixon, E.; Pleasance, S.; Quilliam, M. A.; Walter, J. A.; Wright, J. L. C. *Chem. Commun.* **1992**, *39*, 41.
- (10) Yasumoto, T.; Murata, M.; Oshima, Y.; Sano, M.; Matsumoto, G. K.; Clardy, J. *Tetrahedron* **1985**, *41*, 1019.
- (11) Murata, M.; Kumagai, M.; Lee, J. S.; Yasumoto, T. *Tetrahedron Lett.* **1987**, *28*, 5869.

- (12) Schantz, E. J.; Ghazarossian, V. E.; Schnoes, H. K.; Strong, F. M.; Springer, J. P.; Pezzanite, J. O.; Clardy, J. *J. Am. Chem. Soc.* **1975**, *97*, 1238.
- (13) Landsberg, Jan H. *Reviews in Fisheries Science* **2002**, *10*, 113.
- (14) Baden, D. G. *FASEB J.* **1989**, *3*, 1807.
- (15) McMahon, T.; Silke, J. *Harmful Algae New.* **1996**, *14*, 2.
- (16) Nicolaou, K. C.; Chen, D. Y.; Li, Y.; Qian, Y.; Ling, T.; Vvskovil, S.; Koftis, T. V.; Govindasamy, M.; Uesaka, M. *Angew. Chem. Int. Ed.* **2003**, *42*, 3649.
- (17) Nicolau, K. C.; Vyskocil, S.; Koftis, T. V.; Yamada, Y. M.; Ling, T. T.; Chen, D. Y.; Tang, W. J.; Petrovic, G.; Frederic, M. O.; Li, Y. W.; Satake, M. *Angew. Chem. Int. Ed.* **2004**, *43*, 4312.
- (18) (a) Nicolau, K. C.; Koftis, T. V.; Vyskocil, S.; Petrovic, G.; Ling, T. T.; Yamada, Y. M.; Tang, W. J.; Frederic M. O. *Angew. Chem. Int. Ed.* **2004**, *43*, 4318. (b)
- (19) Ofuji, K.; Satake, M.; McMahon, T.; Silke, J.; James, K. J.; Naoki, H.; Oshima, Y.; Yasumoto, T. *Nat. Toxins.* **1999**, *7*, 99.
- (20) Ofuji, K.; Satake, M.; McMahon, T.; James, K. J.; Naoki, H.; Oshima, Y.; Yasumoto, T. *Biosci. Biotechnol. Biochem.* **2001**, *65*, 740.
- (21) Rehmann, N.; Hess, P.; Quilliam, M. *Rapid Comm. Mass Spectrom.* **2008**, *22*, 549.
- (22) James, K. J.; Moroney, C.; Roden, C.; Satake, M.; Yasumoto, T.; Lehane, M.; Furey, A. *Toxicon.* **2003**, *41*, 145.
- (23) Moran, S., Silke, J., Cusack, C., Hess, P. Sixth International Conference on Molluscan Shellfish Safety, Blenheim, New Zealand, 2007.
- (24) Krock, B.; Tillmann, U.; John, U.; Cembella, A. *Harmful Algae* **2009**, *8*, 254.

- (25) Tillmann, U.; Elbrachter, M.; Krock, B.; John, U.; Cembella, A. *Eur. J. Phycol.* **2009**, *44*, 63.
- (26) Twiner, M. J.; Rehmann, N.; Hess, P.; Coucette, G. J. *Mar Drug.* **2008**, *6*, 39.
- (27) Ito, E.; Satake, M.; Ofuji, K.; Kurita, N.; McMahon, T.; James, K.; Yasumoto, T. *Toxicon.* **2000**, *38*, 917.
- (28) Ito, E.; Satake, M.; Ofuji, K.; Higashi, M.; Harigaya, K.; McMahon, T. *Toxicon.* **2002**, *40*, 193.
- (29) Flanagan, A. F.; Callanan, K. R.; Donlon, J.; Palmer, R.; Forde, A.; Kane, M. *Toxicon.* **2001**, *39*, 1021.
- (30) Twiner, M. J.; Hess, P.; Bottein Dechraoui, M.-Y.; McMahon, T.; Samons, M. S.; Satake, M.; Yasumoto, T.; Ramsdell, J. S.; Doucette, G. J. *Toxicon.* **2005**, *45*, 891.
- (31) Roman, Y.; Alfonso, A.; Louzao, M. C.; de la Rosa, L. A.; Leira, F.; Vieites, J. M.; Vieytes, M. R.; Ofuji, K.; Satake, M.; Yasumoto, T.; Botana, L. M. *Cell. Signal.* **2002**, *14*, 703.
- (32) Roman, Y.; Alfonso, A.; Vieytes, M. R.; Ofuji, J.; Satake, M.; Yasumoto, T.; Botana, L. M.; *Chem. Res. Toxicol.* **2002**, *17*, 1338.
- (33) Alfonso, A.; Vieytes, M. R.; Ofuji, K.; Satake, M.; Nicolau, K. C.; Frederick, M. O.; Botana, L. M. *Biochem. Biophys. Res. Commun.* **2006**, *346*, 1091.
- (34) Dounay, A. B.; Forsyth, C. J. *Org. Lett.* **2001**, *3*, 975.
- (35) Forsyth, C. J.; Hao, J. L.; Aiguade, J. *Angew. Chem. Int. Ed.* **2001**, *40*, 3663.
- (36) Nicolaou, K. C.; Qian, W. Y.; Bernal, F.; Uesaka, N.; Pihko, P. M.; Hinrichs, J. *Angew. Chem. Int. Ed.* **2001**, *40*, 4068.

- (37) Nicolaou, K. C.; Pihko, P. M.; Diedrichs, N.; Zou, N.; Bernal, F. *Angew. Chem. Int. Ed.* **2001**, *40*, 1262.
- (38) Nicolaou, K. C.; Frederick, M. O.; Petrovic, G.; Cole, K. P.; Loizidou, E. *Z. Angew. Chem. Int. Ed.* **2006**, *45*, 2609.
- (39) (a) Evans, D. A.; Dunn, T. B.; Kvarno, L.; Beauchemin, A.; Raymer, B.; Lohava, E. J.; Mulder, J. A.; Juhl, M.; Kagechika, K.; Favor, D. A. *Angew. Chem. Int. Ed.* **2007**, *46*, 4698; (b) Evans, D. A.; Kvarno, L.; Mulder, J. A.; Raymer, B.; Dunn, T. B.; Beauchemin, A.; Olhava, E. J.; Juhl, M.; Kagechika, K. *Angew. Chem. Int. Ed.* **2007**, *46*, 4693.
- (40) Geisler, L. K.; Nguyen, S.; Forsyth, C. J. *Org. Lett.* **2004**, *6*, 4159.
- (41) Li, Y. F.; Zhou, F.; Forsyth, C. J. *Angew. Chem. Int. Ed.* **2007**, *46*, 279.
- (42) Forsyth, C. J.; Xu, J. Y.; Nguyen, S. T.; Samdal, I. A.; Briggs, L. R.; Rundberget, T.; Sandvik, M.; Miles, C. O. *J. Am. Chem. Soc.* **2006**, *128*, 15114.
- (43) Zhou, X. T.; Carter, R. G. *Angew. Chem. Int. Ed.* **2006**, *45*, 1787.
- (44) Zhou, X. T.; Lu, L.; Furkert, D. P.; Wells, C. E.; Carter, R. G. *Angew. Chem. Int. Ed.* **2006**, *45*, 7622.
- (45) (a) Molander, G. A.; Mckie, J. A. *J. Am. Chem. Soc.* **1993**, *115*, 5821; (b) Huemann, L. V.; Keck, G. E. *Org. Lett.* **2007**, *9*, 1951; (c) Saito, T.; Takeuchi, T.; Matsushashi, M.; Nakata, T. *Heterocycles* **2007**, *72*, 151.
- (46) Inanaga, J.; Hirata, K.; Saeki, H.; Katsuki, T.; Yagaguchi, M. *Bull. Chem. Soc. Jpn.* **1979**, *52*, 1989.
- (47) Jin, H. L.; Uenishi, J.; Christ, W.; Kishi, Y. *J. Am. Chem. Soc.* **1986**, *108*, 5644.
- (48) Lewis, M. D.; Cha, J. K.; Kishi, Y. *J. Am. Chem. Soc.* **1982**, *104*, 4976.

- (49) Omura, K.; Swern, D. *Tetrahedron*. **1978**, *34*, 1651.
- (50) Parikh, J. R.; Doering, W. E. *J. Am. Chem. Soc.* **1967**, *89*, 5505.
- (51) Takai, K.; Nitta, K.; Utimoto, K. *J. Am. Chem. Soc.* **1986**, *108*, 7408.
- (52) Miyaura, N.; Yamada, K.; Suzuki, A. *Tetrahedron Lett.* **1979**, *20*, 3437.
- (53) Comins, D.; Dehghani, A. *Tetrahedron Lett.* **1992**, *33*, 6299.
- (54) Milstein, D.; Stille, J. K. *J. Am. Chem. Soc.* **1978**, *100*, 3636.
- (55) Fürstner, A.; Bouchez, L. C.; Funel, J. A.; Liepins, V.; Porée, F. H.; Gilmour, R.; Beaufils, F.; Laurich, D.; Tamiya, M. *Angew. Chem. Int. Ed.* **2007**, *46*, 9265.
- (56) (a) Jacobsen, E. N.; Marko, I.; Mungall, W. S.; Schroder, G.; Sharpless, K. B. *J. Am. Chem. Soc.* **1988**, *110*, 1968; (b) Kolb, H. C.; Van Nieuwenhze, M. S.; Sharpless, K. B. *Chem. Rev.* **1994**, *94*, 2483.
- (57) Mukaiyama, T.; Banno, K.; Narasaka, K. *J. Am. Chem. Soc.* **1974**, *96*, 7503.
- (58) Ding, Y. Ph. D. Thesis, the Ohio State University, 2010.
- (59) Larsen, C. H.; Ridgway, B. H.; Shaw, J. T.; Woerpel, K. A. *J. Am. Chem. Soc.* **1999**, *121*, 12208.
- (60) Mahoney, W. S.; Brestensky, D. M.; Stryker, J. M. *J. Am. Chem. Soc.* **1988**, *110*, 291.
- (61) Lindgren, B. O.; Nilsson, T. *Acta Chem. Scand.* **1973**, *3*, 888.
- (62) Xu, J. Y. Ph. D. Thesis, University of Minnesota, 2006.
- (63) Jianyan Xu, Yue Ding, unpublished results.

- (64) Nicolaou, K. C.; Pihko, P. M.; Bernal, F.; Frederick, M. O.; Qian, W.; Uesaka, N.; Diedrichs, N.; Hinrichs, J.; Koftis, T. V.; Loizidou, E.; Petrovic, G.; Rodriguez, M.; Sarlah, D.; Zou, N. *J. Am. Chem. Soc.* **2006**, *128*, 2244.
- (65) Antoniotti, S.; Genin, E.; Michelet, V.; Genet, J. P. *J. Am. Chem. Soc.* **2005**, *127*, 9976.
- (66) Belting, V.; Krause, N. *Org. Lett.* **2006**, *8*, 4489.
- (67) Aponick, A.; Li, C. Y.; Palmes, J. A. *Org. Lett.* **2009**, *11*, 121.
- (68) Trost, B. M.; O'Boyle, B. M.; Hund, D. *J. Am. Chem. Soc.* **2009**, *131*, 15061.
- (69) Fang, C.; Pang, Y. C.; Forsyth, C. J. *Org. Lett.* **2010**, *12*, 4528.
- (70) Sinibaldi, M. E.; Canet, I. *Eur. J. Org. Chem.* **2008**, *26*, 4391.
- (71) Baldwin, J. E.; Thomas, R. C.; Kruse, L. I.; Silberman, L. *J. Org. Chem.* **1977**, *42*, 3846.
- (72) Shibasaki, M.; Yoshikawa, N. *Chem. Rev.* **2002**, *102*, 2187.
- (73) Corey, E. J.; Fuchs, P. L. *Tetrahedron Lett.* **1972**, *13*, 3769.
- (74) Frantz, D. E.; Fassler, R.; Carreira, E. M. *J. Am. Chem. Soc.* **2000**, *122*, 1806.
- (75) Rychnovsky, S. D.; Rogers, B.; Yang, G. *J. Org. Chem.* **1993**, *58*, 3511.
- (76) Mitsunobu, O. *Synthesis* **1981**, *1*, 1.
- (77) Aponick, A.; Li, C. Y.; Mallng, J. Marques, E. F. *Org. Lett.* **2009**, *11*, 4624.
- (78) Paterson, I.; Wallace, D. J.; Cowden, C. J. *Synthesis* **1998**, 639-652.

Appendix A: Selected NMR Spectra

